Location for Profit Maximization: Applications to On-Demand Warehousing and Pilotless Air Cargo Transportation

by

Hsiu-Chuan Chang

A thesis
presented to the University of Waterloo
in fulfillment of the
thesis requirement for the degree of
Doctor of Philosophy
in
Management Sciences

Waterloo, Ontario, Canada, 2025

© Hsiu-Chuan Chang 2025

Examining Committee Membership

The following served on the Examining Committee for this thesis. The decision of the Examining Committee is by majority vote.

Ext. Examiner:	Borzou Rostami Associate Professor, Alberta School of Business, University of Alberta
Supervisor(s):	Sibel Alumur Alev Associate Professor, Department of Management Science and Engineering, University of Waterloo
	Bissan Ghaddar Associate Professor, Ivey Business School, Western University
Int. Member:	James H. Bookbinder Professor, Department of Management Science and Engineering, University of Waterloo
Int./Ext. Member:	Kumaraswamy Ponnambalam Professor, Department of Systems Design Engineering, University of Waterloo
Other Member(s):	Joe Naoum-Sawaya Associate Professor, Ivey Business School, Western University

Author's Declaration

I hereby declare that I am the sole author of this thesis. This is a true copy of the thesis, including any required final revisions, as accepted by my examiners.

I understand that my thesis may be made electronically available to the public.

Abstract

Modern logistics systems face increasing complexity due to the rapid growth of e-commerce and emerging technologies, particularly in shared warehousing platforms and air freight delivery. Accordingly, advanced approaches are needed to effectively address large-scale network design problems that prioritize profit-oriented objectives. This dissertation develops mathematical models and effective solution methodologies to optimize profitability in on-demand warehousing and pilotless air cargo transportation networks. In particular, the thesis introduces decomposition methods and heuristic algorithms to solve facility location problems arising in these applications with a focus on profit-maximization. First, a Lagrangian relaxation framework combined with a local search heuristic is used to solve a multi-period profit-maximizing facility location model in on-demand warehousing, accounting for price-sensitive demand and dynamic allocation. Next, for pilotless air cargo transportation, two network design models are developed and solved using a branch-and-price and genetic algorithm enhanced with score-based labeling and a hybrid heuristic to optimize business profit, hub placement, and airplane routing. The findings provide practical insights for enhancing profitability and operational responsiveness in both on-demand warehousing and pilotless air cargo logistics.

Keywords: Profit maximization, on-demand warehousing, pilotless air cargo delivery, capacitated facility location problem, hub location problem.

Acknowledgements

I would like to express my sincere gratitude and appreciation to my supervisors, Dr. Sibel Alumur Alev and Dr. Bissan Ghaddar, for giving me the opportunity to work on research projects and for their continuous support throughout the course of my studies. I would like to express my sincere gratefulness to my supervisor Dr. Bissan Ghaddar, for her invaluable support and advice during my research and the writing of this thesis. I am also deeply thankful to my supervisor, Dr. Sibel Alumur Alev, for her continuous research guidance and daily support. Furthermore, I sincerely thank Dr. Joe Naoum-Sawaya for sharing his extensive knowledge and for his valuable advice and insightful comments during my research.

I would also like to express my sincere thanks to Ribbit Ltd. for providing the fellowship that supported my research, and especially to Dr. Jeremy Wang for his constant guidance and generous availability throughout the project. I am grateful to Dr. Jim Bookbinder and Dr. Umair Shah for their support and guidance during my teaching assistantship. In addition, I am thankful to Ms. Lisa Hendel for her kind and efficient administrative support throughout my studies. Moreover, I would like to thank the examiner, Dr. Borzou Rostami, and the committee members — Dr. Jim Bookbinder, Dr. Kumaraswamy Ponnambalam, and Dr. Joe Naoum-Sawaya — for their valuable feedback, insightful questions, and generous support throughout the evaluation process.

Finally, I want to express my thanks to my friends in the Department of Management Science and Engineering, who always provided me with motivation, moral support, and academic advice throughout my time at the University of Waterloo.

Dedication

To my beloved wife, Abby

To my lovely daughters, NaNa and NiNi

To my bright sunshine, Yating

To my kindred spirit, Wiwi

To my dearest parents and younger sister

This is for you, with all my love. Always.

Table of Contents

List of Figures x

List of Tables xii

1 Introduction 1

2 Literature Review 10

2.1 On-Demand Warehousing 11

2.2 Pilotloss Air Cargo Transportation 18

3 Optimizing Locations and Pricing for On-Demand Warehousing 25

3.1 Mathematical Formulation 26

3.1.1 On-Demand Warehousing Formulation 26

3.2 Solution Approach 31

3.2.1 Lagrangian Relaxation (LR) 32

3.2.1.1 Lagrangian Relaxation: Mathematical Process 32

3.2.1.2 Lagrangian Relaxation Improvement: Decomposed Model 35

3.2.2 Lagrangian Relaxation Heuristic Implementation 37
3.3 Computational Results 44
3.3.1 Parameter Setting 44
3.3.2 Computational Performance Analysis 46
3.3.3 Sensitivity Analysis: Pricing and Demand Satisfaction 48
3.4 Chapter Summary 51

4 Optimizing Hub Locations and Flight Assignments 53
4.1 Mathematical Formulation 54
4.1.1 Path-based Formulation (HLPP-P) 54
4.1.2 Arc-based Formulation (HLPP-A) 58
4.2 Solution Approach 62
4.2.1 Branch-and-Price (B&P) 62
4.2.2 Genetic Algorithm (GA) 69
4.2.2.1 Components of GA 69
4.2.2.2 Fitness Function of GA 70
4.2.2.3 Iterative Process of GA 72
4.2.2.4 Genetic Operations of GA 75
4.3 Computational Results 79
4.3.1 Parameter Setting 79
4.3.2 Insights 85
4.3.3 Computational Performance Analysis 91
4.4 Chapter Summary 94

5 Optimizing Hub Locations and Airplane Routes **96**

5.1 Mathematical Formulation 97

5.1.1 Path-based Formulation (HLPP-PR) 97

5.2 Solution Approach 101

5.2.1 Genetic Algorithm for HLPP-PR 103

5.2.1.1 Components and Fitness Function of GA for HLPP-PR . . 103

5.2.1.2 Iterative Process and Genetic Operations of GA for HLPP-PR 104

5.2.2 Score-based Labeling (SL) 106

5.2.3 Hybrid Heuristic (HH) 111

5.3 Computational Results 117

5.3.1 Parameter Setting for HLPP-PR 117

5.3.2 Insights 122

5.3.3 Computational Performance Analysis 125

5.3.4 Sensitivity Analysis 128

5.3.4.1 Effect of Demand Scale on Operational Strategies 128

5.3.4.2 Influence of Airplane's Origin and Destination 133

5.3.4.3 Impact of Revenue-to-Cost Ratio on Profitability 136

5.4 Chapter Summary 140

6 Conclusion and Future Work **142**

References **145**

List of Figures

3.1 Overall process of solution approach. 31

3.2 The Lagrangian Relaxation decomposed model. 37

3.3 The processes of Lagrangian Relaxation Heuristic. 38

3.4 Sample pattern of add/drop procedure. 43

3.5 Demonstration of LRH bounds by iterations. 48

3.6 Scatter plot of the elasticity versus the % of demand satisfied. 49

3.7 Scatter plot of price elasticity versus reduction in demand satisfied given high fixed cost (left) and limited capacity (right). 50

4.1 Overall process of the B&P approach. 68

4.2 The components of GA for solving HLPP. 70

4.3 Encoding and decoding processes of GA. 73

4.4 Detailed process flow of GA. 74

4.5 The nodes in the southeastern region of the US. 82

4.6 The flight assignments and hub location with different nodes. 89

5.1 Overall process of solution approach for HLPP-PR. 102

5.2 Detailed process flow of SL. 107
5.3 Visualization of the path selection comparison for core examples. 124
5.4 Visualization of the effect of demand scale on operational strategies. 130
5.5 Effect of demand scale on operational strategies. 131
5.6 Influence of airplane origin and destinations on results. 134
5.7 Influence of airplane's origin and destination. 135
5.8 Impact of revenue-to-cost ratio on profitability. 137

List of Tables

2.1 Summary of the existing literature on on-demand warehousing. 17

2.2 Summary of the existing literature related to the hub location problem. . . 24

3.1 All possible combinations for the relaxed constraint. 39

3.2 Comparison of the different algorithms. 47

4.1 Parameters: The core southeastern region of the US. 83

4.2 Computational results with flight assignments. 86

4.3 Computational performance: Flight assignments. 92

5.1 Parameters with airplane routing. 119

5.2 Setting for score-based labeling. 121

5.3 Computational results with airplane routing. 122

5.4 Computational performance: Airplane routes. 126

5.5 Location setting of airplanes' origin and destination. 133

Chapter 1

Introduction

As global trade and commerce continue to expand, the demand for reliable and responsive logistics and transportation networks has grown significantly. Efficient network design is critical for minimizing costs, reducing delivery times, and improving customer satisfaction. The rise of advanced technologies, including e-commerce, automation, and artificial intelligence, has created new opportunities to enhance the performance of logistics and transportation systems.

As global supply chains become more complex, many businesses are finding it harder to meet growing customer expectations. The fast growth of e-commerce, frequent changes in demand, and the need for quicker deliveries have made traditional logistics systems less effective. Old models often struggle with flexibility, cost control, and speed. This situation has created a need for better solutions that can adapt quickly and work more efficiently.

At the same time, new technologies such as automation, online platforms, and autonomous vehicles are changing the way logistics works. On-demand warehousing and pilotless air cargo are two examples of these changes. These innovations can reduce costs, improve delivery times, and help businesses respond faster to demand changes. However, they also bring new challenges. For example, it is still not clear how to design large networks that use these technologies while staying profitable and reliable.

Because of this, researchers and companies are now looking for new ways to plan and manage these systems. There is a strong need for better network design methods that consider flexibility, service quality, and profit at the same time. This research is based on that need. It explores how new logistics systems can be planned using modern tools and models that fit today's fast-changing business environment.

From the logistics side, the growth of e-commerce and the shared economy has intensified the need for flexible and responsive on-demand warehousing solutions. On-demand warehousing platforms have emerged in response to the rising complexity and volatility of supply chains, driven primarily by rapid e-commerce growth, shifting consumer expectations, and the limitations inherent in traditional warehousing models [1, 2]. Traditional warehousing arrangements, characterized by rigid contracts and high fixed costs, struggle to offer the flexibility needed to manage fluctuating market demands and short-term inventory needs effectively [3, 4, 5]. Consequently, new collaborative logistics models have arisen, connecting businesses that have excess storage capacity with companies seeking flexible, short-term warehousing solutions [3, 4, 5]. Recent trends highlight these shifts, noting the increasing focus on flexible, modular, and mobile facility solutions to enhance responsiveness in contemporary logistics and supply chain networks [6, 7].

Specifically, the warehouse owner does not serve a single tenant or its own business but can lease the space to generate additional revenue in shared warehousing [4, 8]. On-demand warehousing platforms facilitate this process by connecting small and medium-sized enterprises (SMEs) with warehouse owners and streamlining the matching process through automated algorithms and real-time availability updates [5, 8]. All companies can register their profiles on the on-demand warehousing platform and release warehouse space when they have extra capacity. When SMEs and third-party logistics (3PL) providers encounter sudden increases in demand or require short-term storage, they can quickly secure available space through these platforms. Therefore, SMEs and 3PL providers gain more flexibility to manage fluctuating demand and capitalize on market opportunities as their businesses evolve. Additionally, SMEs can reduce operational costs and meet customer needs by renting partial space from these warehouse owners [5, 8]. This model enhances the adaptability of supply chains and improves overall market efficiency by allowing businesses to scale their storage capacity according to changing market conditions.

Regarding transportation, the rise of autonomous technologies has created new opportunities for pilotless air cargo delivery, offering the potential to revolutionize the industry by enabling faster, more flexible, and environmentally friendly transportation [9, 10]. The rapid growth of e-commerce and increased consumer expectations for quick, reliable delivery have significantly heightened the importance of air cargo transportation, particularly for time-sensitive products. Traditional air cargo systems, frequently organized in hub-and-spoke configurations, consolidate cargo at central locations to improve network efficiency and reduce operational costs [11, 12]. However, traditional air cargo operations often face limitations such as high operational costs, labor-intensive processes, and vulnerability to

human errors, motivating logistics providers to explore more innovative and automated solutions [9]. In response, pilotless air cargo transportation systems have emerged, promising increased efficiency, reduced environmental impacts, and lower operating costs through automation and optimized route planning [9, 10]. These advancements highlight the industry's ongoing transition toward fully automated systems, driven by the need for flexibility, efficiency, and safety enhancements.

One such example is the company Ribbit Ltd. (https://www.flyribbit.com/). Ribbit is a venture-backed startup in Canada that is creating a pilotless airline that will fly cargo shipments to provide just-in-time delivery. These pilotless airplanes are expected to play a crucial role in the resilient and sustainable supply chains of the future. Ribbit's autonomous autopilot technology can perform the equivalent functions of a commercial pilot: taxi, takeoffs, en-route flying, landing, and collision avoidance. By replacing the cockpit with more cargo volume, removing flight time duty limits, and reducing pilot labor costs [13, 14]. The emerging companies, such as Ribbit, anticipate that autonomous planes will increase flight frequency and reliability, thereby reducing delivery times, while expanding the air cargo market to destinations not previously served [9, 10]. To realize the full potential of this autonomy, it is essential to design from the ground up a fast, flexible, and cost-efficient network that will operate a fleet of self-flying airplanes.

Recent studies on on-demand warehousing have predominantly focused on the development and application of advanced optimization techniques, including dynamic facility location models and heuristic algorithms, to facilitate effective network design under uncertain and dynamic conditions [15, 16, 17]. Optimization methodologies, heuristics, and meta-heuristics, are widely employed to efficiently solve large-scale and complex on-demand

warehousing problems, demonstrating significant improvements in computational efficiency and solution quality compared to traditional optimization methods [15, 16, 17]. Recent empirical studies also highlight cost-saving potentials and operational efficiencies achievable through adopting flexible warehousing strategies and integrating shared warehousing platforms [4, 18, 19].

Moreover, the operational challenges and managerial implications associated with on-demand warehousing platforms have gained significant attention. Key research findings underline the critical importance of aligning platform incentives and revenue management strategies to optimize resource allocation between self-use and rental space, thereby ensuring the sustainability and profitability of the warehousing providers [8, 20]. Further investigations into business model evolution reveal a transition from pure on-demand warehousing platforms toward integrated logistics solutions or hybrid fourth-party logistics (4PL) models, aiming to overcome operational complexities and maximize shared value creation [4, 8]. Overall, these recent developments highlight on-demand warehousing as an increasingly vital component in short-term warehousing strategies, facilitating improved capacity utilization, enhanced service responsiveness, and greater operational flexibility [3].

Recent literature on air cargo transportation emphasizes advanced optimization methodologies to manage increasingly complex logistics networks. Significant attention has been given to multimodal network designs, combining air and ground transport to maximize network coverage and efficiency while addressing fluctuating demand and various operational constraints [12]. Furthermore, developed optimization techniques, such as mixed-integer programming, matheuristics, and metaheuristics, have been widely employed to dynamically adapt air cargo networks in response to disruptions, varying cargo volumes, and

different service requirements [11, 12]. These adaptive strategies are essential for pilotless air cargo systems, which require highly responsive network configurations to maximize operational benefits and swiftly adapt to changes in demand and environmental conditions [13, 14].

As air cargo transportation moves toward full automation, selecting optimal hub locations becomes even more critical, as pilotless systems depend significantly on suitable infrastructure, robust connectivity, and precise logistical coordination. Strategic hub placement in automated networks must account for operational requirements, including charging and maintenance facilities, environmental constraints, and regulatory compliance, to fully realize their operational advantages [9]. Additionally, flexible network designs are essential for pilotless cargo operations to ensure reliability and resilience against potential challenges, particularly in path planning and carrying capability [13]. Thus, current research clearly indicates that successful implementation of pilotless air cargo transportation demands a comprehensive and strategic approach to hub location selection, supported by advanced optimization techniques and detailed analysis of operational constraints [9, 10, 14, 21].

While several studies have proposed solid models to address these challenges from different perspectives, significant gaps remain in scaling solutions for large-scale transportation and warehousing networks. Traditional optimization methods, such as mixed-integer programming, often struggle to provide feasible solutions for large-scale networks due to computational complexity. These methods are also limited in effectively balancing profitability with operational efficiency when faced with dynamic market conditions.

Although decomposition methods have shown promise in improving both computational

efficiency and solution quality, existing research has primarily focused on traditional industries with cost-minimization objectives. Limited research has explored the application of these methods to profit-maximization problems in emerging industries such as pilotless air cargo transportation and on-demand warehousing. Moreover, previous studies in these industries have not sufficiently addressed the complex interactions between fluctuating demand patterns, operational costs, and dynamic pricing. Therefore, a comprehensive approach integrating heuristic-based decomposition methods with profit-maximization objectives is needed to deliver scalable, adaptive solutions capable of enhancing both profitability and operational performance.

To address these challenges, this research aims to develop mathematical models and solution methodologies tailored specifically to optimizing profitability and operational performance for on-demand warehousing and pilotless air cargo transportation network design.

In particular, the thesis first focuses on optimizing location and pricing decisions for shared warehousing companies within a multi-period planning horizon. Existing models primarily address cost minimization or single-period decisions, often neglecting the dynamic consideration of customer demand and price sensitivity. This thesis introduces a novel multi-period capacitated facility location model that integrates price sensitivity and demand fluctuations, enabling warehouse owners to make more informed location and pricing decisions. The model considers SMEs as customers with varying demand over multiple periods, allowing the warehouse owner to adjust pricing and facility locations dynamically. By utilizing a Lagrangian relaxation approach combined with heuristic techniques, the model dynamically addresses the complexities of price-sensitive demand and multi-period variability in cus-

tomer requirements. This solution is benchmarked against the commercial solver CPLEX to validate effectiveness and computational efficiency. The solutions obtained from this model provide valuable insights for public warehousing companies, helping them enhance profitability by selecting suitable locations and adjusting pricing strategies in response to market changes.

Second, this thesis also addresses the emerging field of pilotless air cargo transportation, where strategic hub placement and operational efficiency are critical for maximizing profitability. The proposed models offer strategic insights for pilotless air cargo operators by enabling them to optimize hub locations and routing decisions, ultimately enhancing both profitability and service reliability. The models focus on start-up businesses, taking into account the diverse locations of customer demand and limited resources. To solve the proposed models, decomposition approaches are integrated with a Genetic Algorithm substantially improving computational efficiency and solution quality, enabling rapid and informed decision-making. The solutions derived from these models provide valuable guidance for determining optimal flight routes, selecting suitable hub locations, and ensuring customer demand is met effectively. The models enable operators to achieve maximal profit while maintaining high service standards, making it a crucial tool for the growth and success of new entrants in the pilotless air cargo market.

The remaining of this dissertation is organized as follows. Chapter (2) reviews relevant literature. Chapter (3) presents the mathematical model and the proposed algorithm for the on-demand warehousing industry. Chapter (4) introduces mathematical models and related techniques designed to maximize profit by optimizing hub locations and satisfying customer demand for pilotless air cargo transportation. Chapter (5) further extends the models in-

troduced in Chapter (4) by incorporating airplane routing decisions. Finally, Chapter (6) provides concluding remarks and a discussion of future research directions.

Chapter 2

Literature Review

In this chapter, we review the literature pertinent to our research, summarizing research trends and recent key findings in the domains of on-demand warehousing and pilotless air cargo transportation. Additionally, we discuss problem settings relevant to our study, including the Facility Location Problem (FLP) and the Hub Location Problem (HLP), along with their respective solution methodologies. This includes an examination of emerging technologies and their impact on logistics networks, further enhancing our understanding of the dynamic nature of supply chain management. Building on this review, we explore potential opportunities that can be applied to our research, particularly focusing on heuristic approaches and decomposition methods in optimization. Moreover, we assess the scalability of these methods in handling increasingly complex logistics scenarios, which is critical for future applications. The chapter concludes with a summary of key insights, effectively connecting the discussed methodologies and applications to the broader context of network optimization.

2.1 On-Demand Warehousing

Since 1990, warehousing systems have evolved rapidly. The literature indicates that research on warehousing has transitioned from traditional storerooms to more automated and integrated systems, characterized by improved efficiency and effectiveness [7]. Recently, the emergence of on-demand warehousing reflects an important transformation in logistics and supply chain management, driven primarily by the need for increased flexibility and responsiveness amid rapid e-commerce growth and market volatility [6]. On-demand warehousing refers to flexible warehouse rental arrangements facilitated through digital platforms that connect businesses with excess storage capacity to companies requiring temporary or variable warehousing solutions [4]. This concept is vital due to its potential to significantly reduce fixed operational costs and improve the flexibility of supply chains by allowing rapid adjustments to storage capacities in response to fluctuating market demands [3].

Recent investigations have demonstrated that on-demand models are particularly advantageous for addressing fragmented demand, offering rapid responsiveness to SMEs and e-commerce retailers with seasonal or unpredictable needs. For example, Balcazar et al. (2020) and presented a real-world case study in Peru illustrating significant cost and space utilization improvements via an on-demand model for event logistics [18]. Xenou et al. (2021) and Parodos et al. (2022) also analyzed evolving business models of on-demand warehousing platforms in Greek, identifying critical elements such as user interfaces, service pricing, and transition operations [5, 19]. These findings underscore the importance of strategic platform design and continuous innovation to address operational challenges.

In recent years, numerous scholars have extensively researched on-demand warehousing, highlighting its growing importance in enhancing logistics efficiency and responsiveness [8, 22]. A considerable body of literature has investigated the operational and strategic dimensions of on-demand warehousing. Early studies, such as those by Shin (2019) and Lahy (2022), identified significant economic benefits from adopting collaborative logistics systems, emphasizing the efficiency gains and cost reductions achieved through shared storage capacities [3, 4]. More recently, research has shifted towards understanding the complexities involved in implementing on-demand warehousing platforms, focusing on aspects such as financial factors [20], dynamic capacity management [23], and responsiveness to inventory and commitment decisions [17, 24, 25]. For instance, Unnu and Pazour (2022, 2023) demonstrated through simulation models and optimization how hybrid warehousing systems effectively balance the capacity utilization of owned and rented storage spaces, thereby enhancing operational flexibility [1, 15]. Similarly, Ceschia et al. (2023, 2024) highlighted the crucial role of maximizing customer requests and capacity allocation in maintaining the satisfaction of both warehouse owners and customers [2, 16].

While the existing literature shows strong progress in modeling and methods, there are still some limitations. Most methods mainly aim to minimize operational costs and do not focus much on profitability or how pricing changes can impact warehouse performance, even though there is evidence that these factors are crucial [8, 23, 24]. Also, while methods that use heuristics to break down problems have improved how fast computations can be done, their use in strategic, profit-focused decision-making in modern logistics is still limited [15, 17].

Overall, these studies have greatly improved our understanding and optimization of on-

demand warehousing systems using dynamic location models, heuristic methods, and decomposition techniques. However, there is still a lot of room to improve these methods by clearly including ways to maximize profits, analyze price sensitivity, and adapt strategies for dynamic and uncertain operations. Based on these points, future research should thoroughly explore and apply heuristic-based decomposition in contexts that focus on maximizing profits, tackling these limitations, and more accurately reflecting the complexities of modern logistics systems.

Facility Location Problems (FLPs) play a central role in optimizing on-demand warehousing networks by guiding strategic decisions related to warehouse placement, capacity allocation, and service levels. Recent reviews have emphasized the evolution of FLPs and highlighted persistent challenges alongside emerging research directions. Saldanha-da-Gama (2022) reflected on the lasting relevance of FLPs in logistics, underlining the increasing emphasis on reverse logistics, sustainability, and data-driven decision-making in response to globalization and digital transformation [26]. In parallel, Alarcon-Gerbier and Buscher (2022) conducted a systematic review of 125 studies focused on mobile and modular facility location, outlining prevalent modeling approaches, solution techniques, and promising avenues for future exploration in dynamic supply chain contexts [27].

Lagrangian relaxation and its extensions are crucial in solving capacitated facility location problems (CFLPs), and they offer a strong demonstration when addressing on-demand warehousing problems. Beasley (1988) first applied Lagrangian relaxation to large-scale warehouse location problems. His method combined tighter bounds and exclusion rules to speed up exact search performance [28]. Later, he expanded this into a broader heuristic framework that used subgradient optimization and handled various types of FLPs with

different constraints [29]. Wu et al. (2006) further developed this line of work by including nonlinear setup cost functions in a mixed-integer model. They used Lagrangian heuristics to model more realistic warehousing costs [30]. Moreover, Klose and Görtz (2007) proposed a branch-and-price method that used column generation with relaxed constraints to solve large CFLPs more efficiently [31]. Avella et al. (2009) developed a core variable selection method based on Lagrangian dual values and solved the reduced problem using branch-and-cut [32]. These initial efforts highlighted the versatility of Lagrangian relaxation, showing it can function independently or as part of more complex heuristic or exact algorithms.

Building on these foundations, newer studies have used Lagrangian relaxation in hybrid and scalable algorithms to better support modern warehousing needs. Guastaroba and Speranza (2012) introduced a kernel search heuristic guided by Lagrangian relaxation to identify promising variable sets [33], while Sun (2012) used Lagrangian bounds in a memory-based tabu search to improve diversification and intensification during the search [34]. Fischetti et al. (2016) showed that Benders decomposition could still be effective even without separability, especially when combined with Lagrangian-based insights inside a branch-and-cut solver [35]. Alenezy (2020) proposed a volume algorithm that uses tighter Lagrangian-based constraints to improve large-scale CFLP solutions [36]. Caserta and Voß (2020) expanded the landscape with a corridor method that builds search neighborhoods around Lagrangian solutions, enabling near-optimal results for both deterministic and robust CFLP variants [37]. Allman and Zhang (2020) considered the relocation of modular production units using mixed-integer linear programming (MILP) and branch-and-price, quantifying the value of mobility over time [38].

More recently, Ryu and Park (2022) developed a branch-and-price algorithm for single-

source CFLPs with cardinality-constrained demand uncertainty, which enhanced the reliability of solutions with minimal increases in cost [39]. Štádlerová et al. (2023) applied Lagrangian decomposition within a two-stage stochastic framework for planning modular hydrogen infrastructure under conditions of demand uncertainty [40]. Liu et al. (2023) created a two-phase pandemic response framework and utilized Lagrangian Relaxation to manage fluctuating demand and prepositioning requirements [41]. Additionally, some techniques such as ADD/DROP procedures [42] and Relaxation Adaptive Memory Programming (RAMP) algorithms [43] have been integrated with Lagrangian Relaxation, providing good applications for FLPs. In summary, these studies confirm the ongoing value of Lagrangian-based methods in solving complex, large, and flexible facility location problems, particularly in the dynamic context of on-demand warehousing.

Metaheuristic, matheuristic, and hybrid approaches have become increasingly important in solving FLPs, especially when dealing with large datasets, complex constraints, or dynamic features such as demand uncertainty and customer incompatibility. These methods are particularly valuable for on-demand warehousing because they can generate high-quality solutions efficiently. Cabrera et al. (2012) combined artificial bee colony algorithms with mixed-integer programming (MIP) to effectively identify and solve promising subproblems [44]. Rahmani and MirHassani (2014) proposed a hybrid firefly-genetic algorithm inspired by natural signaling behavior, which outperformed the individual methods when used alone [45]. Harris et al. (2014) introduced a multi-objective hybrid model that used a genetic algorithm to balance carbon emissions and financial costs, demonstrating its relevance in green logistics [46]. Lagos et al. (2016) presented a matheuristic that blends local search with mathematical programming, using installation costs and customer distances to guide

facility selection [47].

In recent years, Shoja et al. (2019) incorporated multiple delivery modes into a flexible supply chain design and evaluated ten adaptive metaheuristics, highlighting the superior performance of the adaptive vibration damping optimization (AVDO) algorithm [48]. Pagès-Bernaus et al. (2019) applied a simheuristic approach—integrating simulation with metaheuristics—to effectively address stochastic demand in e-commerce environments, enabling scalable solutions for large instances [49]. Sauvey et al. (2020) modeled delayed demand satisfaction in multi-period FLPs and proposed four constructive heuristics with local improvements, outperforming MIP solvers in both feasibility and quality [50].

More recently, Rabe et al. (2021) further advanced simulation-optimization by combining system dynamics with a multi-period FLP model, supporting adaptive last-mile logistics under varying demand conditions [51]. Silva et al. (2021) addressed modular capacity decisions in dynamic facility models, testing linear relaxation with a genetic algorithm and a variable neighborhood descent (GA+VND) hybrid heuristics across cost scenarios [52]. Maia et al. (2023) tested multiple metaheuristics for CFLPs with customer incompatibilities, identifying data-driven techniques as particularly effective [53]. Similarly, Ozsoydan and Gölcük (2023) proposed a cooperative approach using adaptive mutation within a genetic algorithm, supported by linear programming solvers for final customer-to-facility assignments [54]. In summary, these studies highlight how flexible, hybrid methods can address the unique challenges of on-demand warehousing, balancing practical considerations alongside traditional cost-efficiency goals.

In conclusion, the key literature related to our research is summarized and compared with

our proposed model in Table (2.1).

Table 2.1: Summary of the existing literature on on-demand warehousing.

Paper	Profit Maximization	Multi Period	Demand Uncertainty[3]	Solution Approach[1]	Application Area[2]
Pagès-Bernaus et al. (2019) [49]			✓	S, Sim+LS	OS
Silva et al. (2021) [52]		✓		S, LRH2, GA1+LS	MC
Rabe et al. (2021) [51]		✓	✓	S, Sim	APL
Shi et al. (2021) [23]	✓	✓		ADP	ODW
Correia and Melo (2022) [24]		✓		S, BC	ODW
Ceschia et al. (2023) [2]		✓		S, GA2, MH	ODW
Ceschia et al. (2024) [16]		✓	✓	S, GA2	ODW
Unnu and Pazour (2022) [1]		✓		S, Sim	ODW
Unnu and Pazour (2023) [15]		✓		S, MH	ODW
Lee et al. (2024) [17]		✓	✓	S, BD	ODW
Proposed model	✓	✓		S, LRH1+LS	ODW

[1] Solution Approach: S: CPLEX/Gurobi; Sim: Simulation; LS: Local Search; GA1: Genetic Algorithm; GA2: Greedy Algorithm; ADP: Approximate Dynamic Programming; BD: Benders Decomposition; BC: Branch and Cut; MH: Heuristic; LRH1: Lagrangian Relaxation Heuristic; LRH2: Linear Relaxation Heuristic

[2] Application Area: ODW: On-Demand Warehousing; OS: Outsourcing; APL: Automated Parcel Locker; MC: Modular Capacities

[3] Demand Uncertainty includes stochastic programming, robust consideration, or chance constraint

2.2 Pilotloss Air Cargo Transportation

Air cargo express has become an essential industry in modern logistics, enabling the rapid delivery of time-sensitive or high-value products across vast distances. This sector excels by circumventing the complexities associated with traditional transportation modes, providing direct routes and reduced handling that significantly shorten delivery times. Building on these advantages, many researchers have conducted extensive studies to improve the efficiency of air cargo transportation network design. These efforts are aimed at refining network layouts, boosting the reliability and flexibility of the logistics systems, and simplifying operations to reduce delays and costs. Broader reviews by Gorman et al. and SteadieSeifi et al. highlighted the applications of operations research across freight modes and multimodal freight transportation planning [11, 12]. In particular, much research has concentrated on the necessity for strategically structured networks, especially regarding hub location placement [55] and transportation network connectivity [56, 57]. These studies ensure that service speed and reliability are maintained in express logistics.

Moreover, real-world case studies offer crucial insights into the design of air express networks. Early investigations, such as those by Lin et al. (2012) and Oktal and Ozger (2013), provide thorough analyses based on hub-and-spoke structures in China and Turkey, respectively, setting foundational knowledge in the field [58, 59], Also, Yu et al. (2017) proposed a bi-level network design model for Chinese express firms, optimizing both the transportation network and aircraft capacity usage [60]. More recent studies, such as those by Yildiz et al. (2022, 2023), advance this understanding by proposing an optimization model for package express operations in China that integrates air and ground transportation, multiple service

classes, and resource constraints [61, 62]. Their research expands into transshipment-based multimodal networks, illustrating how express cargo can be managed efficiently through a strategic mix of cargo flights and ground transportation.

Optimization with hybrid techniques broadens the applications to enhance the efficiency and resilience of air cargo express networks. Zhang et al. [63] proposed MIP-based models with a hybrid algorithm to solve large-scale hub and aircraft assignment problems efficiently, while Lee et al. [64] integrated network design and route selection, showing cost savings through smart transshipment planning. Delgado and Mora [65] addressed demand disruptions with a matheuristic rescheduling model using column generation to improve cargo flexibility. Gayialis et al. [66] focused on last-mile logistics, combining operations research (OR) and information technology (IT) tools to optimize dynamic vehicle routing in urban freight systems. These case studies not only highlight practical challenges but also showcase the effectiveness of data-driven and hybrid approaches in optimizing large-scale express logistics operations.

Recently, pilotless air cargo, primarily facilitated by unmanned aerial vehicles (UAVs), has emerged as a new frontier in logistics. UAVs provide several advantages, including rapid deployment, reduced operational costs, and the ability to access remote or congested areas. These capabilities make them particularly valuable for last-mile deliveries and reaching difficult-to-access locations [10, 13]. Betti Sorbelli (2024) highlights the extensive applications of UAVs in critical sectors such as emergency medical services, disaster response, and sustainable logistics, emphasizing their role in modernizing these fields [9]. Additionally, UAVs contribute to reducing emissions, decreasing reliance on traditional infrastructure, and enabling smarter, more flexible routing options. These attributes align well with

the increasing demand for environmentally friendly and cost-effective logistics solutions [14, 21]. As technologies related to airspace management, autonomy, and safety continue to advance, pilotless cargo is expected to become a central component in the evolution of express logistics networks.

Despite growing interest in optimizing air cargo networks, few studies focus on profit-maximizing models for pilotless air express systems under hub placement conditions. Most existing works prioritize cost reduction, schedule recovery, or deterministic planning, often overlooking integrated decision-making across profit consideration with hub placement, customer satisfaction, and airplane routing. It remains a clear gap in adapting to real-time operational shifts and demand fluctuations. Our research aims to fill this gap by developing a heuristic-enhanced decomposition model that facilitates strategic planning for pilotless air express. This model focuses on balancing profitability, service quality, and operational adaptability, offering a comprehensive approach to managing the complexities of modern air logistics.

Besides the literature above, Hub Location Problems (HLPs) in related areas also provide valuable methodologies and insights applicable to air cargo and freight logistics. These problems typically focus on optimizing the placement of hubs and the design of network structures. Over the years, diverse modeling and solution techniques have emerged, ranging from exact methods and classical formulations to decomposition techniques and advanced metaheuristics.

Early foundational reviews structured the growing field. Alumur and Kara (2008) categorized classical and advanced models in HLPs, emphasizing their practical roles in logistics

systems [67], Moreover, Campbell and O'Kelly (2012) reflected on 25 years of research, linking early motivations to modern challenges in transportation network design [68], while Farahani et al. (2013) expanded the scope by summarizing mathematical formulations, solution techniques, and applications of both discrete and continuous HLPs [69]. In a more recent reflection, Alumur et al. (2021) reviewed the historical progression and highlighted new directions, including economies of scale and stochastic elements [70]. Also, Basallo-Triana et al. (2021) reviewed hub-based intermodal networks, noting the limited modeling of internal factors such as vehicles and hub capacity [71]. Similarly, Saldanha-da-Gama (2022) discussed HLPs in the broader context of logistics and transportation, calling for more adaptive and data-driven models under global pressures [26]. These comprehensive reviews provide insights into both the evolution and future challenges of modeling in transportation and logistics, emphasizing the need for innovative approaches to address the complexities of modern networks.

Recently, many studies emphasized the balance between cost and revenue with profit-oriented objectives. Alibeyg et al. (2016) introduced profit-maximizing HLPs that activate different edge types and jointly optimize service coverage, profit, and cost [72]. Taherkhani and Alumur (2019) explored multiple allocation strategies in profit-based networks, comparing scenarios with and without direct links [73]. Building on this, Taherkhani et al. (2020, 2021) further proposed a two-phase Benders decomposition method and a Monte Carlo-based algorithm to solve capacitated profit-maximizing HLPs with multiple demand classes under uncertainty, and introduced robust stochastic models accounting for joint uncertainties in demand and revenue, with different solution frameworks like min-max regret and max-min robustness [74, 75]. More Recently, Oliveira et al. (2022) addressed

incomplete hub networks using Benders decomposition, solving large instances more efficiently than CPLEX [76], while Gao et al. (2022) presented a path-based formulation for hub network design with profits, enhanced by a branch-and-cut approach built on Benders decomposition [77].

Meanwhile, several works have underscored the importance of addressing uncertainty and broader network design with a focus on minimizing operational costs. Alumar et al. (2012) explored HLPs with the consideration of different sources of uncertainty, enhancing the adaptability of network designs to fluctuating conditions [78]. Govindan et al. (2017) provided a comprehensive review of supply chain network design under uncertainty, incorporating stochastic programming and robust optimization to better manage location and transportation planning challenges [79]. Jahani et al. (2024) delved into financial considerations within supply chain network design, emphasizing the need to integrate depreciation, amortization, and valuation models into hub location decisions to achieve a more holistic approach to financial management in logistics [20]. These studies collectively highlight the critical need for incorporating financial and uncertainty aspects into the strategic planning of logistics networks.

Early applications of genetic algorithms were broadly applied in works by Topcuoglu et al. (2005), Naeem and Ombuki-Berman (2010), and Stanimirovic (2010), each refining solution operators and encoding strategies to tackle various variants of HLPs [80, 81, 82]. Moreover, Damgacioglu et al. (2015) proposed a genetic algorithm for uncapacitated planar HLPs, outperforming classical heuristics in solution quality and speed [83]. Continuing this trend, Katoch et al. (2021) provided a comprehensive review on the evolution of genetic algorithms, advocating hybrid strategies and better fitness functions for solving

complex logistics problems [84]. Their review highlights the ongoing advancements in genetic algorithm methodologies, emphasizing their critical role in enhancing the efficiency and effectiveness of solutions in the field of logistics and transportation.

Optimization decomposition techniques continue to be widely used in HLPs. Contreras et al. (2009) introduced a Lagrangian relaxation approach for the capacitated single-assignment hub location problem, which allows the problem to be decomposed into more manageable subproblems that can be solved more efficiently, thus significantly reducing computational effort [85]. Meanwhile, Wu et al. (2024) developed a branch-and-price-and-cut algorithm for the capacitated single allocation HLP with routing considerations, solving intra-city service networks more effectively through bidirectional labeling and column generation [86].

More recently, the use of metaheuristics has proven to be effective for managing large or nonlinear HLPs. Zhang et al. (2023) crafted a Variable Neighborhood Search (VNS) for profit-maximizing HLPs with multiple allocation types, achieving optimal solutions for numerous benchmark cases and surpassing exact methods in larger networks [87]. Similarly, Oliveira et al. (2023) implemented two Iterated Local Search (ILS) algorithms for similar HLPs, demonstrating their effectiveness on instances involving up to 500 nodes [88]. These advancements underscore the evolving complexity and scalability of techniques applied in the optimization of hub location networks.

In summary, these studies not only advance methodologies in hub location modeling but also provide valuable insights for air cargo express systems, particularly in profit maximization, uncertainty, multimodal configurations, and solution approaches.

In conclusion, our research essentially falls under the category of hub location problems, applied in the context of pilotless air cargo transportation. The key literature related to our study is summarized and compared with our proposed model in Table (2.2).

Table 2.2: Summary of the existing literature related to the hub location problem.

Paper	Profit Maximization	Demand Uncertainty[2]	Routing Limit [3]	Solution Approach[1]
Alumur et al. (2012) [78]		✓		S
Damgacioglu et al. (2015) [83]				S, GA
Alibeyg et al. (2016) [72]	✓			S
Taherkhani and Alumur (2019) [73]	✓			S, BD
Taherkhani et al. (2020) [74]	✓	✓	C2	S, BD
Oliveira et al. (2022) [76]	✓			S, BD
Zhang et al. (2023) [87]	✓			S, BD, VNS
Yildiz et al. (2022) [61]	✓		C1, T1	S, CG
Yildiz et al. (2023) [62]			C1, T2	S
Wu et al. (2024) [86]			C1, C2	S, BPC
Proposed model	✓		C1, N, T1, L	S, BP, GA+SL+HH

[1] Solution Approach: S: CPLEX/Gurobi; GA: Genetic Algorithm; SL: Score-Based Labeling; HH: Hybrid Heuristic; BP: Branch and Price; BPC: Branch and Price and Cut; BD: Benders Decomposition; VNS: Variable Neighborhood Search; CG: Column Generation

[2] Demand Uncertainty includes stochastic programming, robust consideration, or chance constraint

[3] Delivery Limit: C1: Truck/Flight Capacity; C2: Hub Capacity; N: Passed Node Number; T1: Delivery Time Limit; T2: Delivery Time Windows(pickup/delivery); L: Route Length

Chapter 3

Optimizing Locations and Pricing for On-Demand Warehousing

In this chapter, we consider shared warehouse owners as the decision-makers and formulate a capacitated facility location problem (CFLP) to model the decision process. Given customer demand across nodes with price functions and time periods, we propose a mixed-integer nonlinear programming (MINLP) model. This model aims to maximize profit over a multi-period planning horizon while incorporating price-sensitive customer demand. To enhance computational efficiency, we exploit the problem structure and apply a Lagrangian relaxation (LR) framework, which disaggregates time periods to establish bounds on the optimal solution. Additionally, we refine feasible solutions through a combination of a Lagrangian Relaxation Heuristic (LRH) and a mixed local search method. To gain further insights, we conduct multiple analyses focusing on customer price sensitivity and demand satisfaction.

3.1 Mathematical Formulation

In this section, we develop a model to optimize warehouse locations and pricing strategies for on-demand warehousing. The goal is to determine the optimal facility locations and customer assignments that maximize the shared warehouse owner's profit over a given planning horizon. In this model, the warehouse owner serves small- and medium-sized businesses with predictable demand that fluctuates based on price sensitivity. To account for these dynamics, we formulate a CFLP that incorporates both storage capacity constraints and customer demand variations.

3.1.1 On-Demand Warehousing Formulation

First, we represent customer locations as a set of demand nodes, $I = \{0, 1, 2, ..., |I|\}$, and potential warehouse locations as a set, $J = \{0, 1, 2, ..., |J|\}$. The planning horizon is divided into discrete time periods, $T = \{1, 2, ..., |T|\}$, such as months, during which decisions can be made. Meanwhile, we define $T^0 = T \cup \{0\}$, where $t = 0$ marks the start point of the planning horizon. Similarly, we introduce J^0 as the set of existing shared warehouses that are already operational at $t = 0$, where $J^0 \subseteq J$.

The index sets required for the formulation are described as follows:

Index Set	**Description**
I	The set of demand nodes, representing the city location of customers.
J	The set of candidate locations for a shared warehouse.

Index Set	Description
T	A planning horizon that consists of a discrete set of periods during which the decisions can be made.

To simplify the calculations, we initially assume that the shared warehouse owner has full control over both fixed and operating costs associated with each warehouse location. Additionally, each warehouse's storage capacity remains constant throughout the planning horizon. Moreover, customer demand is considered deterministic, meaning it is predictable but may vary across different periods within the planning horizon. To account for price sensitivity, we incorporate the relationship between demand elasticity and price. Specifically, a customer's demand is fulfilled only if the unit price is acceptable to both the customer and the warehouse owner. To represent this relationship, we define the price function $P(Q_i)$ as the price of fulfilling the i^{th} customer's demand at a quantity Q_i. We adopt a linear pricing function in this study, which will be detailed in the following section. Based on these assumptions, the parameters required to formulate the problem are outlined below.

Parameters	Description
c_{ijt}	The unit cost of satisfying demand node $i \in I$ from the shared warehouse $j \in J$ at time $t \in T$.
f_{jt}	The fixed cost of locating a shared warehouse at location $j \in J$ in the beginning of period $t \in T$.

Patameters	Description
g_{jt}	The operating cost of the shared warehouse $j \in J$ during period $t \in T$.
q_{jt}	The capacity of the shared warehouse $j \in J$ during period $t \in T$.
d_{it}	The total demand of customer $i \in I$ during period $t \in T$.
a_i	The intercept of the price function for demand node $i \in I$.
b_i	The coefficient of the price function for demand node $i \in I$.

With the parameters established, we can proceed with defining the deicision variables. The aim is to determine the optimal warehouse locations and allocate customer demand efficiently across these facilities over the planning horizon. Based on this, we define the decision variables for the mathematical model as follows:

Decision Variables	Description
y_{jt}	1 if a shared warehouse is operating at candidate site $j \in J$ in the beginning of period $t \in T$; 0 otherwise.
z_{jt}	1 if a new shared warehouse is opened at candidate site $j \in J$ in period $t \in T$; 0 otherwise.
x_{ijt}	The amount of the demand of customer $i \in I$ supplied from the shared warehouse $j \in J$ in period $t \in T$.

The objective is to maximize total profit, which is calculated as the total revenue from satisfying customer demand minus the total costs. These costs include the expenses associated with fulfilling customer demand as well as the operational and fixed costs of the

warehouses. Accordingly, we define the objective function, incorporating a generic pricing function, along with the model constraints as follows:

$$\textbf{[MPCFLP]} \quad \max \quad \left[\sum_{t\in T}\sum_{j\in J}\sum_{i\in I}(P(Q_i))x_{ijt}\right] - \left[\sum_{t\in T}\sum_{j\in J}\sum_{i\in I}c_{ijt}x_{ijt} + \sum_{t\in T}\sum_{j\in J}g_{jt}y_{jt} + \sum_{t\in T}\sum_{j\in J}f_{jt}z_{jt}\right] \tag{3.1}$$

s.t.

$$\sum_{j\in J}x_{ijt} \leq d_{it} \qquad \forall i \in I, \forall t \in T \tag{3.2}$$

$$\sum_{i\in I}x_{ijt} \leq q_{jt}y_{jt} \qquad \forall j \in J, \forall t \in T \tag{3.3}$$

$$z_{jt} \geq y_{jt} - y_{j(t-1)} \qquad \forall j \in J, \forall t \in T \tag{3.4}$$

$$y_{j0} = 1 \qquad \forall j \in J^0 \tag{3.5}$$

$$x_{ijt} \geq 0 \qquad \forall i \in I, j \in J, \forall t \in T \tag{3.6}$$

$$y_{jt} \in \{0,1\} \qquad \forall j \in J, \forall t \in T^0 \tag{3.7}$$

$$z_{jt} \in \{0,1\} \qquad \forall j \in J, \forall t \in T \tag{3.8}$$

The first term in the objective function (3.1) represents the total revenue generated from satisfying customer demand, while the last three terms account for the total costs. Specifically, the first cost term represents the total cost of fulfilling customer demand from each warehouse, the second term captures the operational costs of the warehouses, and the final

cost term corresponds to the fixed costs of opening new shared warehouses. To simplify the calculations, we assume a linear pricing function for the i^{th} customer, expressed as $P(Q_i) = a_i - b_i Q_i$ [89], where $Q_i = \sum_{j' \in J} x_{ij't}$. Additionally, Constraint (3.2) ensures that customer demand is met without exceeding the known demand for each period. Constraint (3.3) enforces capacity limits for shared warehouses operating in a given period. Constraint (3.4) ensures that the fixed cost is incurred when opening a new warehouse, while Constraint (3.5) defines the set of shared warehouses already operating at the beginning of the planning horizon, T^0. Finally, Constraints (3.6) - (3.8) specify the domains of the decision variables.

The proposed model aims to maximize profit over a multi-period planning horizon while considering price-sensitive customer demand. However, the objective function's structure results in a MINLP model, leading to significantly increased solution time. To address this, we introduce an efficient solution approach in the next section.

3.2 Solution Approach

The previous section presents the [MPCFLP] model as a MINLP problem since the objective function contains the revenue item modeled as a nonlinear function. Thus, to find the optimal solution efficiently, we exploit the structure of the problem and propose a Lagrangian Relaxation (LR) to obtain bounds on the optimal objective and a Lagrangian Relaxation Heuristic (LRH) to derive a high quality feasible solution. Figure (3.1) represents the overall process of the proposed solution approach.

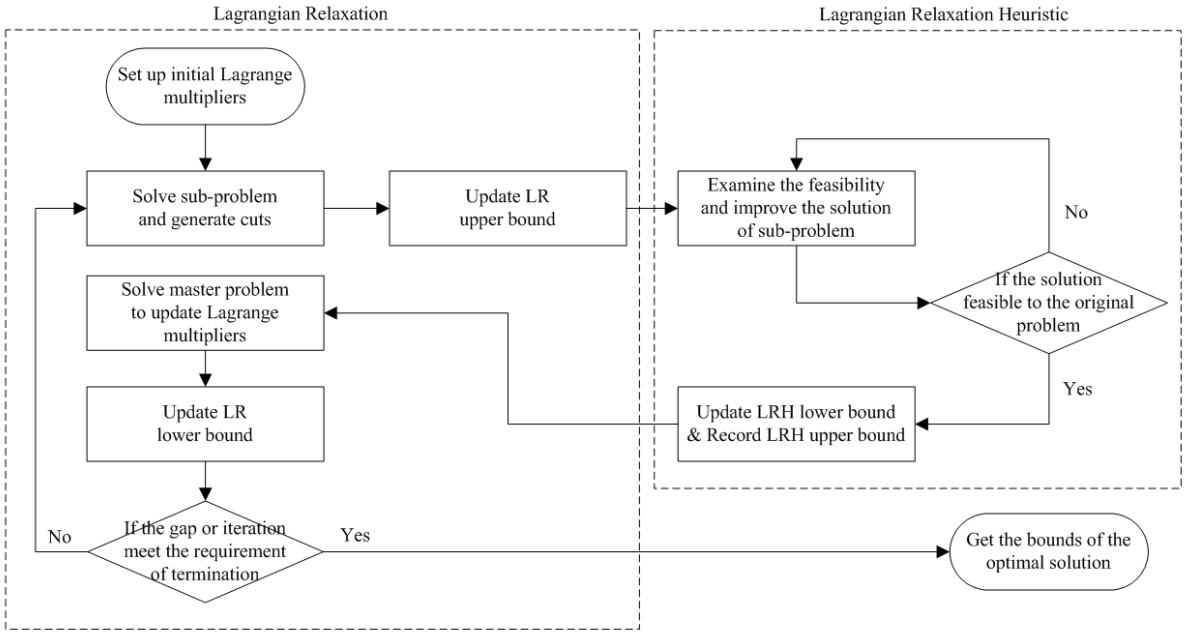

Figure 3.1: Overall process of solution approach.

First, we use the Lagrangian Relaxation method to obtain the LR bounds on the optimal solution. Second, based on the solution from the sub-problem, we examine the resulting solution to determine if it is feasible and improve the obtained solution and thus the

bound through a Lagrangian Relaxation Heuristic combined with a mixed local search method.

3.2.1 Lagrangian Relaxation (LR)

From Section (3.1), the constraints account for multiple periods in warehouse openings, warehouse capacity, and customer demand. Based on these considerations, there are three possible approaches to formulating LR.

- Option 1: Relax Constraint (3.4), new shared warehouse status
- Option 2: Relax Constraint (3.3), shared warehouses capacity
- Option 3: Relax Constraint (3.2), customer demand satisfaction

The model follows a multi-period planning horizon, with Constraint (3.4) being the only link between different periods. This structure allows for a more efficient decomposition of the problem. To take advantage of this, we relax the constraint and apply LR using Option 1, simplifying the overall problem formulation. By doing so, we break the original problem into independent subproblems, each corresponding to a single time period. To further refine the solution, we implement a cutting-plane algorithm, which iteratively strengthens the LR approach by generating additional constraints that guide the optimization process. The detailed formulation of the LR method is presented below.

3.2.1.1 Lagrangian Relaxation: Mathematical Process

First, we present the mathematical formulation of Lagrangian relaxation, which is shown in Figure (3.1). The first step is to define the variable $\lambda \geq 0$ to be the vector of Lagrange

multipliers associated with the new shared warehouse status constraint, i.e., Constraint (3.4), the Lagrangian problem ($Z_{LR}(\lambda)$) of the [MPCFLP] model can be then stated as follows:

$$\begin{aligned} Z_{LR}(\lambda) = \max \quad & \sum_{t\in T}\sum_{j\in J}\sum_{i\in I}(a_i - b_i(\sum_{j'\in J} x_{ij't}))x_{ijt} \\ & - \sum_{t\in T}\sum_{j\in J}\sum_{i\in I} c_{ijt}x_{ijt} - \sum_{t\in T}\sum_{j\in J} g_{jt}y_{jt} - \sum_{t\in T}\sum_{j\in J} f_{jt}z_{jt} \\ & + \sum_{t\in T}\sum_{j\in J}\lambda_{jt}(z_{jt} - y_{jt} + y_{j(t-1)}) \\ s.t. \quad & (3.2),\ (3.3),\ (3.5) - (3.8) \end{aligned} \tag{3.9}$$

Then, we can rearrange the terms in the formulation as given below:

$$\begin{aligned} Z_{LR}(\lambda) = \max \quad & \sum_{t\in T}\sum_{j\in J}\sum_{i\in I}(a_i - b_i(\sum_{j'\in J} x_{ij't}))x_{ijt} \\ & - \sum_{t\in T}\sum_{j\in J}\sum_{i\in I} c_{ijt}x_{ijt} - \sum_{t\in T}\sum_{j\in J}(g_{jt} + \lambda_{jt})y_{jt} \\ & + \sum_{t\in T}\sum_{j\in J}\lambda_{jt}y_{j(t-1)} - \sum_{t\in T}\sum_{j\in J}(f_{jt} - \lambda_{jt})z_{jt} \\ s.t. \quad & (3.2),\ (3.3),\ (3.5) - (3.8) \end{aligned} \tag{3.10}$$

The Lagrangian upper bound, $UB(\lambda)$, is the optimal solution of the sub-problem $Z_{sp}(\lambda)$. In other words, at each iteration, λ will change, and $Z_{sp}(\lambda)$ will approach the optimal solution of the objective function (3.1) from above. The best bound $\min_{\lambda\geq 0}\{Z_{sp}(\lambda)\}$ is the Lagrangian bound. The solution of $Z_{SP}(\lambda)$ is the vector V^h of variables $(x^h_{ijt}, y^h_{jt}, z^h_{jt})$. Suppose that H

is the set of all feasible solutions, then sub-problem $Z_{SP}(\lambda)$ can be written as:

$$\theta = \max_{h=1,2,...H} \quad \sum_{t\in T}\sum_{j\in J}\sum_{i\in I}(a_i - b_i(\sum_{j'\in J} x^h_{ij't}))x^h_{ijt} - \sum_{t\in T}\sum_{j\in J}\sum_{i\in I} c_{ijt}x^h_{ijt}$$
$$- \sum_{t\in T}\sum_{j\in J}(g_{jt}+\lambda_{jt})y^h_{jt} + \sum_{t\in T}\sum_{j\in J}\lambda_{jt}y^h_{j(t-1)} - \sum_{t\in T}\sum_{j\in J}(f_{jt}-\lambda_{jt})z^h_{jt} \quad (3.11)$$

$$s.t. \quad \sum_{j\in J} x^h_{ijt} \le d_{it} \qquad \forall i \in I, \forall t \in T \quad (3.12)$$

$$\sum_{i\in I} x^h_{ijt} \le q_{jt}y^h_{jt} \qquad \forall j \in J, \forall t \in T \quad (3.13)$$

$$y^h_{j0} = 1 \qquad \forall j \in J^0 \quad (3.14)$$

$$x^h_{ijt} \ge 0 \qquad \forall i \in I, j \in J, \forall t \in T \quad (3.15)$$

$$y^h_{jt} \in \{0,1\} \qquad \forall j \in J, \forall t \in T^0 \quad (3.16)$$

$$z^h_{jt} \in \{0,1\} \qquad \forall j \in J, \forall t \in T \quad (3.17)$$

The Lagrangian Dual Problem can be defined as:

$$\min_{\lambda\ge 0}\{Z_{sp}(\lambda)\} \equiv \min_{\lambda\ge 0}\{\theta\} \equiv \min_{\lambda,\theta}\theta \quad (3.18)$$

$$s.t. \quad \theta \ge \sum_{t\in T}\sum_{j\in J}\sum_{i\in I}(a_i - b_i(\sum_{j'\in J} x^h_{ij't}))x^h_{ijt} - \sum_{t\in T}\sum_{j\in J}\sum_{i\in I} c_{ijt}x^h_{ijt}$$
$$- \sum_{t\in T}\sum_{j\in J}(g_{jt}+\lambda_{jt})y^h_{jt} + \sum_{t\in T}\sum_{j\in J}\lambda_{jt}y^h_{j(t-1)}$$
$$- \sum_{t\in T}\sum_{j\in J}(f_{jt}-\lambda_{jt})z^h_{jt} \qquad \forall h \in H \quad (3.19)$$

$$\lambda_{jt} \ge 0 \qquad \forall j \in J, \forall t \in T \quad (3.20)$$

Since x^h_{ijt}, y^h_{jt}, z^h_{jt} are parameters in the problem, the master problem can be rearranged as below:

$$Z_{MP}(\lambda) = \min_{\lambda,\theta} \theta \tag{3.21}$$

$$\begin{aligned} s.t. \quad \theta - & \sum_{t\in T}\sum_{j\in J}(z^h_{jt} - y^h_{jt} + y^h_{j(t-1)})\lambda_{jt} \geq \\ & \sum_{t\in T}\sum_{j\in J}\sum_{i\in I}(a_i - b_i(\sum_{j'\in J} x^h_{ij't}))x^h_{ijt} - \sum_{t\in T}\sum_{j\in J}\sum_{i\in I} c_{ijt}x^h_{ijt} \\ & - \sum_{t\in T}\sum_{j\in J} g_{jt}y^h_{jt} - \sum_{t\in T}\sum_{j\in J} f_{jt}z^h_{jt} \qquad \forall h \in H \end{aligned} \tag{3.22}$$

$$\lambda_{jt} \geq 0 \qquad \forall j \in J, \forall t \in T \tag{3.23}$$

The objective function value of the master problem $Z_{MP}(\lambda)$ is the Lagrangian lower bound, and λ^* is the optimal solution of the master problem. After getting the new λ^* from the master problem, we resolve the sub-problem with the new value of λ. Thus, we iterate between the master problem and the subproblem until we obtain a small gap between the Lagrangian lower and upper bounds. If the gap between the Lagrangian upper bound and Lagrangian lower bound is less than 0.1%, we reach the iteration limit, or a computational time then we terminate the iterative approach and report the results.

3.2.1.2 Lagrangian Relaxation Improvement: Decomposed Model

Based on the model we presented in the previous section, we can further exploit the structure of the subproblem to reduce the computational time. From formulation (3.10), we can re-arrange the λ terms in the formulation as follows:

$$
\begin{aligned}
Z_{LR}(\lambda) = Z_{sp}(\lambda) = \max \quad & \sum_{t\in T}\sum_{j\in J}\sum_{i\in I}(a_i - b_i(\sum_{j'\in J} x_{ij't}))x_{ijt} \\
& - \sum_{t\in T}\sum_{j\in J}\sum_{i\in I} c_{ijt}x_{ijt} \\
& - \sum_{t\in T}\sum_{j\in J}(g_{jt} + \lambda_{jt} - \lambda_{j(t+1)})y_{jt} - \sum_{t\in T}\sum_{j\in J}(f_{jt} - \lambda_{jt})z_{jt} \quad (3.24) \\
s.t. \quad & (3.2),\ (3.3),\ (3.5) - \ (3.8)
\end{aligned}
$$

Since we relaxed the constraint related to time periods, the Lagrangian relaxation sub-problem can be decomposed for each time period separately. So, we can separate the Lagrangian sub-problem into $|T|$ independent sub-problems:

$$
\begin{aligned}
Z^t_{SP}(\lambda) = \max \quad & \sum_{j\in J}\sum_{i\in I}(a_i - b_i(\sum_{j'\in J} x_{ij't}))x_{ijt} - \sum_{j\in J}\sum_{i\in I} c_{ijt}x_{ijt} \\
& - \sum_{j\in J}(g_{jt} + \lambda_{jt} - \lambda_{j(t+1)})y_{jt} - \sum_{j\in J}(f_{jt} - \lambda_{jt})z_{jt} \quad (3.25) \\
s.t. \quad & \sum_{j\in J} x_{ijt} \le d_{it} \qquad \forall i \in I \quad (3.26) \\
& \sum_{i\in I} x_{ijt} \le q_{jt}y_{jt} \qquad \forall j \in J \quad (3.27) \\
& y_{j0} = 1 \qquad \forall j \in J^0 \quad (3.28) \\
& x_{ijt} \ge 0 \qquad \forall i \in I, \forall j \in J \quad (3.29) \\
& y_{jt} \in \{0,1\} \qquad \forall j \in J \quad (3.30) \\
& z_{jt} \in \{0,1\} \qquad \forall j \in J \quad (3.31)
\end{aligned}
$$

For any given value of $\lambda \geq 0$, a Lagrangian upper bound $UB(\lambda)$ is given by $UB(\lambda) = \sum_{t \in T} Z^t_{SP}(\lambda)$. The best bound $\min_{\lambda \geq 0} \{\sum_{t \in T} Z^t_{SP}(\lambda)\}$ is the Lagrangian bound. Then, we proceed to solve the Lagrangian Dual Problem from equation (3.11) to (3.23) to get the optimal solution of the master problem. Compared to the general LR, the disaggregate model can decompose the objective function and constraints to decrease the computational time significantly. In summary, we display the LR process in Figure (3.2).

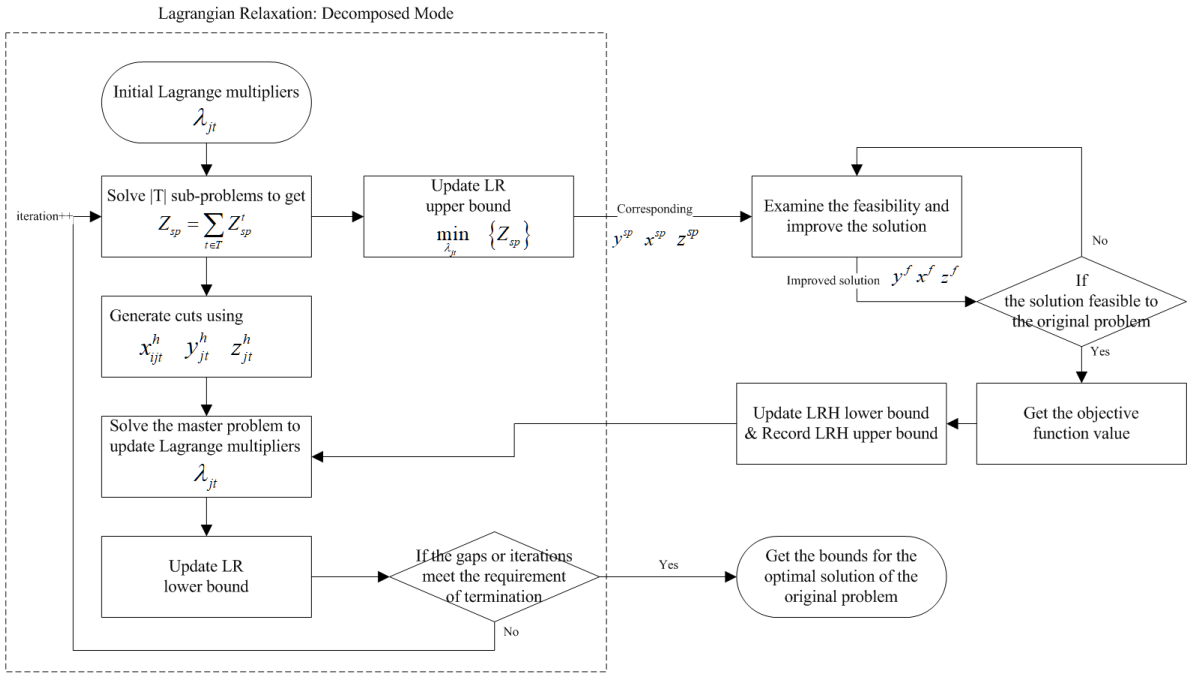

Figure 3.2: The Lagrangian Relaxation decomposed model.

3.2.2 Lagrangian Relaxation Heuristic Implementation

When we relax the constraint (3.4) and obtain the sub-problem solution, the resulting solution might be infeasible. Therefore, based on each sub-problem solution of LR, we

propose a Lagrangian Relaxation Heuristic that examines the solution and aims to make it feasible to obtain a lower bound on [MPCFLP] [29].

In the basic version of the LRH, we first record the solution of the sub-problem x^{sp}, y^{sp}, z^{sp} from LR process, and then examine the solution if it is feasible to the original problem (Equations (3.1) - (3.8)). If the solution is feasible to the original problem, the corresponding objective provides a lower bound. If the solution is not feasible, we modify the variables called x^f, y^f, z^f to a feasible solution based on the described procedure in Figure (3.3).

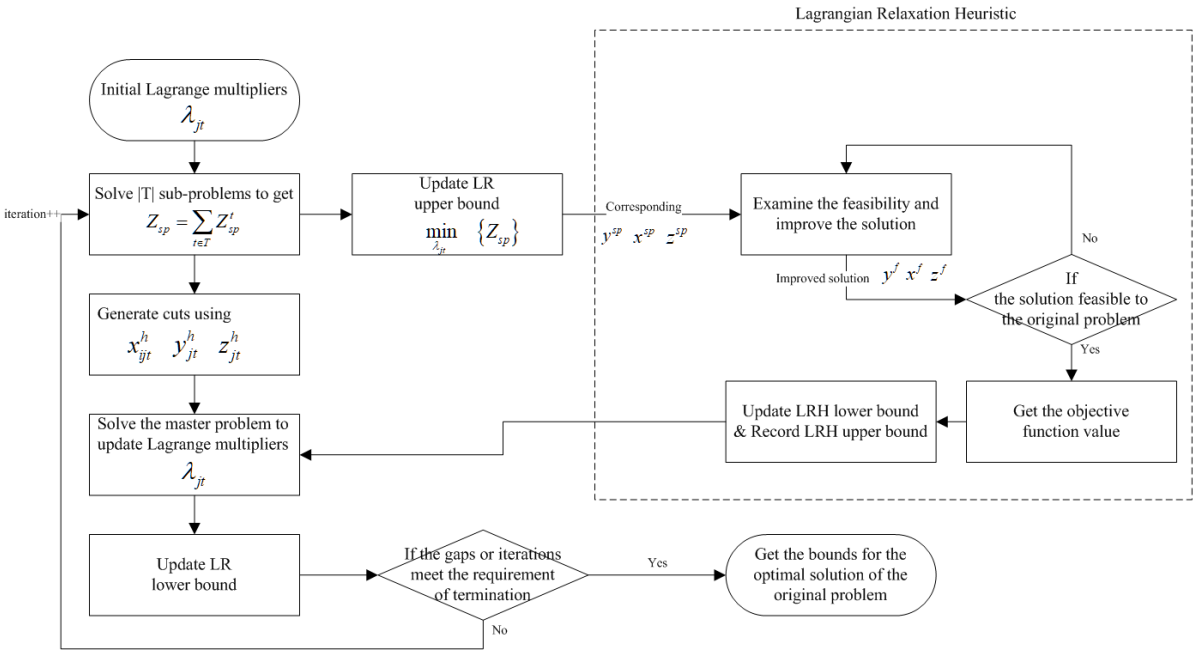

Figure 3.3: The processes of Lagrangian Relaxation Heuristic.

To make the sub-problem solution feasible, we consider all the possible combinations of the binary decision variables y^{sp}, z^{sp} that satisfy constraint (3.4), see Table (3.1). When

we relax the constraint (3.4), there are $2^3 = 8$ combinations based on variables y_{jt}, $y_{j(t-1)}$ and z_{jt}. Considering Scenario (a) - (d), when z_{jt} is 1, the constraint is always feasible though Scenarios (a), (b), and (d) are not optimal, meaning that z_{jt} actually can be set to zero to achieve a lower fixed cost. If we consider Scenarios (e) - (h), then Scenario (g) is the only event that causes the constraint (3.4) to be infeasible. Therefore, the procedure of basic LRH is to fix Scenario (g) to make it feasible. Once the solution is feasible and optimal for the constraint (3.4), we can calculate the objective function value and find a lower bound.

Table 3.1: All possible combinations for the relaxed constraint.

D.V.	z_{jt}	y_{jt}	$y_{j(t-1)}$	Constraint	Solution
Scenario (a)	1	1	1	feasible	not optimal
Scenario (b)	1	0	0	feasible	not optimal
Scenario (c)	1	1	0	feasible	optimal
Scenario (d)	1	0	1	feasible	not optimal
Scenario (e)	0	1	1	feasible	optimal
Scenario (f)	0	0	0	feasible	optimal
Scenario (g)	0	1	0	infeasible	—
Scenario (h)	0	0	1	feasible	optimal

The solution obtained from the LRH can be further improved using a local search. Next we describe the local search details. From the previous part, we find a feasible solution. However, the obtained lower bounds from the feasible solution are typically lower than the bounds from the master problem of the Lagrangian Relaxation. Therefore, to improve the quality of the feasible solution, we propose an algorithm that combined the Lagrangian Relaxation Heuristic with a local search method.

The local search algorithm is a heuristic method that swaps, adds/drops the variables y^{sp}

randomly, evaluates the quality of the objective based on these changes, and finally allocates the variables based on the procedures performed. From the previous related research, Campêlo and Bornstein (2001) [42] consider an ADD/DROP method, and Sun (2012) [34] consider a local search algorithm to solve the capacitated facility location problem directly. However, their methodology focuses on a single period only, and their algorithm included extensive randomness; therefore, this had a negative impact on the computational time. Our algorithm considers the multiple time-period factor and less randomness. Additionally, it includes a weight of opening a facility at each period, the fixed cost reduction, and the revenue from customers' demand. After adjusting the infeasible solution from the sub-problem of the LR iterations, the solution is feasible for the original objective function, and we can have an improved lower bound. In general, the overall process is shown in Algorithm (1) below.

The proposed algorithm includes three parts. The first part considers the weight of the facilities, which is computed based on the median and average of the time periods the facilities are open over the time horizon, as well as the demand being satisfied. From the weights, the facilities are divided to high or low priority. The procedure of calculating the weights and thus the priority of a given facility is shown in Algorithm (2). We first record the opening time periods of facilities and the percentage of demand satisfied over the time horizon, then calculate the priority index based on their median and average values. Finally, considering the number of LR iterations, we select the lowest 30% or 40% ($D3$ and $D4$, respectively) as the low-priority facilities.

Algorithm 1 The proposed algorithm for planning horizon constraint

$J \leftarrow j$, $T \leftarrow t$
Sort $\sum_{t \in T} y_{jt}$ from the highest to the lowest, then mark the priority of j
$j \in j^H$ (high priority), $j' \in j^L$ (low priority)
for $t = 1, 2, ...|T|$ **do**
    for $j = 1, 2, ...|J|$ **do**
        if $j \in j^H$ and $y_{j^H t} = 0$ with certain patterns **then**
            $y_{j^H t} \leftarrow 1$
            $y_{j^L t} \leftarrow 0$
        end if
        if $j \in j^L$ and $y_{j^L t} = 1$ with certain patterns **then**
            $y_{j^L t} \leftarrow 0$
            $y_{jt} \leftarrow 1$
        end if
    end for
end for
for $t = 1, 2, ...|T|$ **do**
    if $z_{jt} = 0$ **then**
        if $y_{jt} - y_{j(t-1)} = 1$ **then**
            $z_{jt} \leftarrow 1$
        end if
    end if
end for
Assign parameters: modified y_{jt}, z_{jt}
Solve the [MPCFLP] with y_{jt}, z_{jt} fixed
Obtain the modified x_{ijt}, and objective function value
Get the lower bound

Algorithm 2 The criteria determining the priority of the facilities

for $j = 1, 2, ...|J|$ **do**
    Record the opening number over the periods $(\sum_{t \in T} y_{jt})$
    Record the percentage of demand satisfied over the periods $(\sum_{t \in T} \sum_{i \in I} x_{ijt} / \sum_{t \in T} d_{it})$
end for
[List1]: Sort the facilities by descending order of the number of opened time periods
[List2]: Sort the facilities by descending order of the percentage of demand satisfied
Calculate the median and average of List 1 and 2
Initialize the priority of the facility j^p
for $j = 1, 2, ...|J|$ **do**
    if j's opening number $\geq$ median and average both **then**
        $j^p \leftarrow j^p + 2$
    else if j's opening number $\geq$ median or average **then**
        $j^p \leftarrow j^p + 1$
    end if
    if j's percentage $\geq$ median and average both **then**
        $j^p \leftarrow j^p + 2$
    else if j's percentage $\geq$ median or average **then**
        $j^p \leftarrow j^p + 1$
    end if
end for
[List3]: Sort the priority by descending order
for $j = 1, 2, ...|J|$ **do**
    if LR iteration ≤ 100 **then**
        if $j^p \leq D4$ **then**
            $j' \in j^L$
        else
            $j \in j^H$
        end if
    else
        if $j^p \leq D3$ **then**
            $j' \in j^L$
        else
            $j \in j^H$
        end if
    end if
end for

Then, the second part is to determine the "add" or "drop" procedure. We consider "adding" facilities at a given time period from the high-priority list if the solution meets a given pattern such as the one described in Figure (3.4). On the other hand, we consider "dropping" facilities at a given time period if they belong to low priority and their solution satisfies a given pattern (see Figure (3.4)). The pattern considers several factors, including the fixed cost reduction, capacity limitation, and the number of opening facility limitations based on the resulting solution of the subproblem of Lagrangian Relaxation. The difference between the number of adding and dropping facilities is no more than two for each period to avoid capacity shortage and revenue loss.

The third part is to modify the variables z_{jt} and x_{ijt}. Once we determine the variables y_{jt}, we reassign the variables of z_{jt}. Then, we put modified y_{jt}, z_{jt} as the parameters to the [MPCFLP] model to recalculate the variable of x_{ijt} and find the optimal solution. The objective value of the generated new solution is the new lower bound.

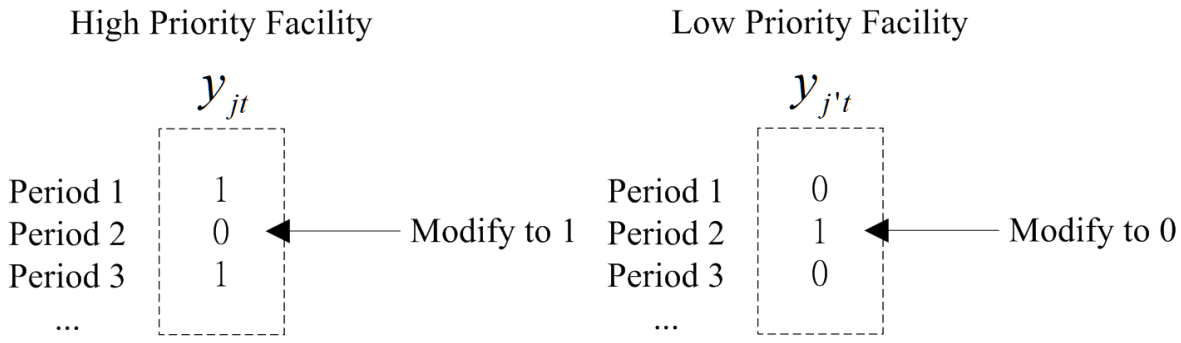

Figure 3.4: Sample pattern of add/drop procedure.

3.3 Computational Results

In this section, we present the computational results to examine the performance of the proposed approach and presenting insights, especially focusing on the impact of price elasticity. Also, we compare the quality of the obtained solution from CPLEX, basic LRH method, LRH with add/drop method, and the proposed approach: LRH with mixed local search method.

3.3.1 Parameter Setting

Referring to the work presented in Section (2.1), our testing instances for the multi-period facility location problem essentially have parameters related to the fixed costs of the facilities, the operating and unit costs to allocate demand between customers and facilities, and the capacity of the facilities. Also, we consider the demand and price function for each customer during each period. Each data set contains five instances generated using different random seeds.

The typical planning horizon is a year and we consider that it is divided into 12 time periods with each time period representing a month [1], i.e., $|T| = 12$. Additionally, we consider the different number of customer nodes and potential facility locations $[I, J]$ as $|I| \geq |J|$. The customers' demand points are randomly generated following a continuous uniform distribution, rounding the x and y coordinates to the next lowest integer value. In this case, we generate customers and potential warehouse locations in an area of 380 km^2.

To simplify the calculation, we assume that all the facilities' parameters stay the same over the planning horizon and do not have the option to extend or reduce their size. In this case, we set up the capacity, q_{jt}, for each facility to be 5,000 at each period. The customer's demand (d_{it}) is assumed to vary for each time period, and the demand trend follows a seasonal pattern. The customer has an average demand generated following a continuous uniform distribution $U(0, 3500)$ units, rounding to the nearest integer. Based on this average, the seasonality for each customer is created by multiplying a time series of random numbers with different peak values following a Poisson distribution with parameter λ in the range of [2, 6]. Regarding the costs, the unit cost, c_{ijt}, was computed based on the Euclidean distance between the nodes.

The unit costs are composed of two components that include the vehicle fuel surcharge cost and driver's payment. Also, since we follow the assumption that all the facilities are the same over the time periods, the fixed cost (f_{jt}) and operating cost (g_{jt}) have the same value of 5,000 at each period. Additionally, we consider the price function $P(Q_i)$ for the i^{th} customer as a linear function of quantity where $P(Q_i)$ is defined as $P(Q_i) = a_i - b_i Q_i$ [89]. The parameters of the price function [a_i, b_i] vary according to several considered scenarios, including high revenue [120, 0.05], average revenue [100, 0.05], and low revenue [80, 0.05] for different customers. For the sensitivity analysis, the parameters are adjusted randomly to examine the impact on the results.

Finally, the computational environment for running the experiments is Windows 10 64-bit with Intel Core i7-6700 CPU 3.4 GHz and 16.0 GB RAM. The software used is Python version 3.7.4, CPLEX version 12.9.0.0 with library "docplex" version 2.20.204. The termination criteria of CPLEX solver wither a relative gap of one percent or a time limit of two

hours. The iteration limit of the LR is 500 iterations for small sizes and 250 iterations for other sizes, and the time limit is also two hours.

3.3.2 Computational Performance Analysis

In this subsection, we compare the performance among the different approaches, including the CPLEX solver, basic LRH, LRH with the add/drop method, and our proposed heuristic: LRH with mixed local search.

First, we solve the [MPCFLP] model through the CPLEX solver. The CPLEX solver uses the primary branch-and-bound method to obtain the optimal solution. The basic LRH from Section (3.2.2) adjusts the infeasible solution from the subproblem of LR directly to obtain a feasible solution. In this case, we repeat $|J|/5$ times with different random seeds for each LR iteration and record the highest value as a lower bound at each iteration. These approaches are compared against the proposed heuristic presented in Section (3.2.2).

The evaluation considers two indices: computational time and gap. Given the initial parameter setting from Section (3.3.1), we test the algorithms with 3 different instances for each sample size and provide a summary, which is shown below:

From Table (3.2), the gap is calculated by comparing to the optimal solution from CPLEX solver and the best feasible solution across the LRH iterations, which is $\frac{(LRH-cplex)}{cplex} * 100\%$. We notice that the computational time and gap increase significantly when the revenue is low for the shared warehouse company; the CPLEX solver usually reaches the time limit with the gap between 1.2 to 3.8% even when the instance size is small. Compared to the other approaches, the basic LRH is the best in terms of computational performance,

Table 3.2: Comparison of the different algorithms.

Size (I, J)	Price Function	Iterations	CPLEX Solver		Basic LRH		LRH w. add/drop		LRH w. mixed LS	
			Time (sec)	MIP Gap (%)	Time (sec)	Gap (%)	Time (sec)	Gap (%)	Time (sec)	Gap (%)
(15, 15)	Low	500	7,200	4.34	800.2	-0.72	837.5	-0.69	2,029.4	0.01
(15, 15)	Average	500	7,200	2.27	637.5	-1.06	654.6	-0.46	1,868.1	0.19
(15, 15)	High	500	7,200	1.32	517.9	-0.82	620.1	-0.53	1,749.7	0.04
(30, 15)	Low	500	7,200	2.44	970.8	-1.17	1,392.1	-0.76	2,497.1	-0.29
(30, 15)	Average	500	4954.4	1.22	747.1	-0.68	1,196.8	-0.67	2,274.5	-0.22
(30, 15)	High	500	77.6	1.00	528.8	-0.45	736.1	-0.16	2,055.8	-0.35
(30, 30)	Low	250	7,200	4.36	7,065.2	-0.59	7,149.8	-0.43	7,200	-0.40
(30, 30)	Average	250	7,200	2.55	1564.1	-1.05	2490.9	-0.56	3,480.2	0.09
(30, 30)	High	250	7,200	1.41	457.5	-0.90	2426.6	-0.60	2,374.0	-0.40
(60, 30)	Low	250	7,200	2.69	2968.9	-0.45	4781.6	-0.34	5,284.4	0.21
(60, 30)	Average	250	7,200	1.31	793.2	-0.62	3264.2	-0.34	3,109.5	-0.02
(60, 30)	High	250	160.6	1.00	427.7	-0.28	2110.5	-0.65	2,843.6	-0.05

[1]The iteration limit of the LR is 500/250 iterations based on sample size
[2]The time limit is 7200 seconds and CPLEX MIP gap setting is 1.00%.

but the gap is worse than the CPLEX solver and the other two heuristics. This implies that the decomposed model solves the LR efficiently; however, it causes the solution to be farther away from the optimal one. Furthermore, the add/drop method has a better lower bound than the basic LRH, and the computational time increases since we iterate to search for more opportunities to get better bounds. It implies that the randomness factor of the add/drop method cannot handle the connection between the different periods in the multi-period planning framework, which causes the lower bound not to be further improved.

Finally, generally speaking, the proposed algorithm has a better performance than the CPLEX solver mainly for computational time. In some instances, the gap is close or even better than the CPLEX solver, especially on small-size instances. Figure (3.5) demonstrates a small-size sample [15,15] where the gap is better than the CPLEX solver. It implies that the proposed algorithm can approach the lower bound more effectively than

the other algorithms, but computational time is the trade-off for better bounds.

In summary, the proposed algorithm provides a better option to implement than LRH to obtain higher quality feasible solutions within reasonable computational time.

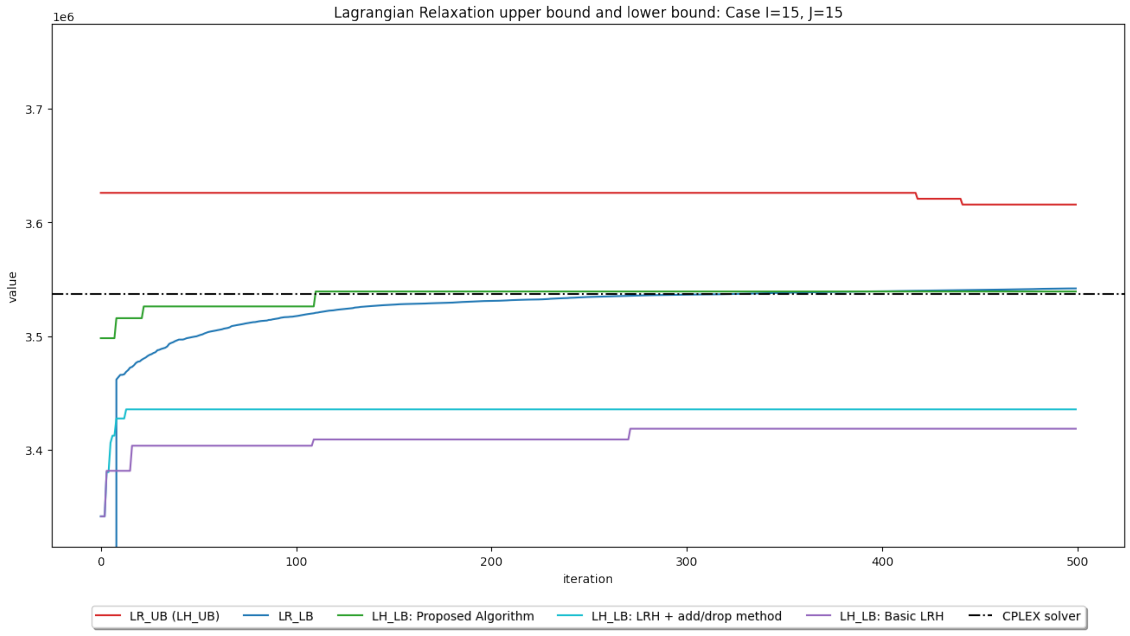

Figure 3.5: Demonstration of LRH bounds by iterations.

3.3.3 Sensitivity Analysis: Pricing and Demand Satisfaction

In this subsection, we present sensitivity analyses considering the relationship between the price elasticity and demand satisfaction.

The planning time horizon was $|T| = 12$ and the combination of customer nodes I and potential facility location J is [60, 30]. The parameters including the unit cost (c_{ijt}), fixed cost (f_{jt}), operating cost (g_{jt}), and customer demand (d_{it}) are similar as before. The inter-

cept (a_i) and coefficient (b_i) of the price function for demand nodes are generated randomly by following the uniform distribution with $a_i \sim U(400, 600)$ and $b_i \sim U(0.05, 0.25)$.

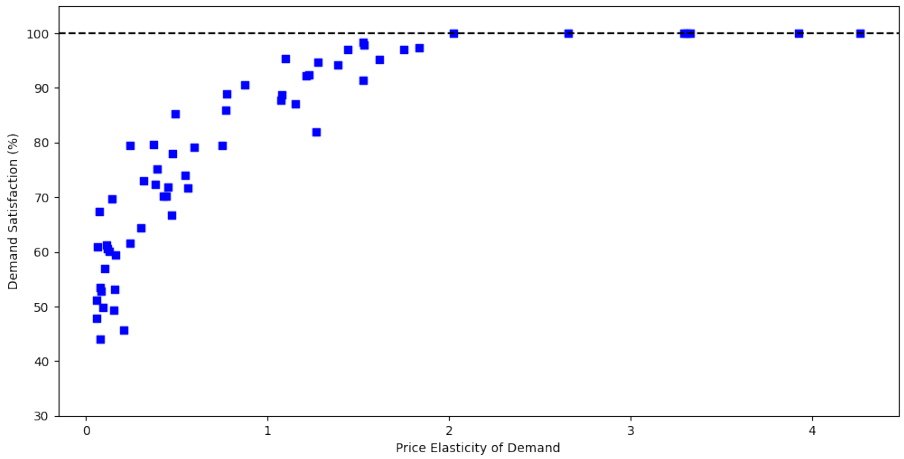

Figure 3.6: Scatter plot of the elasticity versus the % of demand satisfied.

Figure (3.6) presents the scatter plot of the elasticity versus the % of the demand satisfied. The scatter plot shows a relationship between the elasticity and the demand satisfied. It implies that when the price elasticity is relatively high, the demand can be satisfied entirely since the customers can accept the alternative matched price. It also shows that the amount of demand can be completely satisfied once the elasticity is high enough. In this case, when the elasticity is higher than two, the customer demand can be fully satisfied.

Additionally we examine the relationship with different capacities and different fixed costs. In one case, we decrease the capacity of each shared warehouse from 5,000 to 1,500 to simulate the scenario if the warehouses' capacities are low or high in the market. In another scenario, we increase the fixed cost from 5,000 to 5,000,000 to see the effect of the fixed cost. The results are shown in Figure (3.7).

Figure (3.7) shows that the facilities still satisfy the customer's demand with a higher elasticity of price, which is similar to the previous analysis. Given the limited capacity of the shared warehouse, the reduction of the demand for customers with lower elasticity is more significant. Similarly, for the fixed cost the reduction in demand satisfied is greater for customers with lower elasticity compared to one with higher values.

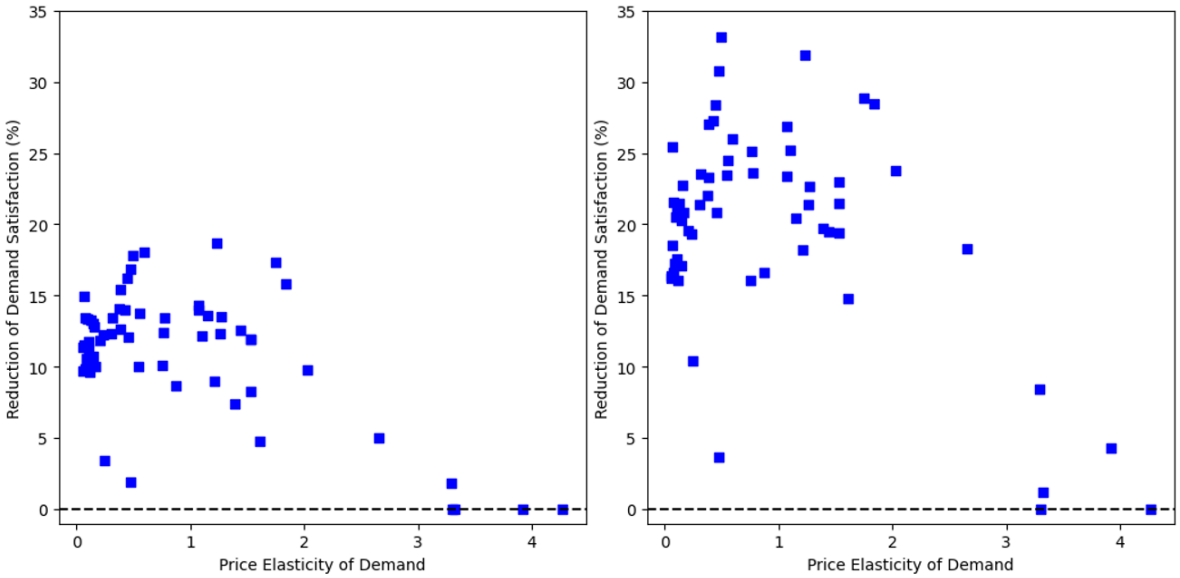

Figure 3.7: Scatter plot of price elasticity versus reduction in demand satisfied given high fixed cost (left) and limited capacity (right).

In summary, the presented sensitivity analyses proposes a significant relationship between the elasticity of the customer and demand satisfaction.

3.4 Chapter Summary

This research considers shared warehouse owners as the decision-maker and formulate a CFLP to model the underlying decision problem. The proposed MINLP aims to maximize the profit, considering a multi-period planning horizon and price-sensitive demand from the targeted customers. We exploit the structure of the problem and disaggregate the time periods using an LR framework to obtain bounds on the optimal solution. Moreover, we extract and improve the feasible solution through a combination of an LRH and a mixed local search method.

The presented research shows two analyses. First, considering the proposed model, the LR approach yields tighter bounds than CPLEX, and the mixed local search method combined with LRH produces high-quality feasible solutions, resulting in a relatively small gap from the optimal objective value of the original problem. Beyond numerical performance, this study introduces an adaptive optimization framework that effectively accommodates dynamic storage demand and evolving pricing conditions, both of which are common in on-demand warehousing environments.

Under price-sensitive demand, the proposed model provides valuable insights into the trade-offs between revenue and cost by analyzing the effects of price elasticity on customer satisfaction and demand fulfillment. Sensitivity analysis demonstrates that when the price function $P(Q_i)$ is linear, higher price elasticity encourages facilities to offer services more actively, resulting in greater demand satisfaction over the planning horizon. The model also underscores the value of demand segmentation, as differentiated pricing strategies

across time periods can better align with customer willingness to pay. Additionally, the timing of facility openings and dynamic capacity allocation are shown to be critical to profitability, particularly in highly elastic markets. From a managerial perspective, the model provides strategic decision-making by offering actionable guidance on pricing adjustments and resource allocation in response to market fluctuations.

In conclusion, this chapter presented a profit-maximizing CFLP formulation for on-demand warehousing that incorporates multi-period planning and price-sensitive customer demand. The integration of Lagrangian relaxation and a mixed local search heuristic significantly improved solution quality and computational efficiency, offering near-optimal solutions with small optimality gaps. This chapter establishes a framework that supports strategic pricing and resource allocation, which provides valuable insights into the effects of price elasticity, demand segmentation, and capacity timing on profitability.

Chapter 4

Optimizing Hub Locations and Flight Assignments

In this chapter, we present the problem of designing pilotless air express cargo networks. Our framework aims to optimize profitability by considering critical factors such as demand volumes between origin-destination (O-D) pairs, adherence to delivery deadlines, associated revenue, and the operational costs of both airplanes and hubs, while factoring in the constraints of limited airplane capacity. Given this, the model determines the most profitable network configuration by optimizing hub locations, flight assignments, and shipment routing. To achieve these objectives, we present the Hub Location Problem with Profit Maximization (HLPP), and introduce two formulations: Arc-based (HLPP-A) and Path-based (HLPP-P). Solving these formulations is computationally challenging, and thus we present a Genetic Algorithm (GA) as a solution approach. These formulations allow us to evaluate various network dynamics and operational limitations.

4.1 Mathematical Formulation

In this session, we introduce two formulations—Path-based and Arc-based models—to address the problem of maximizing profitability by determining the optimal locations of hubs and the optimal quantities of commodities to be transported along suitable paths.

4.1.1 Path-based Formulation (HLPP-P)

Let (N, A) represent a directed graph, where N is the set of nodes and A is the set of arcs (i, j) from node $i \in N$ to node $j \in N$. Customer demand is modeled as a set of commodities K, where $o(k) \in N$ and $d(k) \in N$ denote the origin and destination of commodity $k \in K$. For simplicity, we assume that airplanes can transport these commodities under all conditions, without additional operational constraints (e.g., product dimension). We further define P_k as the set of directed feasible paths for commodity $k \in K$, where "feasible" refers to paths meeting delivery time requirements, typically within half a day or a full day. The index sets required for the formulation are described as follows:

Index Set	**Description**
N	The set of nodes, representing the city location of customers.
A	The set of arcs, where (i, j) represents the arc from node $i \in N$ to node $j \in N$.
K	The set of commodities, where $o(k) \in N$ represents the origin and $d(k) \in N$ represents the destination of commodity $k \in K$.

Index Set	Description
P_k	The set of all directed feasible paths from origin $o(k) \in N$ to destination $d(k) \in N$ for commodity $k \in K$, where $\mathcal{P}^k = \bigcup_{k \in K} P_k$.

Moreover, we assume that the amount of each commodity $k \in K$ is deterministic, and the unit revenue is dependent on the value of commodity $k \in K$. Additionally, we assume an unlimited number of airplanes are available. However, the fixed costs (e.g., maintenance, overhaul, airport charges, load insurance, IT services, general and administrative expenses) and operational costs (e.g., software/hardware engineers, fuel surcharge, flight equipment replacement, navigation) for each flight depend on both the airplane model and the selected path. Finally, we assume a fixed cost for operating a hub, along with a handling time for loading, unloading, and sorting at the hub. The rest of the parameters are as follows:

Parameters	Description
w_k	Amount of commodity $k \in K$ to be shipped from origin $o(k) \in N$ to destination $d(k) \in N$.
r_k	Unit revenue of satisfying commodity $k \in K$.
f_i	Fixed cost of operating a hub at $i \in N$.
$c_{(i,j)}$	Overall cost of a flight on arc $(i, j) \in A$.
t_k^p	Time spent on path $p \in \mathcal{P}^k$ including traveling and material handling time.
$\Gamma_{(i,j)}$	Remaining capacity of an airplane on arc $(i, j) \in A$.

Parameters	Description
β_k	Delivery time limit for commodity $k \in K$ (e.g., 12 or 24 hours).

The objective is to maximize profitability by determining the optimal hub locations and the most suitable quantities of commodities to be transported along their respective paths by the flights. Accordingly, we define the indicators as follows:

Indicators	Description
$\delta^p_{(i,j)}$	1, if arc $(i,j) \in A$ is contained in the path $p \in \mathcal{P}^k$; 0, otherwise.
ϕ^p_i	1, if the hub $i \in N$ is contained on the path $p \in \mathcal{P}^k$; 0, otherwise.

The indicator $\delta^p_{(i,j)}$ establishes the relationship between the paths and arcs, while ϕ^p_i ensures the connection between the paths and the locations of potential hubs. Additionally, we define the decision variables for the mathematical model below:

Decision Variables	Description
x^p_k	1, if commodity $k \in K$ is shipped on path $p \in P_k$, where $t^p_k \leq \beta_k$; 0, otherwise.
y_i	1, if a hub is operated at node $i \in N$; 0, otherwise.
$z_{(i,j)}$	Number of the flights to be operated on arc $(i,j) \in A$.

The decision variable x^p_k represents the path selected for commodity $k \in K$, focusing on entire paths rather than individual arcs (i,j). Additionally, the decision variables y_i and $z_{(i,j)}$ indicate the status of the hubs and the number of flights on arc (i,j), respectively.

The objective of the problem is to maximize total profit, which is calculated by subtracting the total costs from the total revenue. Total revenue is generated by satisfying customer demand, while total costs include the expenses of assigning flights on arcs (i, j) and the fixed costs associated with operating the hubs. Thus, the HLPP-P model is formulated with the following objective function and constraints:

$$\textbf{[HLPP-P]} \quad \max \quad \sum_{k \in K} \sum_{p \in P_k} r_k w_k x_k^p - \sum_{(i,j) \in A} c_{(i,j)} z_{(i,j)} - \sum_{i \in N} f_i y_i \tag{4.1}$$

s.t.

$$\sum_{p \in P_k} x_k^p \leq 1 \qquad k \in K \tag{4.2}$$

$$\phi_i^p x_k^p \leq y_i \qquad i \in N, k \in K, p \in P_k \tag{4.3}$$

$$\sum_{k \in K} \sum_{p \in P_k} w_k \delta_{(i,j)}^p x_k^p \leq \Gamma_{(i,j)} z_{(i,j)} \qquad (i,j) \in A \tag{4.4}$$

$$y_i \in \{0, 1\} \qquad i \in N \tag{4.5}$$

$$x_k^p \in \{0, 1\} \qquad k \in K, p \in P_k \tag{4.6}$$

$$z_{(i,j)} \in \mathbb{Z}_0^+ \qquad (i,j) \in A \tag{4.7}$$

Constraint (4.2) ensures the commodity $k \in K$ can be satisfied through the selected path(s) $p \in P_k$. Constraint (4.3) makes sure the hub $i \in N$ is operational when the selected path $p \in P_k$ passes through its location. Constraint (4.4) limits the capacity of the commodities transported by the airplanes on arc $(i, j) \in A$. The remaining constraints (4.5) - (4.7)

denote the domains of the decision variables.

The path-based formulation offers several advantages, including a reduction in problem size when the number of feasible paths is limited, as it focuses on pre-defined paths rather than individual arcs. This approach simplifies modeling and proves particularly effective in scenarios where demand between O-D pairs can be captured through a manageable set of paths—such as in our case of designing a shipment network for pilotless airplane operations. However, if the number of potential paths is large, the formulation requires the enumeration or generation of paths beforehand, leading to a significant increase in the number of decision variables. This exponential growth in variables can substantially increase computational time and complexity, posing challenges in solving the problem efficiently.

Next, we introduce an alternative approach: the arc-based formulation.

4.1.2 Arc-based Formulation (HLPP-A)

To formulate HLPP-A, we introduce the following new parameters.

Parameters	**Description**
$t_{(i,j)k}$	Overall time spent of a flight on arc $(i,j) \in A$ for commodity $k \in K$.
a_k	The maximum allowed number of arcs traversed by commodity $k \in K$.

We also introduce the following decision variables.

Decision Variables	Description
$x_{(i,j)k}$	1, if commodity $k \in K$ is routed on arc $(i,j) \in A$; 0, otherwise.
u_k	1, if commodity $k \in K$ is satisfied through a direct connection; 0, otherwise.
v_k	1, if commodity $k \in K$ is satisfied through the hub network; 0, otherwise.

The decision variable $x_{(i,j)k}$ represents if arc (i,j) is selected for transporting commodity $k \in K$ with the hub network. The variables u_k and v_k indicate if commodity $k \in K$ is satisfied through a direct connection or the hub network, respectively. Finally, the decision variables y_i and $z_{(i,j)}$ are identical to those in the HLPP-P formulation. These variables represent the operational status of hubs and the number of flights assigned to arc (i,j), respectively.

The objective of the arc-based formulation is identical to that of the HLPP-P, aiming to maximize total profit by subtracting total costs from total revenue. However, the total revenue in this formulation explicitly accounts for the delivery method, whether through direct shipment or the hub network. Accordingly, the arc-based formulation is structured to include the objective function and associated model constraints, as detailed below:

$$\textbf{[HLPP-A]} \quad \max \quad \sum_{k \in K} r_k w_k (u_k + v_k) - \sum_{(i,j) \in A} c_{(i,j)} z_{(i,j)} - \sum_{i \in N} f_i y_i \tag{4.8}$$

s.t.

$$u_k + v_k \leq 1 \qquad k \in K \qquad (4.9)$$

$$\sum_{j:(i,j)\in A} x_{(i,j)k} - \sum_{j:(j,i)\in A} x_{(j,i)k} = \begin{cases} v_k, \text{if } i = o(k) \\ -v_k, \text{if } i = d(k) \\ 0, \text{ otherwise} \end{cases} \qquad i \in N, k \in K \qquad (4.10)$$

$$\sum_{k\in K: i=o(k), j=d(k)} w_k u_k + \sum_{k\in K} w_k x_{(i,j)k} \leq \Gamma_{(i,j)} z_{(i,j)} \qquad (i,j) \in A \qquad (4.11)$$

$$x_{(i,j)k} \leq y_j \qquad (i,j) \in A, k \in K : j \neq d(k) \qquad (4.12)$$

$$x_{(i,j)k} \leq y_i \qquad (i,j) \in A, k \in K : i \neq o(k) \qquad (4.13)$$

$$x_{(i,j)k} \leq 0 \qquad (i,j) \in A, k \in K : i = o(k), j = d(k) \qquad (4.14)$$

$$t_{(i,j)k} u_k \leq \beta_k \qquad k \in K \qquad (4.15)$$

$$\sum_{(i,j)\in A} t_{(i,j)k} x_{(i,j)k} \leq \beta_k \qquad k \in K \qquad (4.16)$$

$$\sum_{(i,j)\in A} x_{(i,j)k} \leq a_k \qquad k \in K \qquad (4.17)$$

$$u_k, v_k \in \{0,1\} \qquad k \in K \qquad (4.18)$$

$$x_{(i,j)k} \in \{0,1\} \qquad (i,j) \in A, k \in K \qquad (4.19)$$

(4.5), (4.7)

Constraint (4.9) determines whether commodity $k \in K$ is routed through hub(s) or shipped directly. Constraint (4.10) ensures flow balance for each commodity $k \in K$. Additionally, Constraint (4.11) enforces the capacity limit on arc $(i,j) \in A$. Constraint (4.12) - (4.14)

activate the opening of hubs when the commodities pass through them. Constraint (4.15) and (4.16) apply delivery time limits for commodity $k \in K$, whether via direct shipment or through hubs. Furthermore, Constraint (4.17) is an optional constraint that limits the maximum number of arcs traversed by commodity $k \in K$, thereby reducing potential shipping risks and ensuring the delivery time limit from another perspective. Lastly, Constraint (4.5), (4.7), (4.18), (4.19) define the domains of the decision variables.

4.2 Solution Approach

The previous section introduces the HLPP model (i.e., HLPP-P, HLPP-A) to address the optimization problem of strategically maximizing profit within air express cargo networks. However, solving the model is challenging, as the decision variables—such as potential routes, hub locations, and customer demand—increase exponentially with the consideration of additional nodes. To address this problem, we introduce a Branch-and-Price (B&P) as an exact solution approach and then present a Genetic Algorithm (GA) to obtain a high-quality feasible solution efficiently.

4.2.1 Branch-and-Price (B&P)

B&P is an optimization technique that combines column generation with branch-and-bound to efficiently solve large-scale integer programming problems. When HLPP-P is set as the Master Problem [MP], column generation iteratively adds promising paths, while branch-and-bound ensures integer solutions by systematically exploring feasible path assignments. The Restricted Master Problem [RMP] is then formulated on a subset $\bar{P}_k \subset P_k$, where P_k represents the full set of feasible paths for commodity $k \in K$.

Since $\bar{P}_k$ must be initialized, we construct the first subset by randomly selecting one or more paths for each commodity $k \in K$ to ensure feasibility. The [RMP] model is formulated as follows:

$$\textbf{[RMP]} \quad \max \quad \sum_{k \in K} \sum_{p \in \bar{P}_k} r_k w_k x_k^p - \sum_{(i,j) \in A} c_{(i,j)} z_{(i,j)} - \sum_{i \in N} f_i y_i \tag{4.20}$$

s.t.

$$\sum_{p \in \bar{P}_k} x_k^p \leq 1 \qquad k \in K \tag{4.21}$$

$$\phi_i^p x_k^p \leq y_i \qquad i \in N, k \in K, p \in \bar{P}_k \tag{4.22}$$

$$\sum_{k \in K} \sum_{p \in \bar{P}_k} w_k \delta_{ij}^p x_k^p \leq \Gamma_{(i,j)} z_{(i,j)} \qquad (i,j) \in A \tag{4.23}$$

$$y_i \in \{0,1\} \qquad i \in N \tag{4.24}$$

$$x_k^p \in \{0,1\} \qquad k \in K, p \in \bar{P}_k \tag{4.25}$$

$$z_{(i,j)} \in \mathbb{Z}_0^+ \qquad (i,j) \in A \tag{4.26}$$

We then relax the decision variables in the [RMP], transforming it into a linear programming relaxation [RMP-relaxed] as follows:

$$\textbf{[RMP-relaxed]} \quad \max \quad \sum_{k \in K} \sum_{p \in \bar{P}_k} r_k w_k x_k^p - \sum_{(i,j) \in A} c_{(i,j)} z_{(i,j)} - \sum_{i \in N} f_i y_i \tag{4.27}$$

s.t.

$$\sum_{p \in \bar{P}_k} x_k^p \leq 1 \qquad k \in K \tag{4.28}$$

$$\phi_i^p x_k^p \leq y_i \qquad i \in N, k \in K, p \in \bar{P}_k \tag{4.29}$$

$$\sum_{k \in K} \sum_{p \in \bar{P}_k} w_k \delta_{ij}^p x_k^p \leq \Gamma_{(i,j)} z_{(i,j)} \qquad (i,j) \in A \tag{4.30}$$

$$0 \leq y_i \leq 1 \qquad i \in N \tag{4.31}$$

$$0 \leq x_k^p \leq 1 \qquad k \in K, p \in \bar{P}_k \tag{4.32}$$

$$z_{(i,j)} \geq 0 \qquad (i,j) \in A \tag{4.33}$$

By evaluating the reduced costs of columns in the [RMP-relaxed], we can determine whether the current set of paths is optimal or if additional columns need to be introduced. If all remaining columns have non-positive reduced costs, this indicates that the current solution is optimal, and no further columns are required. However, if some columns have positive reduced costs, this suggests that adding new columns (paths) could improve the objective value. In the context of HLPP-P, positive reduced costs indicate the existence of alternative paths that could contribute to a higher maximal profit. By incorporating these new columns, the model iterates towards the optimal outcome.

The dual variables can also be obtained by solving the dual of [RMP-relaxed] which is formulated next.

Decision Variables	Description
θ_k	The dual variable associated with Constraint (4.28)
λ_{ik}^p	The dual variable linked to Constraint (4.29).
$\mu_{(i,j)}$	The dual variable referred to Constraint (4.30).

$$\textbf{[Dual of RMP-relaxed]} \quad \min \quad \sum_{k \in K} \theta_k \tag{4.34}$$

s.t.

$$\theta_k + \sum_{i \in N} \phi_i^p \lambda_{ik}^p + \sum_{(i,j) \in A} w_k \delta_{(i,j)}^p \mu_{(i,j)} \geq r_k w_k \qquad k \in K, p \in \bar{P}_k, \tag{4.35}$$

$$\sum_{k \in K} \sum_{p \in \bar{P}_k} \lambda_{ik}^p \leq f_i \qquad i \in N \tag{4.36}$$

$$\Gamma_{(i,j)} \mu_{(i,j)} \leq c_{(i,j)} \qquad (i,j) \in A \tag{4.37}$$

$$\theta_k \geq 0 \qquad k \in K \tag{4.38}$$

$$\lambda_{ik}^p \geq 0 \qquad i \in N, k \in K, p \in \bar{P}_k \tag{4.39}$$

$$\mu_{(i,j)} \geq 0 \qquad (i,j) \in A \tag{4.40}$$

Accordingly, based on (4.35), the reduced cost c_p for each path $p \in P_k$, $k \in K$ is defined as follows:

$$c_p = r_k w_k - \sum_{i \in N} \phi_i^p \lambda_{ik}^p - \sum_{(i,j) \in A} w_k \delta_{(i,j)}^p \mu_{(i,j)} \tag{4.41}$$

The new paths are generated by solving the Sub-problem [PSP]

$$[PSP_k] \quad \max \quad r_k w_k - \sum_{i \in N} \sum_{p \in \bar{P}_k} \phi_i^p \lambda_{ik}^p y_i - \sum_{(i,j) \in A} w_k \mu_{(i,j)} x_{(i,j)k} - \sum_{(i,j) \in A} \varepsilon x_{(i,j)k} - \sum_{i \in N} \varepsilon y_i \tag{4.42}$$

s.t.

$$\sum_{j:(i,j) \in A} x_{(i,j)k} - \sum_{j:(j,i) \in A} x_{(j,i)k} = \begin{cases} 1, \text{if } i = o(k) \\ -1, \text{if } i = d(k) \\ 0, \text{ otherwise} \end{cases} \qquad i \in N \tag{4.43}$$

$$x_{(i,j)k} \leq y_j \qquad (i,j) \in A, k \in K : j \neq d(k) \tag{4.44}$$

$$x_{(i,j)k} \leq y_i \qquad (i,j) \in A, k \in K : i \neq o(k) \tag{4.45}$$

$$x_{(i,j)k} \leq 0 \qquad (i,j) \in A, k \in K : i = o(k), j = d(k) \tag{4.46}$$

$$x_{(i,j)k} \in \{0,1\} \qquad (i,j) \in A \tag{4.47}$$

$$y_i \in \{0,1\} \qquad i \in N \tag{4.48}$$

The [PSP] is decomposed for each commodity $k \in K$ as $[PSP_k]$. The objective function (4.42) includes an extremely small value, ε, to encourage the selection of paths with the minimal number of $x_{(i,j)k}$ and y_i. By solving $[PSP_k]$, we obtain a feasible path (column) and evaluate its corresponding reduced cost. If the reduced cost for any commodity k is positive, the newly generated path is added to [RMP], and the optimization process is repeated. This iterative procedure continues until no path with a positive reduced cost

remains. Once all reduced costs are non-positive, we terminate the loop and verify whether the variables in [RMP-rel] satisfy integer constraints. If fractional values exist, a branching step is applied to enforce integrality, following the branch-and-price framework.

For the branching scheme, we focus on the hub variable y_i and the flight variable z_{ij}. The hub variable y_i is of primary importance as it has a significant impact on the path and flight number decisions. If y_i is fractional, two branches are created: one branch fixes $y_i = 0$, and the other fixes $y_i = 1$ to establish bounds. When solving the pricing subproblem $[PSP_k]$, we forbid the hub variable if it is fixed to 0. Next, we proceed with branching on the flight variable z_{ij}. Similar to the hub variable, if the value of z_{ij} is fixed to 0, we forbid the corresponding arc (i, j) in the subproblem. For each branch, we incorporate the corresponding constraints into [RMP-rel] and repeat the process to approach the bounds. In summary, the B&P process as shown in Figure (4.1).

While the B&P approach improves the computational efficiency of the HLPP-P, it still requires significant time to obtain the optimal solution. For business purposes, however, faster response times are more critical than achieving the optimal solution. Therefore, we introduce the Genetic Algorithm (GA) to further reduce computational time while providing a high-quality feasible solution. The next subsection will present the GA approach in detail.

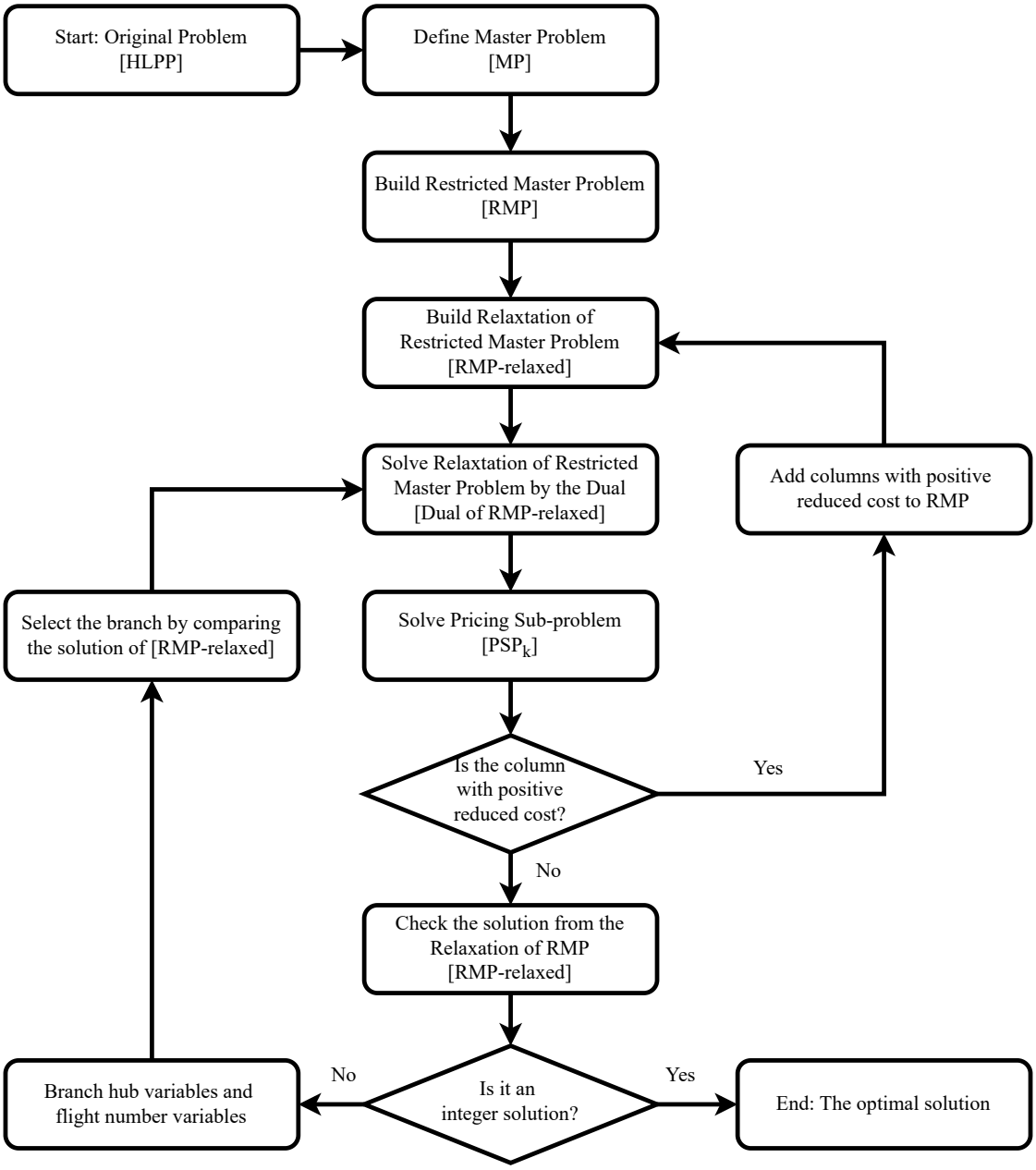

Figure 4.1: Overall process of the B&P approach.

4.2.2 Genetic Algorithm (GA)

4.2.2.1 Components of GA

The GA comprises several essential components that collaborate to identify high-quality solutions for optimization problems. These components include three key elements: Gene, Chromosome, and Population. Their definitions and roles within GA are outlined below:

- Gene: A gene is the smallest unit of the solution representation. It typically represents a single decision variable in the problem, such as a hub location or an arc selection in a transportation network.
- Chromosome: A chromosome is a collection of genes that represents a complete solution to the problem. For example, in this context, a chromosome consists of a set of selected hubs, which subsequently determines the available paths for commodities based on the chosen hubs.
- Population: The population is a group of chromosomes that serves as the search space for the algorithm. Each chromosome in the population represents a potential solution, and the size of the population determines the diversity of solutions being explored.

Based on the definitions above, Figure (4.2) illustrates the definitions of the components in GA.

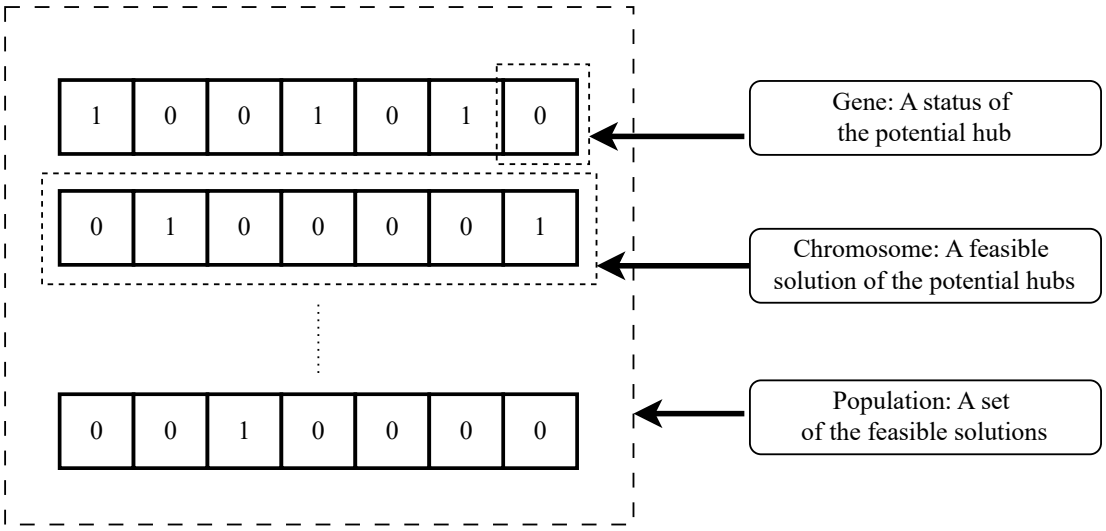

Figure 4.2: The components of GA for solving HLPP.

In our problem, we firstly define the decision variable y_i as a gene, with its opening status denoted by $\hat{y}_i$, where a value of 1 indicates that the potential hub is open, and a value of 0 signifies it is closed. Subsequently, we define a feasible solution for the potential hubs as a chromosome, representing one of the possible combinations regarding the list of potential hubs. Finally, the population comprises the collection of possible solutions related to the potential hubs.

4.2.2.2 Fitness Function of GA

The fitness function evaluates how well a chromosome meets the problem's objective. It assigns a fitness value to each chromosome based on the quality of the solution it represents. In our case, a higher profit results in a better fitness value for the chromosome.

(1) Sub-problem of HLPP-P

Let m denote the number of chromosomes in the population, and n denote the number of the generation, then $Y^n = \{Y_1^n, Y_2^n, ...Y_m^n\}$ represent the set of the individuals in the n^{th} population and Y_m^n represent the m^{th} chromosome. Each chromosome is considered a sub-problem of the HLPP, which can be solved to obtain the optimal solution. For each sub-problem of HLPP-P, since the decision variable y_i transformed into $\hat{y}_i$, the corresponding feasible paths for the commodities are reduced. Consequently, the sets P_k can be reduced to $\hat{P}_k$, with $\hat{\mathcal{P}}^k = \bigcup_{k \in K} \hat{P}_k$. As a result, the sub-problem for each chromosome of the GA can be written as follows:

$$\textbf{[sub-HLPP-P]} \quad \max \quad \sum_{k \in K} \sum_{p \in \hat{P}_k} r_k w_k x_k^p - \sum_{(i,j) \in A} c_{(i,j)} z_{(i,j)} - \sum_{i \in N} f_i \hat{y}_i \tag{4.49}$$

s.t.

$$\sum_{p \in \hat{P}_k} x_k^p \leq 1 \qquad k \in K \tag{4.50}$$

$$\sum_{k \in K} \sum_{p \in \hat{P}_k} w_k \delta_{(i,j)}^p x_k^p \leq \Gamma_{(i,j)} z_{(i,j)} \qquad (i,j) \in A \tag{4.51}$$

$$x_k^p \in \{0,1\} \qquad k \in K, p \in \hat{P}_k \tag{4.52}$$

(4.7)

Since the potential paths of the commodities are limited by $\hat{y}_i$ as $\hat{P}_k$, the reduced domain (4.52) and sets in the objective function (4.49), constraint (4.50) and (4.51) are presented. Additionally, the original constants (4.3) and (4.5) are removed as the status of the potential hubs is now confirmed. Consequently, sub-problem's size is significantly smaller than the original problem, allowing for faster computations and enabling the determination of an

optimal solution more efficiently.

(2) Sub-problem of HLPP-A

Similarly, for HLPP-A, the objective function and constraints are decomposed by converting the decision variable y_i into $\hat{y}_i$, as shown below:

$$\textbf{[sub-HLPP-A]} \quad \max \quad \sum_{k \in K} r_k w_k (u_k + v_k) - \sum_{(i,j) \in A} c_{(i,j)} z_{(i,j)} - \sum_{i \in N} f_i \hat{y}_i \tag{4.53}$$

s.t.

$$x_{(i,j)k} \leq \hat{y}_j \qquad (i,j) \in A, k \in K : j \neq d(k) \tag{4.54}$$

$$x_{(i,j)k} \leq \hat{y}_i \qquad (i,j) \in A, k \in K : i \neq o(k) \tag{4.55}$$

(4.7), (4.9), (4.10), (4.11), (4.14), (4.15), (4.16), (4.17), (4.18), (4.19)

Similar to the sub-HLPP-P, the domain constraint for y_i (4.5) is removed, and the third term of the objective function is fixed by $\hat{y}_i$, as shown in (4.53). Additionally, the original constraints (4.12) and (4.13) are replaced by the decomposed constraints (4.54) and (4.55), significantly simplifying the calculations associated with hub activation.

4.2.2.3 Iterative Process of GA

After the initial population is generated, the GA begins progressing toward the best feasible solution through encoding and decoding processes. The encoding and decoding processes work on two types of spaces alternatively: coding space and solution space, or in other terms, genotype space and phenotype space [84]. The encoding and decoding processes of

GA are illustrated below in Figure (4.3):

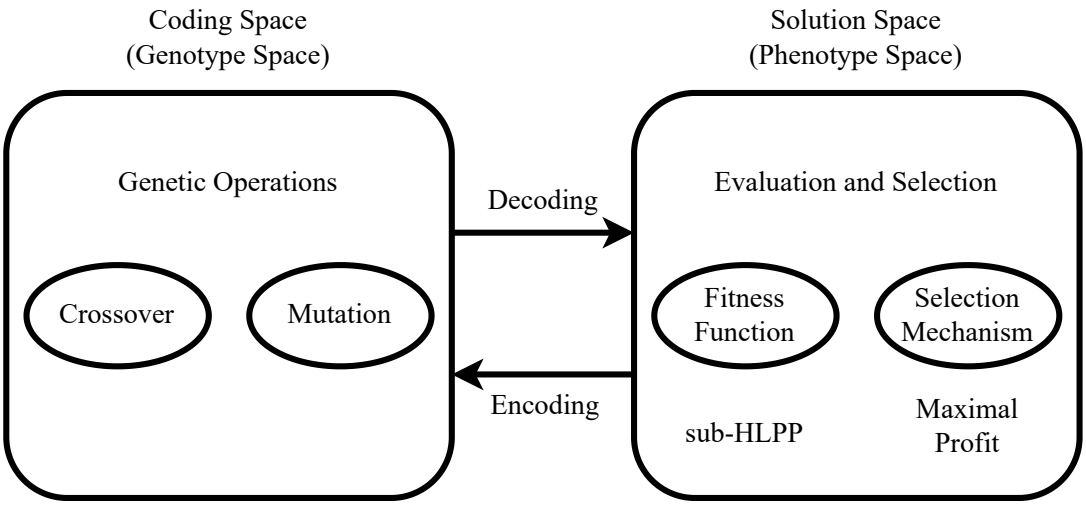

Figure 4.3: Encoding and decoding processes of GA.

Genetic operators work in the genotype space, generating offspring from the parents through crossover and mutation. Additionally, evaluation and selection operate in the phenotype space, selecting the maximal profit based on the evaluations of the sub-problems. Through iterative generations, the fitness value of the chromosome ultimately leads to the best feasible solution when the specified requirements, such as the generation limit or computational time limit, are satisfied.

Considering the detailed flow process of GA, we represent a visualization of the GA below in Figure (4.4).

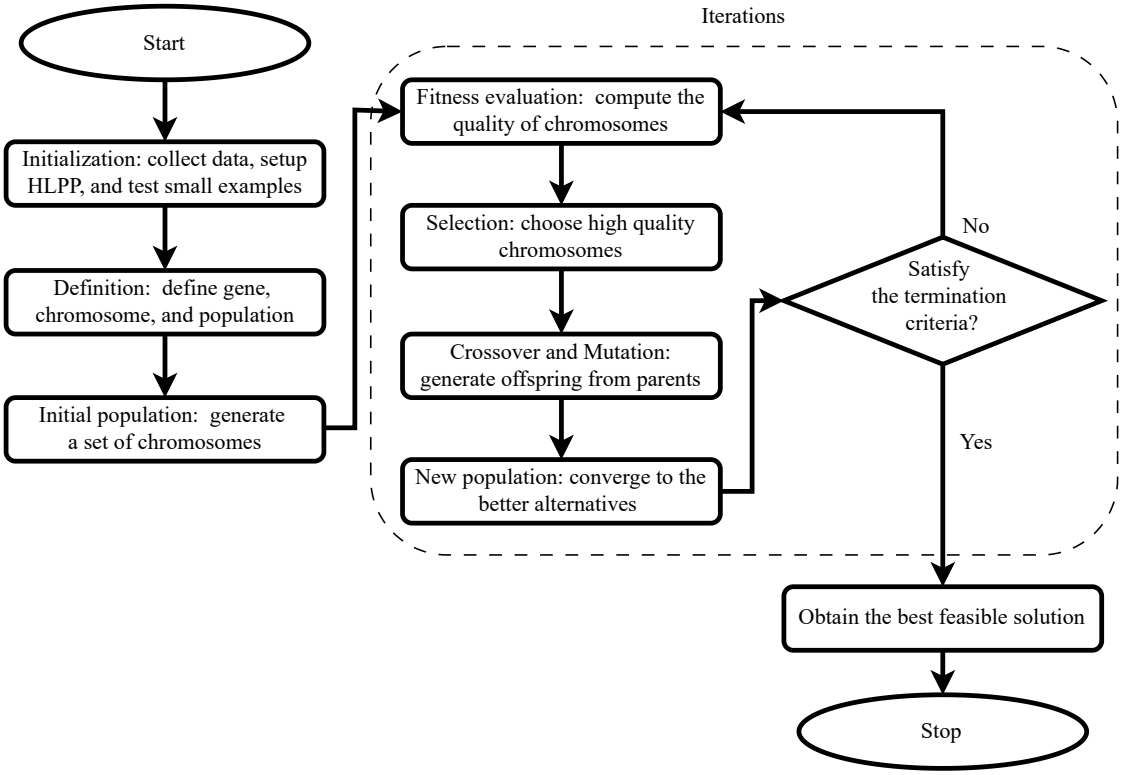

Figure 4.4: Detailed process flow of GA.

We first initialize a population of potential solutions during the encoding phase, where genes, chromosomes, and populations are defined to represent potential solutions for the hub list. Next, we generate a set of potential solutions as the initial population based on the initial settings. By evaluating the fitness of each chromosome in the population, we select the better individuals based on their fitness value (i.e., higher profit) for reproduction. These selected individuals are treated as the parents and offspring are generated through genetic operators (i.e., crossover and mutation). This process replaces the least

fit chromosomes in the population. Repeating these steps over several generations leads to convergence, eventually yielding the best feasible solution based on the fitness values of the chromosomes in the final population. Finally, the termination criteria in our study are based on several factors such as the number of generations, the computational time limit, and the convergence of fitness values. Specifically, the evolution process is stopped if the fitness value remains unchanged for a specified number of consecutive generations.

4.2.2.4 Genetic Operations of GA

Crossover and mutation are two fundamental genetic operations in GA that drive the search process within the genotype space. These operations enable the algorithm to explore a broad solution space, refine promising solutions, and maintain genetic diversity throughout the evolutionary process. As a result, they contribute to efficiently identifying high-quality solutions. Both operations occur in every generation of the GA. Once a population of chromosomes is generated, crossover is performed on selected parent chromosomes with a predefined probability, facilitating the exchange of genes to create offspring. Following this, mutation is applied to the newly generated offspring based on a specified mutation probability, introducing variations that prevent premature convergence. These steps continue iteratively until the stopping criterion is satisfied.

(1) Crossover in GA

Crossover involves combining two parent chromosomes to produce offspring for the next generation. This process simulates biological reproduction, where genetic material is exchanged between two individuals. In GA, crossover helps explore new regions of the solution space by merging features from both parents. Common crossover methods include single-

point crossover, two-point crossover, uniform crossover, and scattered crossover [84]. In our study, we modified the single-point crossover and established custom conditions to suit our specific requirements. The custom crossover function (3) is outlined as follows:

Algorithm 3 Custom Crossover Function

Input: `parents` (array of parent solutions), `offspring_size` (desired size of offspring)
Output: `offspring` (array of generated offspring)

```
offspring ← [ ]
idx ← 1
while length(offspring) ≠ offspring_size do
    crossover_candidate ← single_point(parents[idx], parents[idx+1])
    if if_customize = True then
        num_hubs ← count_opening_hubs(crossover_candidate)
        if_passed ← check_attributes(num_hubs, ratio_cost, cur_gen)
        if if_passed = True then
            Append crossover_candidate to offspring
        end if
    else
        Append crossover_candidate to offspring
    end if
    idx ← idx + 1
    if (idx = length(parents)) and (length(offspring) < offspring_size) then
        idx ← 1
    end if
end while
return offspring
```

First, we apply the single-point crossover based on the parents' index. Once the crossover is performed, we assess the offspring candidate's attributes to maintain feasibility and diversity. These attributes include the number of opening hubs, the ratio of unit revenue to fixed hub opening costs, and the current generation number. The number of hubs and the revenue-to-cost ratio act as filters to exclude impractical solutions, while the generation

parameter progressively relaxes constraints across iterations. This adjustment encourages greater diversity, allowing the algorithm to explore a wider solution space and improve overall search efficiency.

(2) Mutation in GA

Mutation introduces random alterations to a chromosome, promoting genetic diversity and preventing premature convergence. It involves changing one or more elements of the chromosome, potentially leading to a new solution. This randomness helps the algorithm escape local optimal solution by exploring new regions of the solution space. By adjusting mutation rates appropriately, the balance between exploration and exploitation is maintained, ensuring that the search process remains effective throughout the generations.

Common mutation methods include random mutation, swap mutation, inversion mutation, scramble mutation, and adaptive mutation [84]. In our study, we adopt a modified version of the random mutation, incorporating custom conditions specific to the problem's requirements. After completing the crossover process, the custom mutation function is applied to further enhance genetic diversity. The detailed mutation process is presented in the custom mutation function (4).

Algorithm 4 Custom Mutation Function

Input: `offspring` (current offspring solutions)
Output: `offspring` (mutated offspring)

```
for i = 1 to length(offspring) do
    offspring_candidate ← [ ]
    for j = 1 to num_expected_trial do
        mutation_candidate ← random_mutation(mut_prob, potential_hub_loc)
        if mutation_candidate exist then
            if if_customize = True then
                num_hubs ← count_opening_hubs(mutation_candidate)
                if_passed ← check_attributes(num_hubs, ratio_cost, cur_gen)
                if if_passed = True then
                    Append mutation_candidate to offspring_candidate
                end if
            else
                Append mutation_candidate to offspring_candidate
            end if
        end if
    end for
    offspring[i] ← replace_criteria(offspring_candidate)
end for
return offspring
```

Each gene in the offspring chromosomes initially undergoes random mutation based on a predefined mutation probability and the constraints associated with potential hub locations. Similar to the crossover mechanism, we incorporate a rigorous filtering step after the mutation process to eliminate infeasible solutions by assessing key attributes. Multiple candidate chromosomes are then generated, with the expected number of trials through the mutation process. These candidates are carefully evaluated based on selection criteria such as uniqueness and the number of hubs. Ultimately, the best candidate replaces the original chromosome, ensuring the population evolves toward higher-quality solutions.

4.3 Computational Results

In this section, we conduct extensive computational experiments to assess the performance of the proposed methods. By considering the specifications of the airplanes and city populations, we selected the core southeastern region of the U.S. as our target area, which includes the states: Tennessee, North Carolina, Mississippi, Alabama, Georgia, South Carolina, and Florida. The populous cities in these states, which have facilities such as airports nearby, are selected as our demand nodes and potential hub locations.

Computational experiments were conducted on a workstation equipped with an AMD Ryzen 9 5900X 12-Core Processor (3.70 GHz) and 64GB of RAM. The mathematical models were solved using IBM ILOG CPLEX 22.1.1.0, Python version 3.10.11, and docplex version 2.25.236. All instances were solved to optimality by one thread, with a 1% gap tolerance and within a two-hour time limit.

This section is organized as follows: Subsection (4.3.1) introduces the parameter settings of the dataset and GA. Next, subsection (4.3.2) discusses managerial insights focusing on the economies of scale factor. Lastly, to evaluate the computational performance of the proposed algorithms, numerical results from larger-sized instances based on the dataset are displayed in subsection (4.3.3).

4.3.1 Parameter Setting

Firstly, we define the set of nodes, N, which represent customer locations across various cities. We used publicly available information and utilized population data from the 2022

U.S. Census Bureau to estimate demand across different cities. We ranked cities in the southeastern U.S. by population, focusing on the most populous ones with at least one nearby airport. This analysis assumes no geographical barriers between cities and airports, enabling us to concentrate solely on pilotless air express while excluding ground shipments. For areas with high population density, such as the Miami region, we used the K-means method to cluster cities and evenly distribute them among nearby airports. Ultimately, we selected the top 50 cities in the southeastern U.S. for our study. The coordinates of these cities conform to the World Geodetic System 1984 (WGS-84), maintained by the United States National Geospatial-Intelligence Agency. With the nodes defined, we establish the set of arcs, A, where (i, j) denotes the arc from node $i \in N$ to node $j \in N$. The length of arc (i, j), denoted as $Dist(i, j)$, is calculated as the geodesic distance according to the WGS-84 standard.

Furthermore, based on the population data, we scale them and filter out unrealistic scenarios, such as excessively short distances between nodes, to create a commodity matrix among nodes from $i \in N$ to $j \in N$. In this study, we assume that the commodity unit is measured in kilograms (kg), and that the dimensions of the commodities do not present any constraints. Based on these parameters, we define the set of commodities, K, and demand matrix (w_k). Motivated by postal delivery applications, where the cost of sending a letter remains the same between any two locations, the revenue per unit demand (r_k) is assumed to be independent of the O-D pair.

Next, we define the parameters related to the airplanes. To simplify the calculations, we assume that all airplanes in the set have uniform specifications. Specifically, we use the Pilatus PC-12 NG model, as aligned by Ribbit Ltd., a start-up pilotless air cargo

transportation company. Fixed flight costs, aircraft speed, average operating cost per hour, total capacity, and fuel consumption per hour are all derived from the specifications of this model. These parameters serve as the basis for calculating the total cost ($c_{(i,j)}$), travel time ($t_{(i,j)}$), and the remaining capacity ($\Gamma_{(i,j)}$) for the arcs.

Additionally, the potential hub locations are chosen based on the size of nearby airports and their geographical locations. The fixed cost of opening a hub, denoted as f_i, is relatively larger than the unit revenue within a reasonable range. For hub operations, the loading, unloading, and sorting times are assumed to be the same regardless of the hub's size. Based on the settings above, we present the visualization of the largest case (50 nodes, 20 potential hubs) of the dataset in Figure (4.5).

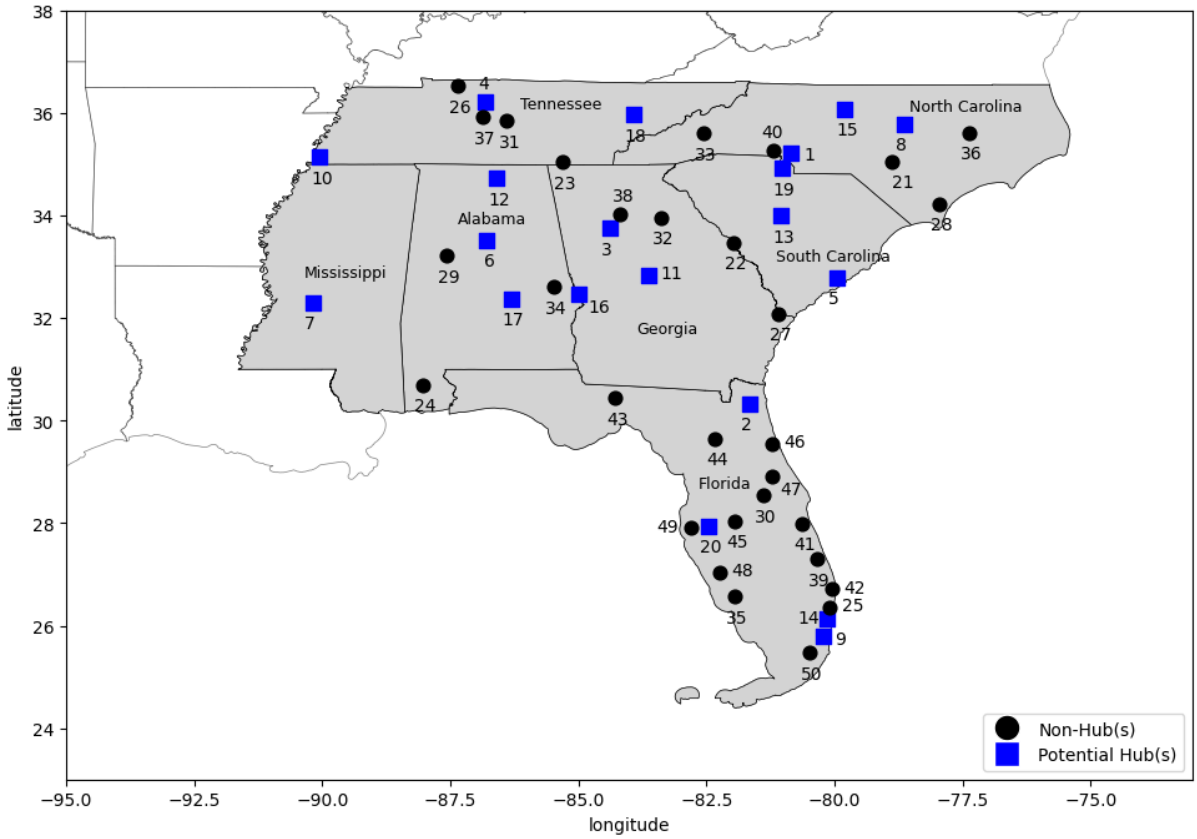

Figure 4.5: The nodes in the southeastern region of the US.

Finally, For HLPP-P, we generate the set of all feasible directed paths, P_k, for each commodity $k \in K$, ensuring that the time spent on path (t_k^p) is within the delivery time limit (β_k) and the number of arcs in path p does not exceed the maximum allowed (a_k), in order to avoid physical carry risks. In summary, the detailed information regarding these parameters are displayed in Table (4.1).

We now move to describe the setup for our Genetic Algorithm. We configure the GA by defining several parts: components (i.e., gene, chromosome, population), fitness func-

Table 4.1: Parameters: The core southeastern region of the US.

Parameter	Value	Unit	Descriptions
d_{ng}	1,400	\$	fixed cost of a flight by Pilatus PC-12 NG
Γ_{ng}	1,800	kg	total capacity by Pilatus PC-12 NG
sp_{ng}	280	km/hr	aircraft speed by Pilatus PC-12 NG
op_{ng}	1,097	\$/hr	average operating cost per hour by Pilatus PC-12 NG
fu_{ng}	175	kg/hr	fuel spent per hour by Pilatus PC-12 NG
t_k^l	1	hr	loading time of the commodity $k \in K$ at a node
t_k^u	1	hr	unloading time of the commodity $k \in K$ at a node
t_k^s	1	hr	sorting time of the commodity $k \in K$ at a hub
β_k	12	hr	delivery time limit for commodity $k \in K$
a_k	3		maximal allowed arcs in a path for commodity $k \in K$
r_k	20	\$/kg	unit revenue of the commodity
f_i	10,000	\$	fixed cost of operating hub $i \in N$
$t_{(i,j)}$	$vary^1$	hr	time spent of a flight for an airplane on arc $(i,j) \in A$
$\Gamma_{(i,j)}$	$vary^2$	kg	remaining capacity of an airplane on arc $(i,j) \in A$
$c_{(i,j)}$	$vary^3$	\$	overall cost of a flight on arc $(i,j) \in A$
$t_{(i,j)k}$	$vary^4$	hr	time spent for commodity $k \in K$ on arc $(i,j) \in A$

[1] Formula: $t_{(i,j)} = (Dist(i,j)/sp_{ng})$
[2] Formula: $\Gamma_{(i,j)} = \Gamma_{ng} - (fu_{ng} * t_{(i,j)})$
[3] Formula: $c_{(i,j)} = d_{ng} + op_{ng} * t_{(i,j)}$
[4] Formula: $t_{(i,j)k} = t_{(i,j)} + f(t_k^l, t_k^u, t_k^s)$; $f(t_k^l, t_k^u, t_k^s)$ follows shipping operations

tion (i.e., sub-HLPP-P, sub-HLPP-A), genetic operations (i.e., crossover, mutation), and iterative process.

We initially setup the decision variable y_i as a gene, with its opening status denoted by $\hat{y}_i$. A value of 1 indicates that the potential hub is open, while 0 signifies it is closed. Subsequently, a feasible solution for the potential hubs is represented as a chromosome. For instance, if there are 20 potential hubs, the chromosome size is 20, comprising 20 binary values (0 or 1) to indicate whether each hub is open. Meanwhile, the population size is manually defined. In our research, we set the population to consist of 10 chromosomes. The initial population is generated randomly; however, to improve computational

efficiency, we assign a higher probability to configurations reflecting trends observed in small testing examples of HLPP-A and HLPP-P. Specifically, the likelihood of opening fewer hubs (e.g., one or two) is set to be twice as high as other scenarios when generating the initial population in our study.

The fitness value for each chromosome in GA is determined using the sub-HLPP-P fitness function. Similarly, for the HLPP-A model, the fitness function used is sub-HLPP-A. We set a 2-hour overall time limit for GA, with a maximum of five minutes allocated to compute a feasible solution for each chromosome and consider a 1% gap tolerance.

In the iterative process of generating offspring, we select the top 50% of the population based on fitness value as parents for crossover and mutation operations. This process produces nine offspring while retaining one elite individual from the parent generation to preserve high-quality solutions. For GA operators, we employ a custom crossover function and custom mutation function shown in Algorithms (3) and (4) to filter out unrealistic scenarios, thereby simplifying calculations. These limitations are gradually relaxed after the 10th generation as the first stage and the 15th generation as the second stage, at which point all restrictions are removed. In addition to the number of generations, the custom functions are designed to prevent the creation of an excessive number of open hubs by considering the number of nodes ($|N|$) and other relevant parameters, such as the revenue-cost ratio (e.g., r_k, f_i). The mutation probability is set to a standard level of 10%, meaning each gene has a 10% chance of mutating during the mutation process. At the end of the mutation process, we exclude chromosomes that have appeared in previous populations when selecting the offspring from the candidate list. This approach prevents redundant computations and enhances computational efficiency.

Finally, we establish the termination criteria as follows: a maximum of 50 generations, no improvement in fitness value over five consecutive generations, or a 2-hour time limit. The iteration process stops once any of these conditions are met, and the chromosome with the highest fitness value is selected as the best feasible solution.

4.3.2 Insights

This section examines key insights by analyzing net profit and the decision variables y_i, $z_{(i,j)}$, and x_k^p (or u_k, v_k, and $x_{(i,j)k}$) in response to parameter variations. We focus on three critical parameters: the number of nodes ($|N|$), unit revenue (r_k), and the fixed cost of opening a hub (f_i). The number of nodes is primarily determined by market demand, making it difficult to modify. Similarly, the fixed cost of opening a hub depends on market size and is not easily reduced. Analyzing variations in these parameters provides valuable insights into decision variables and net profit.

In this study, we analyze multiple scenarios by expanding the network size from 10 to 30 nodes, varying unit revenue from 10 (50% of the normal setting) to 40 (200%), and adjusting the fixed cost of opening a hub from 5,000 (50%) to 20,000 (200%). Meanwhile, we keep the number of potential hubs fixed at 10, along with their locations. Based on these combinations, we evaluate the network's profitability, commodity demand satisfaction, the number of open hubs, the number of flight assignments, and the average utilization of airplanes. Each performance index provides valuable insights into the network's profitability, operational efficiency, and service performance across different parameter configurations. The detailed results are presented in Table (4.2).

Table 4.2: Computational results with flight assignments.

Parameters			**Performance Indexes**					
$\|N\|$	r_k	f_i	Net Profit	# of Open Hubs	# of Flights	Avg. Flight Utilization (%)	Demand Satisfaction by Weights (%)	Demand Satisfaction by Orders (%)
10	10	5,000	100,167.0	2	28	76.47	95.13	93.33
10	10	10,000	92,723.4	1	26	85.04	89.72	74.44
10	10	20,000	82,723.4	1	26	85.04	89.72	74.44
10	20	5,000	311,955.8	2	28	81.38	99.63	98.89
10	20	10,000	301,955.8	2	28	81.38	99.63	98.89
10	20	20,000	291,326.0	1	32	75.83	99.33	97.78
10	40	5,000	738,058.8	2	29	78.07	100.00	100.00
10	40	10,000	727,395.8	2	28	81.38	99.63	98.89
10	40	20,000	716,890.2	1	34	68.65	100.00	100.00
20	10	5,000	265,761.4	2	71	77.84	97.48	98.14
20	10	10,000	255,111.1	2	71	77.42	97.34	97.87
20	10	20,000	235,761.4	2	71	77.56	97.48	98.14
20	20	5,000	765,641.6	2	78	75.70	99.86	98.67
20	20	10,000	759,718.2	2	74	75.23	98.88	97.61
20	20	20,000	739,658.8	2	74	75.99	98.89	98.67
20	40	5,000	1,793,011.3	2	78	71.44	100.00	100.00
20	40	10,000	1,783,011.3	2	78	71.44	100.00	100.00
20	40	20,000	1,763,094.9	2	77	72.90	100.00	100.00
30	10	5,000	410,723.8	2	110	80.18	99.29	98.50
30	10	10,000	400,763.8	2	110	80.25	99.29	98.61
30	10	20,000	380,373.8	2	110	80.08	99.24	98.38
30	20	5,000	1,190,016.1	2	112	79.64	99.89	99.77
30	20	10,000	1,180,016.1	2	112	79.60	99.89	99.77
30	20	20,000	1,157,710.6	2	113	79.09	99.93	99.88
30	40	5,000	2,744,376.5	2	116	76.77	100.00	100.00
30	40	10,000	2,734,157.1	2	116	77.15	100.00	100.00
30	40	20,000	2,714,157.1	2	116	77.15	100.00	100.00

Firstly, when the unit revenue and fixed hub opening costs are held constant, an increase in the number of nodes from 10 to 30 results in a net profit that grows slightly faster than linearly. This suggests that the network's profitability improves more than proportionally with the addition of nodes. Additionally, the number of flights required increases at a

nonlinear rate. For instance, when the number of nodes is doubled from 10 to 20, the number of flights increases significantly from approximately 30 to 75, which is more than double the initial value. This indicates a high sensitivity of flight demand to the number of nodes in the network.

Additionally, when comparing scenarios with the same unit revenue and hub costs, increasing the number of nodes intensifies route complexity, yet average flight utilization remains relatively stable, and the demand satisfaction levels show a steady increase. This indicates that additional nodes primarily expand routing flexibility rather than overburdening existing routes. For example, as the number of nodes increases from 10 to 30, demand satisfaction increases from 95% to 100%.

Under different combinations of unit revenue and fixed hub opening costs, the results indicate that unit revenue has a significantly greater impact on net profit than hub opening costs. For example, at 30 nodes and a hub cost of 5,000, net profit increases substantially from 410,723.8 ($r_k = 10$) to 2,744,376.5 ($r_k = 40$). Higher unit revenue also leads to full demand satisfaction, reaching 100% for both weight and orders when $r_k = 40$. This is because higher unit revenue not only absorbs most operational costs but also expands the range of viable shipping options. As a result, the network can accommodate a wider variety of orders and routes, thereby maximizing demand fulfillment.

In contrast, raising hub opening costs has a relatively minor effect on net profit and little impact on operational efficiency. For instance, with 20 nodes at $r_k = 20$, increasing hub costs from 5,000 to 20,000 results in a slight net profit reduction from 765,641.6 to 739,658.8, while flight utilization remains stable at approximately 75–76%. However, when

unit revenue is low and hub opening costs are high, the network faces a trade-off in accepting orders based on the demand structure. In this scenario, with 10 nodes, $r_k = 10$, and hub costs of 10,000 or 20,000, demand satisfaction by orders declines to 74.44%, highlighting the impact of cost-pressure on service performance.

Our evaluation also reveals that the number of open hubs remains stable at two in most scenarios, indicating that the model prioritizes a small number of high-capacity hubs over multiple smaller hubs. Notably, when unit revenue is low and hub opening costs are high, the model reduces the number of hubs to a single location to minimize expenses. For example, with $|N| = 10$, $r_k = 10$, and hub costs $f_i = 10,000$ or $20,000$, only one hub is opened.

Moreover, hub location selection considers both high-demand routes and location centrality. Figure (4.6) presents examples from the results with different numbers of nodes ($|N| = 10, 20, 30$) and varying unit revenue levels ($r_k = 10, 40$).

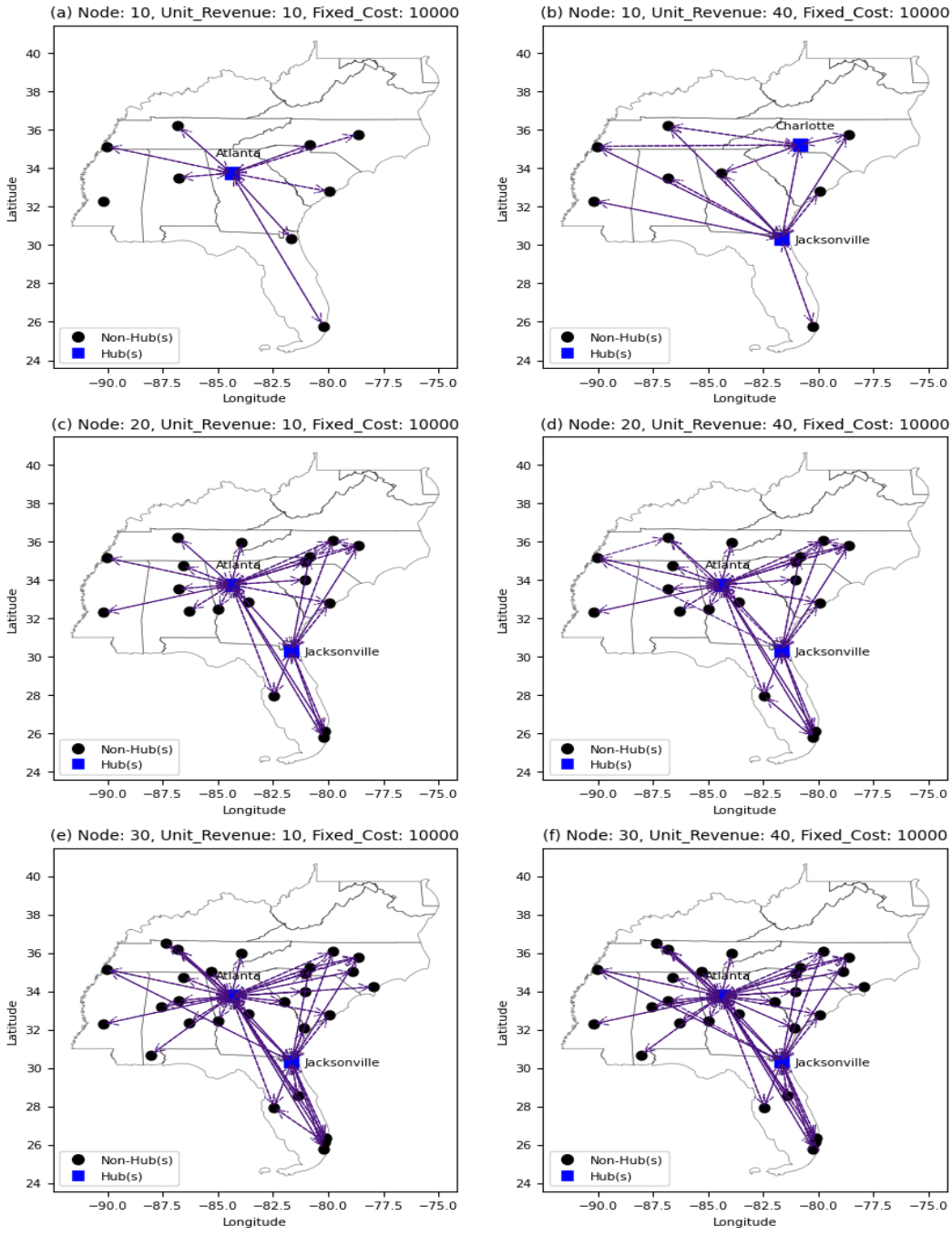

Figure 4.6: The flight assignments and hub location with different nodes.

Ideally, Charlotte and Jacksonville are identified as the optimal hub candidates, as they cover the highest proportion of demand, as shown in case (b). However, in scenarios with low unit revenue and high fixed opening costs, or with more flexible route options (e.g., 20 or 30 nodes), Charlotte, despite covering the highest demand, is generally not selected as a hub due to its peripheral location on the map. In contrast, Atlanta, which has lower overall demand than Charlotte and Jacksonville, becomes the preferred hub candidate because of its central location within the network, as illustrated in cases (a) and (c)-(f). This demonstrates that the model strategically balances demand coverage with geographical centrality, prioritizing hubs that can efficiently serve multiple routes.

4.3.3 Computational Performance Analysis

In this subsection, we evaluate the performance of our proposed models using datasets of varying sizes from the core southeastern U.S. region. Given the initial parameters in Table (4.1), we vary the number of nodes and potential hubs, which are combined in different configurations to comprehensively assess our models. The experiments involve the original HLPP-P and HLPP-A formulation, as well as HLPP-P and HLPP-A with GA, tested under diverse parameter settings. The results are summarized in Table (4.3).

Firstly, the results in the table emphasize the growing complexity of the HLPP models as the number of nodes and potential hubs increases. When the network size reaches 20 nodes, both HLPP-P and HLPP-A are unable to achieve an optimal solution within the 2-hour computational limit, highlighting scalability issues. As the problem size expands further, the LP gap consistently exceeds 3.5%. HLPP-P generally outperforms HLPP-A in both computational efficiency and objective function value. Although HLPP-A performs well in smaller instances, it struggles with feasibility in larger networks, particularly for cases with 40 or 50 nodes and 20 potential hubs, where it fails to provide a feasible solution within the time limit.

The introduction of the GA improves both solution quality and computational efficiency for both formulations. In almost all instances, the GA-enhanced models provide better feasible solutions with reduced computational effort. On average, GA increases net profit by about 1% for HLPP-P and 1.5% for HLPP-A, indicating its effectiveness in refining solutions. Although the improvement is modest for smaller networks, it becomes more significant for larger networks, especially for cases with 40 to 50 nodes and 20 hubs. For

Table 4.3: Computational performance: Flight assignments.

Parameters			**HLPP-P**						**HLPP-A**					
			Normal			with GA			Normal			with GA		
$\|N\|$	Potential Hub	$\|\mathcal{P}^k\|$	Net Profit (A^*)	LP Gap (%)	CPU Time (sec)	Net Profit (B^*)	Gap w. Normal (%)[1]	CPU Time (sec)	Net Profit (C^*)	LP Gap (%)	CPU Time (sec)	Net Profit (D^*)	Gap w. Normal (%)[2]	CPU Time (sec)
10	5	520	301,955.8	1.00	23.7	301,955.8	0.00	22.1	301,996.4	1.00	114.3	301,326.0	-0.22	26.1
10	10	906	301,966.4	1.00	133.7	301,955.8	-0.01	43.8	301,996.4	1.48	7200.0	301,326.0	-0.22	44.9
20	5	3,032	751,106.3	3.89	7200.0	759,718.2	1.13	2299.7	757,611.5	3.55	7200.0	758,340.5	0.10	2458.6
20	10	5,708	757,590.9	3.47	7200.0	759,718.2	0.28	4273.7	757,752.1	3.93	7200.0	758,262.4	0.07	4658.8
20	20	22,994	749,532.0	6.63	7200.0	754,154.8	0.61	7200.0	716,768.0	12.75	7200.0	754,281.6	4.97	7200.0
30	5	7,368	1,170,976.8	2.69	7200.0	1,180,016.1	0.77	2082.1	1,165,681.0	3.42	7200.0	1,177,721.5	1.02	1956.4
30	10	14,050	1,166,213.6	3.56	7200.0	1,180,016.1	1.17	4245.5	1,140,298.9	6.19	7200.0	1,177,721.5	3.18	4321.5
30	20	56,530	1,116,849.7	9.77	7200.0	1,175,633.7	5.00	4804.4	964,600.9	27.16	7200.0	1,176,950.0	18.04	6897.5
40	5	13,936	1,429,690.9	3.49	7200.0	1,447,374.6	1.22	2856.0	1,411,833.9	5.01	7200.0	1,445,054.6	2.30	2800.6
40	10	26,530	1,424,314.9	3.99	7200.0	1,445,556.4	1.47	6620.9	1,400,704.0	6.18	7200.0	1,444,794.6	3.05	6062.4
40	20	109,854	1,318,159.4	15.29	7200.0	1,432,995.7	8.01	5540.3	0.0	∞	7200.0	1,433,169.1	100.00	5077.7
50	5	20,768	1,700,712.0	4.34	7200.0	1,721,078.1	1.18	3000.6	1,705,889.6	4.44	7200.0	1,718,769.6	0.75	3173.5
50	10	38,168	1,671,077.4	6.43	7200.0	1,721,078.1	2.91	6543.2	1,653,494.7	8.24	7200.0	1,718,129.6	3.76	7200.0
50	20	149,856	1,287,396.0	42.90	7200.0	1,730,233.2	25.59	7200.0	0.0	∞	7200.0	1,727,112.5	100.00	7200.0

[1] Gap with normal HLPP-P: (B^* - A^*)/B^* * 100%

[2] Gap with normal HLPP-A: (D^* - C^*)/D^* * 100%

example, in the 50-node case, HLPP-P with GA results in a gap of 25.6%, while HLPP-A with GA produces a higher-quality feasible solution compared to the standard HLPP-A, which fails to find any feasible solution. This underscores the benefits of incorporating GA in large-scale networks. This suggests that GA is particularly beneficial in complex scenarios where the original formulations struggle to find high-quality solutions within the time limit.

A comparison between HLPP-P with GA and HLPP-A with GA highlights notable differences in solution quality and computational efficiency. In terms of net profit, HLPP-P with GA consistently outperforms HLPP-A with GA across most instances. Additionally, HLPP-P with GA maintains a lower gap than HLPP-A with GA in nearly all cases. While HLPP-P with GA generally requires less computational time for smaller instances, HLPP-A with GA occasionally performs better in certain mid-sized cases due to its reduced number of decision variables. However, as network size increases, HLPP-A's computational time escalates significantly, whereas HLPP-P with GA maintains better scalability.

4.4 Chapter Summary

This chapter aimed to analyze the net profit and operational efficiency of the transportation network design model, focusing on how variations in customer demand, unit revenue, and fixed hub opening costs influence outcomes. To achieve this, we introduced two formulations: the HLPP-P and HLPP-A models.These formulations ensured that demand satisfaction was effectively balanced with profitability in the optimization process. Additionally, we implemented the GA methodology to enhance the models' solvability.

This chapter presented an application for the pilotless air cargo industry, focusing on the core southeastern region of the U.S. The chapter also highlighted key managerial insights and provides an in-depth comparison of the HLPP-P and HLPP-A models across various scenarios, offering valuable perspectives for transportation network design and decision-making.

The results demonstrated that increasing the number of nodes significantly enhances both profitability and demand satisfaction, with net profit rising more than proportionally due to expanded routing flexibility and improved service coverage. Additionally, unit revenue proved to be the most critical factor influencing profitability, as higher revenue not only boosted net profit but also ensured full demand satisfaction by accommodating a wider range of orders and routes. In contrast, fixed hub opening costs had a relatively minor impact on both net profit and operational efficiency, although high costs combined with low revenue caused a decline in service performance.

Hub deployment patterns revealed that the model consistently prioritized cost efficiency

by maintaining a small number of high-capacity hubs, typically two, and reducing to a single hub in low-revenue, high-cost scenarios. Strategic hub selection balanced demand coverage with geographic centrality, with Atlanta emerging as a preferred hub due to its central location, even when other cities, such as Charlotte, had higher demand. Overall, these insights emphasize that expanding the network and optimizing revenue generation are crucial for profitability, while a cost-efficient, centrally located hub structure enhances service performance and operational resilience.

Additionally, the performance analyses highlighted the increasing complexity of HLPP models as network size expands. Compared to both models, HLPP-P generally outperforming HLPP-A in both computational efficiency and solution quality. HLPP-A struggles with feasibility in larger networks due to exponential constraint growth, whereas HLPP-P remains more robust despite its growing number of decision variables.

The introduction of GA enhances both formulations by improving solution quality and reducing computational effort, particularly for larger networks where standard methods struggle to find feasible solutions. Notably, HLPP-P with GA consistently delivers higher net profits and better scalability compared to HLPP-A with GA, further validating its effectiveness for large-scale transportation network optimization.

Chapter 5

Optimizing Hub Locations and Airplane Routes

Building on the previous chapter, which examined hub location, profit maximization, and flight assignments, this chapter addresses the challenge of limited airplane availability. To resolve this issue, we introduce a model that optimizes the same objectives while incorporating airplane availability constraints. This updated model enhances hub location decisions, improves demand fulfillment, and optimizes both shipment and airplane routing. Specifically, we propose the Hub Location Problem with Profit Maximization with Airplane Routes (HLPP-PR), which captures key network dynamics and operational constraints. Additionally, we implement Score-based Labeling (SL) and a Hybrid Heuristic (HH) approach to improve computational efficiency. Finally, we present computational results and conduct sensitivity analyses to evaluate the model's robustness and effectiveness.

5.1 Mathematical Formulation

In this session, we modify the HLPP-P formulation to obtain HLPP-PR by incorporating additional constraints related to airplane routing. These constraints ensure that the optimal transportation plan takes into account the operational limitations of the airplanes.

5.1.1 Path-based Formulation (HLPP-PR)

We introduce the set of airplanes $G = \{0, 1, 2, ..., g\}$, where each airplane $g \in G$ is unique and subject to specific operational constraints. Accordingly, we define P_g as the set of directed feasible paths for airplane $g \in G$. The additional index sets required for formulating the problem are described as follows:

Index Set	**Description**
G	The set of available airplanes.
P_g	The set of all directed feasible paths from origin $o(g) \in N$ to destination $d(g) \in N$ for airplane $g \in G$, where $\mathcal{P}^g = \bigcup_{g \in G} P_g$.

Compared with P_k and P_g, a "feasible" path for a commodity satisfies delivery time requirements, typically within either half a day or a full day, while airplane paths account for operational constraints, typically one or two full days. Additionally, airplane routes are either round-trip or directed to a specific destination. Moreover, feasible paths consider the maximum allowable number of arcs to minimize the risk of physical damage during

transport for commodities and account for daily airplane maintenance.

Similar to the previous setting, the fixed and operational costs for each flight are determined by both the airplane model and selected path, with the remaining capacity varying based on the travel distance along $(i, j) \in A$. The additional parameters required to formulate the problem are described as follows:

Parameters	**Description**
c_g^p	Overall cost of a flight for the airplane $g \in G$ on path $p \in P_g$.
t_g^p	Time spent on path $p \in \mathcal{P}^g$ including traveling and material handling time.
$\Gamma_{g(i,j)}$	Remaining capacity of an airplane $g \in G$ on arc $(i, j) \in A$.
β_g	Available time for airplane $g \in G$ (e.g., 24 or 48 hours).

We also define the following indicator parameters.

Indicators	**Description**
$\Delta_{(i,j)}^p$	1 if arc $(i, j) \in A$ is contained in the path $p \in \mathcal{P}_k \cup \mathcal{P}_g$, 0 otherwise.

The new indicator $\Delta_{(i,j)}^p$ establishes the relationship between paths and arcs while accounting for both commodity and airplane routes.

Decision Variables	Description
x_k^p	The fraction of commodity $k \in K$ shipped on path $p \in P_k$, where $t_k^p \leq \beta_k$;
z_g^p	1, if airplane $g \in G$ is operated on path $p \in P_g$, where $t_g^p \leq \beta_g$; 0, otherwise.

The decision variable x_k^p is redefined as a fractional value, representing the fraction of multiple paths being selected for commodity $k \in K$. Meanwhile, z_g^p indicates the path chosen for airplane $g \in G$. Lastly, the decision variable y_i retains its original function, indicating the operational status of the hubs.

The objective of this problem is to maximize overall profit by balancing revenue and costs. Revenue is generated by meeting customer demand, while costs include the expenses associated with airplane route selection and hub operations. The parameters required for this formulation are derived from customer specifications, aircraft types, potential route options, and hub details, ensuring that the model aligns with operational and logistical requirements. Accordingly, the HLPP-PR presents the objective function along with the model constraints as outlined below:

$$\textbf{[HLPP-PR]} \quad \max \quad \sum_{k \in K} \sum_{p \in P_k} r_k w_k x_k^p - \sum_{g \in G} \sum_{p \in P_g} c_g^p z_g^p - \sum_{i \in N} f_i y_i \tag{5.1}$$

s.t.

$$\sum_{p \in P_k} x_k^p \leq 1 \qquad k \in K \qquad (5.2)$$

$$\sum_{p \in P_g} z_g^p \leq 1 \qquad g \in G \qquad (5.3)$$

$$\phi_i^p x_k^p \leq y_i \qquad i \in N, k \in K, p \in P_k \qquad (5.4)$$

$$\sum_{k \in K} \sum_{p \in P_k} \Delta_{(i,j)}^p w_k x_k^p \leq \sum_{g \in G} \sum_{p \in P_g} \Gamma_{g(i,j)} \Delta_{(i,j)}^p z_g^p \qquad (i,j) \in A \qquad (5.5)$$

$$0 \leq x_k^p \leq 1 \qquad k \in K, p \in P_k \qquad (5.6)$$

$$y_i \in \{0,1\} \qquad i \in N \qquad (5.7)$$

$$z_g^p \in \{0,1\} \qquad g \in G, p \in P_g \qquad (5.8)$$

Constraint (5.2) ensures the commodity $k \in K$ can be satisfied through the selected path(s) $p \in P_k$. Constraint (5.3) ensures that each airplane $g \in G$ select at most one path $p \in P_g$. Constraint (5.4) makes sure the hub $i \in N$ is operational when the selected path $p \in P_k$ passes through its location. Constraint (5.5) limits the capacity of the commodities transported by the airplanes $g \in G$ on arc $(i,j) \in A$. The remaining constraints (5.6) - (5.8) denote the domains of the decision variables.

5.2 Solution Approach

Similar to the HLPP-P model, the HLPP-PR model is very challenging to solve. This is due to the exponential growth of decision variables (i.e., x_k^p, z_g^p, y_i) as more nodes are considered. Therefore, to address this challenge, we go beyond simply applying the GA. We further exploit the problem's structure and introduce an enhanced approach that combines GA with Score-based Labeling and a Hybrid Heuristic technique (GA+SL+HH). This integrated method enables us to obtain high-quality feasible solutions more effectively. Figure (5.1) illustrates the overall process of the proposed solution approach.

To efficiently solve the HLPP-PR problem, we decompose it into multiple sub-problems using GA. In each iteration, these sub-problems are solved individually, and their solutions are compared. The GA then filters out less optimal solutions, gradually refining the results through successive iterations. To further enhance efficiency, we apply Score-based Labeling (SL) and a Hybrid Heuristic (HH) technique while solving each sub-problem, allowing us to quickly obtain feasible solutions. The process continues until the termination condition is met, at which point the best feasible solution is identified.

The following subsections provide additional explanations of the GA in subsection (5.2.1), expanding on the content discussed in Section (4.2). Furthermore, the details of the SL and HH methods are also presented in subsection (5.2.2) and (5.2.3).

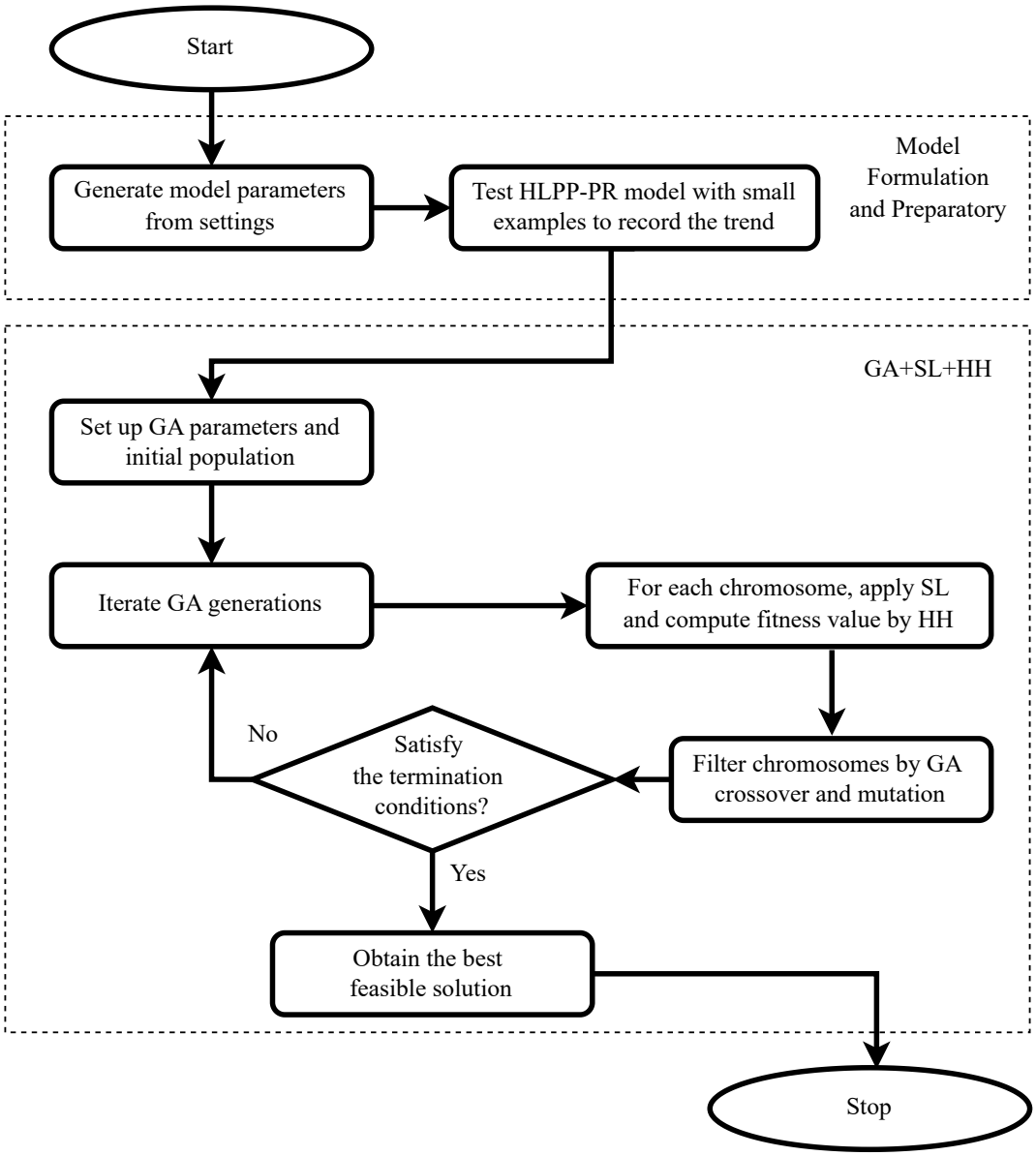

Figure 5.1: Overall process of solution approach for HLPP-PR.

5.2.1 Genetic Algorithm for HLPP-PR

In this subsection, we introduce additional GA settings, building on the content discussed in Section (4.2), to compute the best feasible solution for the HLPP-PR model.

5.2.1.1 Components and Fitness Function of GA for HLPP-PR

As with the HLPP-P model, we begin by defining the decision variable y_i as a gene, where its opening status is represented by $\hat{y}_i$. A value of 1 indicates that the potential hub is open, while a value of 0 signifies that it remains closed. Next, we define a chromosome as a feasible configuration of potential hubs, representing a specific combination of selected hubs. Lastly, the population consists of a set of possible solutions, each corresponding to a different arrangement of potential hubs.

In the context of the fitness function, each chromosome can be treated as a sub-problem of the HLPP-PR, which is then solved to obtain its optimal solution. Since the decision variable y_i is transformed into $\hat{y}_i$, it directly affects not only the feasible paths for commodities but also those for airplanes. Consequently, the sets P_k can be reduced to $\hat{P}_k$, with $\hat{\mathcal{P}}^k = \bigcup_{k \in K} \hat{P}_k$. Similarly, the sets P_g can be reduced to $\hat{P}_g$, and corresponding $\hat{\mathcal{P}}^g = \bigcup_{g \in G} \hat{P}_g$. As a result, the GA sub-problem corresponding to each chromosome can be formulated as follows:

$$\textbf{[sub-HLPP-PR]} \quad \max \quad \sum_{k \in K} \sum_{p \in \hat{P}_k} r_k w_k x_k^p - \sum_{g \in G} \sum_{p \in \hat{P}_g} c_g^p z_g^p - \sum_{i \in N} f_i \hat{y}_i \tag{5.9}$$

s.t.

$$\sum_{p \in \hat{P}_k} x_k^p \leq 1 \qquad k \in K \tag{5.10}$$

$$\sum_{p \in \hat{P}_g} z_g^p \leq 1 \qquad g \in G \tag{5.11}$$

$$\sum_{k \in K} \sum_{p \in \hat{P}_k} \Delta_{(i,j)}^p w_k x_k^p \leq \sum_{g \in G} \sum_{p \in \hat{P}_g} \Gamma_{g(i,j)} \Delta_{(i,j)}^p z_g^p \qquad (i,j) \in A \tag{5.12}$$

$$0 \leq x_k^p \leq 1 \qquad k \in K, p \in \hat{P}_k \tag{5.13}$$

$$z_g^p \in \{0,1\} \qquad g \in G, p \in \hat{P}_g \tag{5.14}$$

Due to the constraints imposed by $\hat{y}_i$, the feasible paths for both commodities and airplanes are restricted, leading to a reduction in the corresponding sets within the objective function and constraints (5.10), (5.11), and (5.12). Moreover, the original constraints (5.4) and (5.7) are eliminated, as the status of potential hubs is set in advance. As a result, the sub-problem becomes significantly smaller than the original problem, allowing for more efficient computations and facilitating the identification of an optimal solution in a shorter time.

5.2.1.2 Iterative Process and Genetic Operations of GA for HLPP-PR

The GA flow process for HLPP-PR is mostly the same as HLPP-P (i.e., Figure (4.4)), except for differences in the formulation and algorithm used in the fitness function. It starts with population initialization, where potential solutions are encoded as genes, chromosomes, and populations. The algorithm then goes through selection, crossover, and

mutation to refine solutions, gradually converging to the best feasible outcome. The termination criteria remain the same, stopping the process when the fitness value stabilizes over consecutive generations or when a computational limit is reached.

Also, the genetic algorithm process for HLPP-PR remains similar to HLPP-P, where crossover and mutation are used to explore and refine solutions over multiple generations, as shown in Function (3) and (4). The primary distinction lies in the incorporation of the `check_attributes()` function, which enhances the evaluation process by considering the number of airplanes in addition to the number of opening hubs. During the crossover operation, after generating offspring through single-point crossover, the algorithm checks whether the offspring satisfy the required constraints. It evaluates the locations of the hubs and the number of available airplanes to determine feasibility. Similarly, in the mutation process, candidate solutions are randomly generated. However, only those that meet the attribute requirements for hub allocation and airplane availability are accepted. This filtering step helps remove unrealistic candidates early, increases computational efficiency, and directs the population toward better solutions.

However, when evaluating the quality of the chromosomes, even though we decompose the HLPP-PR into sub-problems using GA to accelerate computation, solving each sub-problem still requires considerable time. Achieving a feasible solution with a lower gap within a short time limit remains challenging. Therefore, we implemented two approaches to obtain a good feasible solution—whether local or global—while further reducing computational time. The first approach is the score-based labeling approach (5.2.2), and the second is the hybrid heuristic technique (5.2.3). The score-based labeling approach aims to reduce the number of decision variables x_k^p and z_g^p thereby accelerating the computa-

tional process, while the hybrid heuristic technique focuses on computing sub-HLPP-PR and obtain local or global optimal solution more efficiently.

5.2.2 Score-based Labeling (SL)

A labeling algorithm is a computational method used to assign labels or scores to elements based on predefined criteria. It is widely applied in optimization, machine learning, and network analysis to evaluate and prioritize paths, nodes, or items. In network design, labeling algorithms are essential for assessing paths or nodes based on factors such as cost, capacity, and reliability. While traditional methods, such as Ford-Fulkerson and Dijkstra's, focus on finding optimal flow or shortest paths, our score-based labeling approach extends this by incorporating additional weighted criteria, including airplane specifications, node centrality, and demand requirements. This allows for more dynamic path evaluation, optimizing profitability and operational efficiency while reducing decision variables.

The SL approach distinguishes itself by using ranking evaluation rather than the domination rule. This enables more efficient filtering of less feasible paths and provides flexibility in selecting a subset of paths based on an acceptable level of risk. The reduction in decision variables leads to faster computation, particularly in large-scale network design problems. Figure (5.2) illustrates the detailed process flow of SL.

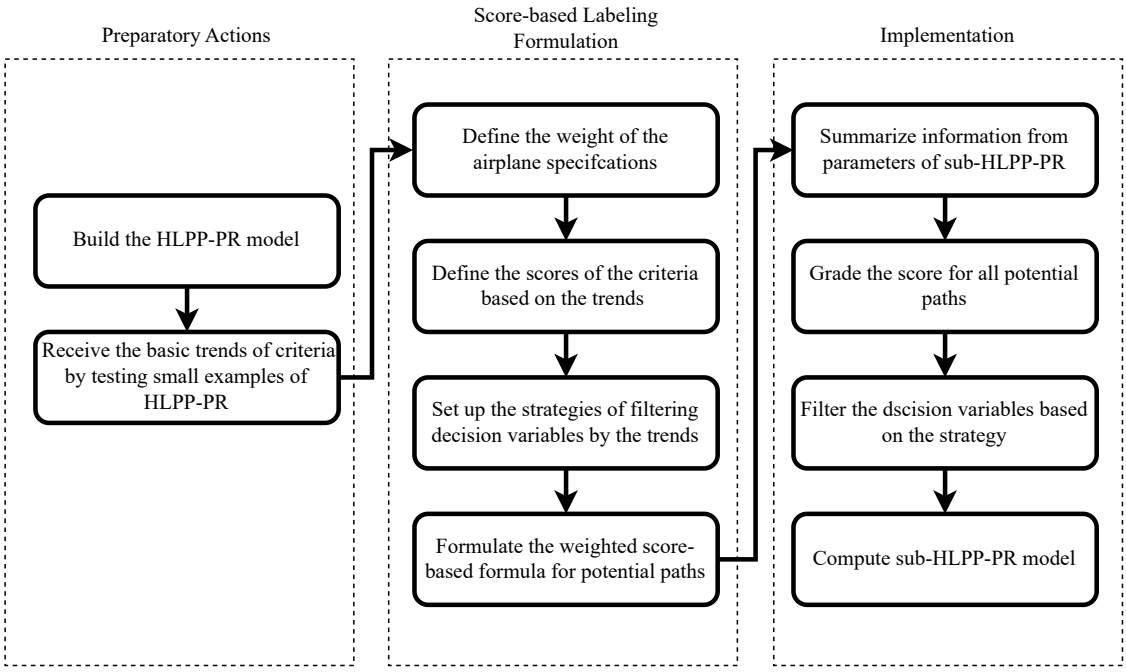

Figure 5.2: Detailed process flow of SL.

The first step of SL is to have a preparatory action on the parameters. In our study, once we build the HLPP-PR model, we can determine that the paths of commodities (x_k^p) and airplanes (z_g^p) have a specific likelihood of passing through hubs to generate revenue. This is achieved by analyzing trends derived from training the model on small-scale examples. For example, when the cost of operating a hub is low and the unit revenue of the commodity is high, airplanes are more likely to pass through hubs. Therefore, by examining these small-scale scenarios, we gain insights that help define the weights of the evaluation criteria effectively.

Secondly, we establish a weighted score-based formula to evaluate all potential paths. In our

study, the geographic positions of nodes, including the airplane's origin, destination, and potential hub numbers, node centrality (e.g., central or peripheral on the map), as well as the total demand at each node, encompassing both outgoing and incoming demand, play a critical role in the path selection process. By incorporating these factors, we assign weights to each criterion derived from training results on small-scale examples. This allows us to compute the scores for potential paths, enabling a ranking based on their suitability. Accordingly, we initially define the index set and variables below:

Variables	**Description**
$N(p)$	Set of nodes in path $p \in P_g$.
S_g^p	Score indicating whether airplane $g \in G$ is operated on path $p \in P_g$.
w_g	Weight of airplane $g \in G$.
w_i^c	Weight of position centrality for node $i \in N(p)$.
w_i^d	Weight of demand summation for node $i \in N(p)$.
s_i	Basic score of node $i \in N$.
s_i^h	Score indicating whether node $i \in N(p)$ is in the open hub list; $s_{o(g)}^h$ and $s_{d(g)}^h$ represent scores for the origin and destination of the airplane $g \in G$ is in the open hub, respectively.

The score S_g^p for operating airplane $g \in G$ on path $p \in P_g$, corresponding to the decision variable z_g^p, is calculated based on the weighted criteria, reflecting factors such as hub locations, demand levels, and operational efficiency of the airplanes. Additionally, the weight of the node i included in path $p \in P_g$ accounts for three primary factors: airplane's specifi-

cation, position centrality and demand requirements [90]. Airplane specification considers the model of the airplane. Position centrality evaluates the strategic significance of the node within the network (e.g., central or peripheral location), while demand requirements reflect the node's ability to generate or fulfill transportation needs effectively.

Specifically, the weight of the airplane, w_g, reflects the airplane's specification, which accounts for its economic efficiency in transporting commodities. The weight of position centrality, w_i^c, reflects the strategic importance of the node $i \in N(p)$ within the network [90]. Nodes with higher centrality (e.g., those located centrally on the geographic map) are typically assigned higher weights, as they are more likely to serve as effective hubs for connecting multiple paths and meeting demand efficiently. Also, the weight of demand summation, w_i^d, indicates the total demand associated with the node, including both its sending and receiving demand [90]. This weight highlights the significance of nodes with high demand levels, as they are critical in optimizing the network's profitability and efficiency. Nodes with greater demand summation are typically prioritized when selecting paths, as they contribute more to the overall throughput and revenue potential of the system.

The formula used to calculate these path scores is defined as follows:

$$S_g^p = w_g * \Big(\sum_{i \in N(p)} (w_i^c * (s_{o(g)}^h + s_{d(g)}^h + s_i^h)) + \frac{\sum_{i \in N(p)} w_i^d * s_i}{|N(p)|} \Big) \tag{5.15}$$

The first and second scores, $s_{o(g)}^h$ and $s_{d(g)}^h$, evaluate whether the origin and destination of the airplane $g \in G$ are located at an open hub $\hat{y}_i = 1$. Airplanes operating from open hubs

have greater flexibility in delivering commodities compared to those operating from non-hub cities. The third score s_i^h assesses the number of open hubs the airplane passes through. Paths that pass through more open hubs are typically assigned a higher probability of utilization. Finally, we account for the demand level of the path by calculating the average demand requirements of the nodes along the path, which indicates the path's efficiency in achieving higher revenue.

Once the score S_g^p is obtained for each path $p \in P_g$, various strategies can be implemented to reduce the decision variables x_k^p and z_g^p according to the level of risk tolerance. In our research, we suggest three different strategies, which include aggressive, standard, and defensive strategies. The choice of strategy varies based on the trends observed in the small examples. Typcially, an aggressive strategy represents the most likely scenarios, while a standard strategy assumes general, expected situations. In contrast, a defensive strategy eliminates low-probability scenarios only. For example, if the distribution of the scores follows a normal distribution, different strategies can be devised based on the statistical thresholds. We can define the aggressive strategy that includes approximately the top 10.6% of potential paths, corresponding to scores that are 1.25 standard deviations (σ) above the mean (μ). The standard strategy considers about 31.9% of paths with scores that are 0.5 standard deviations (σ) above the mean (μ), and defensive strategy includes a broader selection, approximately 69.1% of paths, covering scores that fall within 0.5 standard deviations (σ) below the mean (μ).

Finally, based on these scores, we can filter paths according to the selected strategy, effectively reducing the decision variable set when solving a sub-problem of HLPP-PR. While this reduction may carry a risk of excluding the global optimal solution, the SL approach

offers the significant advantage of substantially decreasing the number of variables.

5.2.3 Hybrid Heuristic (HH)

In GA, we fix the hubs as chromosomes and define a set of chromosomes as the population. To calculate the fitness value of a chromosome, we build a sub-HLPP-PR and compute the optimal solution as the fitness value. When constructing the sub-HLPP-PR, the index set N includes two components: the fixed nodes (either with or without open hubs) and other non-hub nodes. Initially, all non-hub nodes are considered together to calculate the optimal solution. However, as the number of non-hub nodes in the sub-problem increases, the size of the decision variables grows exponentially. To find a locally optimal solution for the sub-HLPP-PR within a short time limit, we employ a hybrid heuristic technique to decompose the non-hub nodes, allowing the problem to be solved heuristically. This significantly accelerates the computation of the sub-problem.

Inspired by the traditional reinforcement learning (RL) approach, which involves an agent interacting with an environment by taking actions, receiving rewards, and updating its policy based on feedback, the hybrid heuristic approach shares similar mechanisms but with less emphasis on the learning component. In RL, an agent learns to maximize cumulative reward through trial and error, typically following steps such as initializing the environment, observing states, selecting actions, receiving rewards, and updating the policy or value function. In HH, we adopt similar concepts from RL and define five key components: Agent, Environment, Action, Reward, and State. These definitions are applied to the sub-HLPP-PR as follows:

- Agent: The agent is the learner or decision-maker that interacts with the environment. In our study, the agent aims to optimize profit by selecting suitable nodes, including both hub and non-hub nodes, for delivery.
- Environment: The environment encompasses everything that the agent interacts with. In this scenario, the environment includes the total nodes, the costs associated with traveling between each pair of nodes, and customer demand.
- Action: An action is a decision made by the agent at a given state. In our study, actions involve selecting the next node for delivery from the current node. For instance, if airplane $g \in G$ is currently at City A, the action could be to travel to City B, City C, or another city along the route.
- State: A state represents the agent's current situation. In this case, a state is defined by the current city where the airplane is located, along with the set of cities already confirmed for delivery. For instance, if airplane $g \in G$ has confirmed deliveries to City A and City B, and is currently in City C, the state can be represented as (C, A, B).
- Reward: The reward is a feedback signal received by the agent after performing an action. In our study, the agent seeks to maximize the total reward, which corresponds to maximizing the profit generated by the selected actions.

When we compute a sub-HLPP-PR, the state S_t and the action A_t^M at step t is defined. For each potential action A_t^m, we calculate the corresponding reward R_t^m and subsequently update the state by selecting the nodes (action) that yield higher profits. It is important to note that the reward calculation becomes increasingly time-consuming as the number

of nodes chosen grows, particularly in the final state. To address this, once a certain state $S_{t'}$ is reached, actions are limited by focusing only on high-value potential nodes based on prior rewards rather than evaluating all possible non-hub nodes. As we continue updating the state, the reward converges, eventually allowing us to identify the local optimal solution. Based on the concepts above, we propose the hybrid heuristic algorithm displayed as follows:

Algorithm 5 Hybrid Heuristic Algorithm

$G \leftarrow g$, $N \leftarrow i$, $T \leftarrow t$
$t = 1$
$\tilde{D} = \emptyset$
$R_t = -inf$
$S_t \leftarrow$ `initialize_state`$(o(g), d(g), \hat{y}_i)$
$A_t^M = \{A_t^1, A_t^2, ..., A_t^{|M|}\} \leftarrow$ `update_potential_actions`$(S_t, \tilde{D})$

while $S_t \leq S_{|T|}$ **do**
    for $m = 1, 2, ...|M|$ **do**
        $A_t^{m'} \leftarrow$ `score-based_labeling`(A_t^m)
        $R_t^m \leftarrow$ `sub-HLPP-PR`$(A_t^{m'})$
        $\tilde{D} \leftarrow$ `record_reward`(R_t^m)
    end for
    $A^{best}, R^{best} \leftarrow$ `rank_reward`$(R_t^M = \{R_t^1, R_t^2, ..., R_t^{|M|}\})$
    if $R_t \leq R^{best}$ **then**
        $t \leftarrow t + 1$
        $R_t \leftarrow R^{best}$
        $S_t \leftarrow$ `update_state`(A^{best})
        $A_t^M \leftarrow$ `update_potential_actions`$(S_t, \tilde{D})$
    else
        `break`
    end if
end while

The proposed algorithm employs a heuristic framework to iteratively select actions and

update states with the goal of maximizing profits over successive iterations. The key steps are outlined as follows:

Step 1 (Initialization): The algorithm begins by initializing key variables, where the set of the airplanes $G \leftarrow g$, nodes $N \leftarrow i$, and the iteration status of the states $T \leftarrow t$. The reward at iteration $t = 1$, denoted as R_t, is initialized to negative infinity, and the database $\tilde{D}$ is initially set to empty. The initial state, S_t, is set through the function `initialize_state`$(o(g), d(g), \hat{y}_i)$, which considers the origin of the airplane $o(g)$, destination $d(g)$, and an estimated open hubs $\hat{y}_i$ to define the starting conditions. The set of potential actions A_t^M is then generated using the function `update_potential_actions`$(S_t, \tilde{D})$ based on the initial state.

Step 2 (Main Iterative Process): The algorithm proceeds through an iterative process while the current state S_t remains unequal to the final state $S_{|T|}$. For each potential action $A_t^m \in A_t^M$ at iteration t, the following operations are executed:

- The score-based labeling function `score-based_labeling`(A_t^m) is applied to filter the decision variables and update the action to $A_t^{m'}$.
- The reward R_t^m associated with the action $A_t^{m'}$ is calculated using the sub-problem `sub-HLPP-P`$(A_t^{m'})$ (objective function (5.1)). Then the computed reward is stored in the dataset $\tilde{D}$ for future decision reference.

Step 3 (Action Selection and State Update): Once the rewards for all potential actions have been calculated, the set of rewards $R_t^M = \{R_t^1, R_t^2, ..., R_t^{|M|}\}$ is ranked, and the best action A^{best} with the highest reward R^{best} is selected through the function `rank_reward(`R_t^M`)`. If the current reward R_t is less than or equal to R^{best}, the following updates occur:

- The iteration index t is incremented.
- The reward R_t is updated to R^{best}.
- The state S_t is updated based on the the best potential actionvia the function `update_state`(A^{best}).
- The set of potential actions A_t^M is updated by referring to the new state S_t and the stored dataset $\tilde{D}$.

Step 4 (Termination): The algorithm iterates until the final state $S_{|T|}$ is reached, marking the termination of the process. Additionally, the heuristic stops if the best reward R^{best} is worse than the current reward R_t. The total number of states, T, is determined by several factors, including the number of airplanes, the requirement for a round trip, and adjustments such as the desired hubs to be used and the expected overlap of paths that the airplanes will traverse. Alternatively, T can be left to unlimited until the stopping criterion is met, which either the best reward is found or all the non-hub nodes are considered. To enhance randomness, we assign an equal probability to increasing or decreasing the total number of states by one, ensuring that T varies rather than remaining constant.

In summary, the algorithm operates within a heuristic framework, starting with the initialization of key variables and the establishment of the initial state, which incorporates factors like the airplane's origin, destination, and estimated open hubs. At each iteration, the algorithm first evaluates potential actions to identify feasible options. It then calculates the reward for each action and selects the one with the highest reward. Finally, the state is updated based on the chosen action. This iterative refinement continues until the terminal state is reached, or if no improvement in reward is observed, ensuring the algorithm

converges efficiently toward a locally optimal solution.

By employing the HH approach, the main advantage lies in its ability to rapidly converge toward a feasible solution. This efficiency is achieved through a focused exploration of feasible solutions, prioritizing high-value actions based on previous rewards. However, a potential drawback of the HH approach is that it does not guarantee a global optimal solution.

5.3 Computational Results

Similar to the approach in Section (4.3), we conducted extensive computational experiments to assess the effectiveness of the proposed methods while integrating airplane-related parameters. This analysis considers airplane specifications and their associated operational costs, ensuring a comprehensive evaluation of the model's performance under varying conditions. The experiments were carried out on the same workstation and software environment (AMD Ryzen 9 5900X 12-Core Processor, 3.70 GHz, 64GB RAM; IBM ILOG CPLEX 22.1.1.0, Python 3.10.11, docplex 2.25.236). The solution criteria remained the same as in HLPP-P, ensuring that each instance was solved to optimality with a 1% gap tolerance and a maximum computational time of two hours.

This section is organized as follows: Subsection (5.3.1) introduces the additional parameter settings of the dataset for HLPP-PR. The managerial insights, which provide key takeaways from the computational experiments and their implications for decision-making, are presented in subsection (5.3.2). To evaluate the computational performance of the proposed algorithms, numerical results from larger-sized instances based on the dataset are displayed in subsection (5.3.3). Lastly, subsection (5.3.4) discusses sensitivity analysis focusing on the economies of scale factor.

5.3.1 Parameter Setting for HLPP-PR

Firstly, we set up the sets N, A, and K following the same approach as in subsection (4.3.1). Nodes N represent customer locations based on 2022 U.S. Census Bureau population data,

with cities near airports selected under the assumption of no geographical barriers. The set of arcs A is determined using the geodesic distance based on the WGS-84 standard, where (i, j) denotes the arc from node $i \in N$ to node $j \in N$. Commodities K and the demand matrix w_k are measured in kilograms, with unit revenue r_k remaining constant across O-D pairs.

Next, we define the set of available airplanes G. Following the same approach as before, we define each airplane $g \in G$, assuming all airplanes in the set have uniform specifications based on the Pilatus PC-12 NG model. As a result, all airplane-related parameters, such as fixed flight costs, aircraft speed, average operating cost per hour, total capacity, and fuel consumption per hour, are derived from the specifications of this model. These parameters are used to calculate various costs associated with each airplane $g \in G$, including the flight cost $c_{g(i,j)}$, travel time $t_{g(i,j)}$, and the remaining capacity $\Gamma_{g(i,j)}$ for the arcs. Additionally, in a similar way to P_k, for each airplane $g \in G$, we generate the set of all feasible directed paths, denoted as P_g. These paths are subject to the condition that the trip is round-trip and the time required t_g^p does not exceed the available time β_g. Then, we summarize c_g^p, the overall cost of a flight for the airplane $g \in G$ on path $p \in P_g$ based on the cost summation of the arcs $c_{g(i,j)}$. Finally, we define the origin $o(g)$ and destination $d(g)$ for each airplane. These are placed in the most populous cities within the states; specifically, we assign each airplane to one of the cities for each state: Charlotte, Jacksonville, Atlanta, Nashville, and Charleston.

In summary, the detailed information regarding these parameters in displayed in Table (5.1).

Table 5.1: Parameters with airplane routing.

Parameter	Value	Unit	Descriptions
d_g	1,400	\$	fixed cost of a flight for airplane $g \in G$
Γ_g	1,800	kg	total capacity for airplane $g \in G$
sp_g	280	km/hr	aircraft speed for airplane $g \in G$
op_g	1,097	\$/hr	average operating cost per hour for airplane $g \in G$
fu_g	175	kg/hr	fuel spent per hour for airplane $g \in G$
t^l	1	hr	loading time of the commodity at a node
t^u	1	hr	unloading time of the commodity at a node
t^s	1	hr	sorting time of the commodity at a hub
β_k	12	hr	delivery time limit for commodity $k \in K$
β_g	24	hr	delivery time limit for airplane $g \in G$
a_k	3		maximal allowed arcs in a path for commodity $k \in K$
a_g	4		maximal allowed arcs in a path for airplane $g \in G$
r_k	20	\$/kg	unit revenue of the commodity
f_i	30,000	\$	fixed cost of operating hub $i \in N$
$t_{g(i,j)}$	$vary^1$	hr	time spent of a flight for airplane $g \in G$ on arc $(i,j) \in A$
$\Gamma_{g(i,j)}$	$vary^2$	kg	remaining capacity of airplane $g \in G$ on arc $(i,j) \in A$
$c_{g(i,j)}$	$vary^3$	\$	overall cost of a flight for airplane $g \in G$ on arc $(i,j) \in A$

[1] Formula: $t_{g(i,j)} = (Dist(i,j)/sp_g)$
[2] Formula: $\Gamma_{g(i,j)} = \Gamma_g - (fu_g * t_{g(i,j)})$
[3] Formula: $c_{g(i,j)} = d_g + op_g * t_{g(i,j)}$

Similar to the previous chapter, we configure the GA by defining its components (gene, chromosome, population), fitness function (sub-HLPP-PR), genetic operations (crossover, mutation), and iterative process. Specifically, the decision variable y_i is represented as a gene, where $\hat{y}_i$ indicates hub status (1 for open, 0 for closed). A chromosome consists of binary values corresponding to potential hubs, and the population is set at 10 chromosomes. Moreover, the initial population is randomly generated with a bias toward fewer open hubs and airplane origins to enhance efficiency. The fitness function follows sub-HLPP-PR, with a 2-hour time limit and a 1% gap tolerance.

Furthermore, we employ custom crossover and mutation functions to prevent unrealistic

solutions, gradually relaxing constraints over generations. The mutation probability is set at 10%, meaning each gene has a 10% chance of mutating. Also, to enhance computational efficiency, duplicate chromosomes are excluded from the selection process. During offspring generation, we select the top 50% of solutions based on fitness value, ensuring high-quality solutions by retaining one elite chromosome. Finally, the algorithm terminates when it reaches 50 generations, shows no improvement for five consecutive generations, or meets the 2-hour time limit.

In the SL approach, priority is given to the number of open hubs an airplane passes through, as well as whether its origin and destination are located at open hubs. Additionally, we emphasize the average score derived from the demand summation of nodes along each path. After calculating these scores, we implement an aggressive strategy to select the top 10% of potential paths, effectively reducing approximately 90% of lower-scoring paths. The detailed settings are provided in Table (5.2).

Table 5.2: Setting for score-based labeling.

Variables	Value	Descriptions
w_g	1	weight of airplane $g \in G$.
w_i^c	$vary$[1]	weight of position centrality for node $i \in N(p)$.
w_i^d	$vary$[1]	weight of demand summation for node $i \in N(p)$
s_i	0.2	basic score for the nodes $i \in N(p)$
s_i^h	0.5	basic score for node $i \in N(p)$ is in the open hub list
$s_{o(g)}^h$	0.25	basic score for the origin of the airplane $g \in G$
$s_{d(g)}^h$	0.25	basic score for the destination of the airplane $g \in G$

[1] Values are calculated as referred to [90] and normalized to relative values.

The values of the basic scores (i.e., s_i, s_i^h, $s_{o(g)}^h$, $s_{d(g)}^h$) are defined by considering their relative relationships. In this study, we emphasize the importance of airplanes passing through open hubs, assigning the highest score to this factor. For weight settings, we assume uniform weights for airplanes to simplify calculations, as their specifications are identical. Additionally, a node $i \in N$ with higher position centrality and demand summation is assigned a higher weight [90]. In our research, the weights for position centrality and demand summation are normalized to reflect relative values among the nodes.

Finally, the HH algorithm limits the scope of action exploration by restricting the evaluation of non-hub nodes once a certain state is reached, as discussed in subsection (5.2.3). For instance, when three airplanes are considered, the algorithm evaluates the top five actions (A_6^5) upon reaching the 6th state (S_6) and further narrows the evaluation to the top three actions (A_7^3) upon reaching the 7th state (S_7). All the restrictions during the HH process are dynamically adjusted by the dataset $\tilde{D}$ and state S_t, which is function `update_potential_actions`(S_t, $\tilde{D}$). Finally, the selection of actions is guided by previous rewards and the frequency of node occurrences stored in the dataset $\tilde{D}$, according to the

factors outlined in subsection (5.2.3).

5.3.2 Insights

We explore the key insights derived from the computational results, focusing on net profit and the decision variables y_i, x_k^p, and z_g^p in relation to parameter variations. While the number of nodes, typically determined by the customer market, is a fixed factor that heavily influences the complexity of the problem, the ability to adjust the selection of potential hubs and the number of airplanes provides opportunities for strategic optimization. Modifying these parameters allows businesses to analyze the resulting decision variables and net profit, offering valuable guidance for enhancing the performance of the transportation network. The table presenting the combinations of parameters is displayed as follows:

Table 5.3: Computational results with airplane routing.

Parameters					**Performance Indexes**				
$\|N\|$	Potential Hub	$\|G\|$	$\|\mathcal{P}^k\|$	$\|\mathcal{P}^g\|$	Net Profit	# of Open Hubs	Avg. Flight Utilization (%)	Demand Satisfaction by Weights (%)	Open Hub Locations[1]
10	10	3	906	1,681	97,749.6	2	86.49	46.84	[0, 2]
10	10	4	906	2,234	153,063.2	2	89.32	63.98	[0, 2]
10	10	5	906	2,789	196,435.5	2	92.85	76.50	[2, 4]
20	10	3	5,708	18,173	112,931.7	2	93.17	21.05	[0, 1]
20	10	4	5,708	24,102	179,435.1	2	97.94	28.91	[0, 1]
20	10	5	5,708	30,151	231,245.1	2	94.39	35.05	[0, 1]
20	20	3	22,994	18,173	112,931.7	2	92.82	21.05	[0, 1]
20	20	4	22,994	24,102	179,435.1	2	98.81	28.91	[0, 1]
20	20	5	22,994	30,151	231,245.1	2	94.39	35.05	[0, 1]
30	10	3	14,050	67,141	112,931.7	2	92.82	13.79	[0, 1]
30	10	4	14,050	88,886	179,435.1	2	97.98	18.95	[0, 1]
30	10	5	14,050	111,243	231,245.1	2	94.39	22.96	[0, 1]
30	20	3	56,530	67,141	112,931.7	2	92.82	13.79	[0, 1]
30	20	4	56,530	88,886	179,435.1	2	97.98	18.95	[0, 1]
30	20	5	56,530	111,243	231,245.1	2	94.37	22.96	[0, 1]

[1] 0: Charlotte. 1: Jacksonville. 2: Atlanta. 4: Charleston

Firstly, the number of airplanes plays a crucial role in determining net profit across networks of varying sizes and configurations. A higher number of airplanes consistently leads to increased net profit, provided that market conditions remain favorable. For instance, when the number of airplanes increases from 3 to 5, the system gains greater flexibility in handling complex routes and accommodating higher demand, regardless of the number of nodes. Additionally, the demand satisfaction column indicates that there is still room for further fulfillment of customer demand, suggesting potential opportunities for network expansion or operational adjustments. This finding emphasizes the importance of additional airplanes in strengthening the network's capacity, particularly as the network grows in size and complexity. However, further sensitivity analyses involving changes in revenue and costs are needed to determine the optimal number of airplanes for varying network conditions.

As the network size increases from 10 to 30 nodes, the system's complexity and resource requirements grow significantly. For example, with 10 potential hubs and 5 airplanes, the number of possible airplane paths increases from 2,789 to 111,243 as the network expands from 10 to 30 nodes—an almost 40-fold increase. However, the number of nodes appears to have minimal impact on net profit when the number of airplanes and potential hubs is fixed. Across different scenarios with the same configurations of airplanes and hubs, net profit remains relatively stable, even as the network expands. Meanwhile, the path selection for airplanes (z_g^p) shows a preference for routes passing through hubs located in populous cities, maximizing the utilization of high-demand paths. This demonstrates that the system can maintain consistent performance levels despite increasing network complexity, provided that resource allocation, such as the number of airplanes and hubs, remains unchanged. Consequently, resource availability proves to be a more critical factor than the size of

the network in optimizing net profit. A key reason for this is the selection of populous cities as potential hubs, which naturally attract demand and serve as efficient origins and destinations for the airplanes. In most network designs, the algorithm prioritizes identifying valuable routes, which in this case align with high-demand paths, as long as the associated costs remain reasonable.

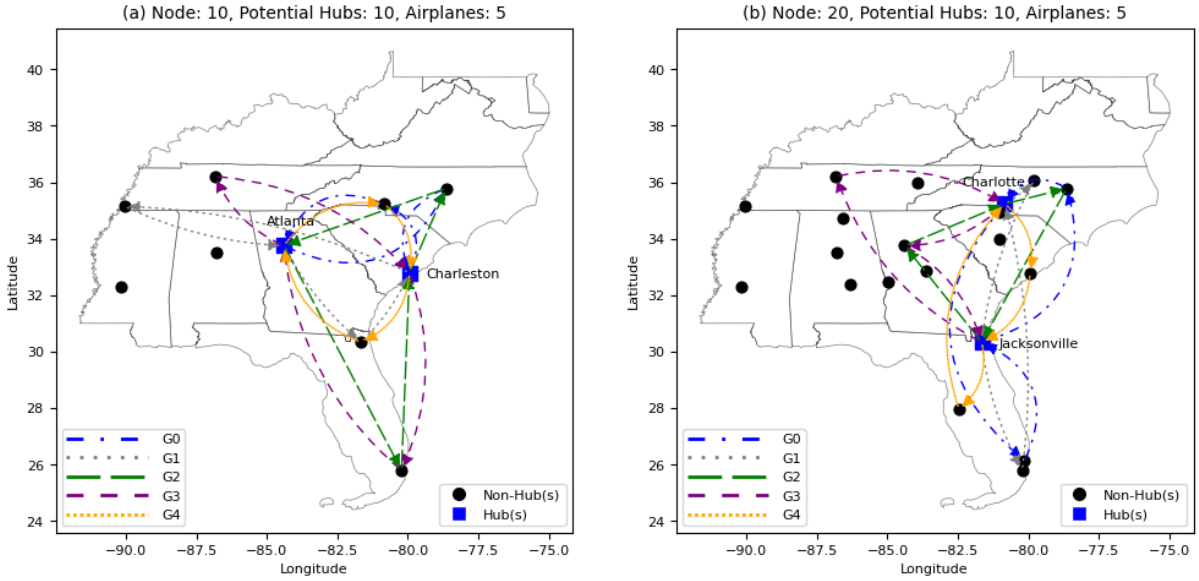

Figure 5.3: Visualization of the path selection comparison for core examples.

Specifically, expanding the nodes still has the potential to increase profit. For example, as shown in Figure (5.3), comparing scenarios with (a) 10 nodes/10 hubs/5 airplanes and (b) 20 nodes/10 hubs/5 airplanes reveals a significant increase in net profit. This improvement occurs because the transportation network increases the flexibility in flight assignments, allowing airplanes to select routes that pass through high-demand cities such as Tampa and Fort Lauderdale, thereby enhancing profitability. However, when the number of nodes

increases from 20 to 30, the profit remains stable, indicating that the additional nodes do not contribute valuable routes to enhance profitability. This suggests that beyond a certain threshold, expanding the network does not necessarily lead to better financial performance, as the newly added nodes may lack sufficient demand or strategic positioning to generate meaningful revenue.

5.3.3 Computational Performance Analysis

In this subsection, we evaluate the performance of our proposed algorithms on instances from the core southeastern U.S. region. The experiments involve the original HLPP-PR formulation, HLPP-PR with GA, and HLPP-PR with GA+SL+HH, tested under diverse parameter settings. The results are summarized in Table (5.4).

Firstly, the table presents the computational performance of the algorithms across different problem sizes, with key parameters such as the number of nodes ($|N|$), potential hubs, and the number of airplanes ($|G|$). The problem size increases from 10 to 50 nodes, with potential hubs ranging from 10 to 20, and the number of airplanes varying from three to five. This increase in parameters progressively raises the complexity of the problem, resulting in a significant expansion of potential paths for commodities ($\mathcal{P}^k$) and airplanes ($\mathcal{P}^g$).

The table also provides computational performance results. The 'CPU Time' column indicates the time taken to solve each instance within a 2-hour limit, while the 'Net Profit' and 'Gap' columns offer insights into the performance of each method in terms of solution quality. Notably, the gap with HLPP-PR serves as a key performance measure, where

Table 5.4: Computational performance: Airplane routes.

Parameters			**HLPP-PR**			**HLPP-PR w. GA**		**HLPP-PR w. GA+SL+HH**	
$\|N\|$	Potential Hubs	$\|G\|$	Net Profit	LP Gap (%)	CPU Time (sec)	Gap with HLPP-PR (%)	CPU Time (sec)	Gap with HLPP-PR (%)	CPU Time (sec)
10	10	3	97,749.6	1.00	453.7	0.00	93.85	0.00	90.2
10	10	4	153,063.2	1.00	302.8	-0.03	419.1	0.00	346.1
10	10	5	196,435.5	1.00	1708.1	0.00	1591.4	0.00	785.4
20	10	3	112,931.7	6.26	7200.0	0.00	1551.0	0.00	193.8
20	10	4	179,435.1	1.00	3487.8	0.00	2414.6	0.00	1183.3
20	10	5	231,245.1	1.00	6407.7	0.00	3855.2	0.00	3312.1
20	20	3	112,931.7	50.39	7200.0	0.00	3564.7	0.00	366.3
20	20	4	179,435.1	12.42	7200.0	0.00	5037.7	0.00	2365.3
20	20	5	231,245.1	22.49	7200.0	0.00	7200.0	0.00	5281.2
30	10	3	112,931.7	16.04	7200.0	0.00	4333.2	0.00	198.2
30	10	4	178,955.1	6.29	7200.0	0.27	6343.2	0.27	1399.5
30	10	5	231,145.1	22.90	7200.0	-1.71	7200.0	0.04	4655.4
30	20	3	105,949.0	65.15	7200.0	6.18	6903.3	6.18	301.5
30	20	4	159,943.2	45.21	7200.0	10.86	7200.0	10.86	3087.4
30	20	5	231,245.1	24.91	7200.0	0.00	7200.0	0.00	5049.6
40	10	3	109,179.6	58.52	7200.0	3.32	6248.1	3.32	210.7
40	10	4	178,315.1	27.66	7200.0	0.62	7004.5	0.62	1200.8
40	10	5	231,245.1	25.19	7200.0	0.00	7200.0	0.00	4059.8
40	20	3	93,174.9	90.11	7200.0	17.49	7200.0	17.49	370.5
40	20	4	0	∞	7200.0	100.00	7200.0	100.00	4472.6
40	20	5	0	∞	7200.0	100.00	7200.0	100.00	7200.0
50	10	3	110,714.7	58.52	7200.0	1.96	7200.0	1.96	227.2
50	10	4	170,487.5	36.76	7200.0	4.99	7200.0	4.99	2213.0
50	10	5	226,127.3	28.48	7200.0	2.21	7200.0	2.21	4587.2
50	20	3	0	∞	7200.0	100.00	7200.0	100.00	350.6
50	20	4	0	∞	7200.0	100.00	7200.0	100.00	2649.8
50	20	5	0	∞	7200.0	100.00	7200.0	100.00	7200.0

positive values indicate improved performance compared to the base HLPP-PR method, and negative values indicate a decrease in performance. For smaller problem sizes, such as those with 10 nodes, all three methods performed well within the 2-hour time limit, with HLPP-PR with GA+SL+HH consistently achieving faster execution times averagely. For example, in a 10-node scenario with five airplanes and 10 potential hubs, HLPP-PR required 1,708.1 seconds, HLPP-PR with GA reduced the time to 1,591.4 seconds, and HLPP-PR with GA+SL+HH further decreased it to 785.4 seconds.

As the problem size increases, HLPP-PR showed significant limitations, reaching the 2-hour time limit for nearly all instances with 30 or more nodes. In contrast, HLPP-PR with GA and HLPP-PR with GA+SL+HH demonstrated superior computational efficiency. For example, while HLPP-PR failed to compute solutions for most instances with 50 nodes, HLPP-PR with GA+SL+HH achieved considerable time reductions, completing computations faster than HLPP-PR with GA in several cases. Specifically, in a 50-node scenario with four airplanes and 20 potential hubs, HLPP-PR exceeded the 2-hour limit without producing a solution, while HLPP-PR with GA completed the computation in 2-hour limit as well, and HLPP-PR with GA+SL+HH further reduced it to 2,649.8 seconds. These results show the computational advantages of the enhanced methods, particularly in handling large-scale problems.

Also, gap analysis further highlights the superior solution quality of HLPP-PR with GA and HLPP-PR with GA+SL+HH compared to the base HLPP-PR method. For most tested scenarios, these enhanced methods achieved positive gap values, indicating better performance. HLPP-PR with GA+SL+HH frequently delivered the highest solution quality, especially for larger problem sizes. For instance, in scenarios involving 50 nodes, HLPP-PR with GA+SL+HH consistently improved gap values, whereas HLPP-PR failed to compute solutions for such cases. However, in some instances where HLPP-PR with GA concluded computations prematurely since the randomness of GA, its performance was slightly inferior to the original model (e.g., 30 nodes, 10 potential hubs, 5 airplanes). Despite these occasional deviations, the overall trend shows clear superiority.

5.3.4 Sensitivity Analysis

This section presents a sensitivity analysis to examine how key factors influence the performance of the transportation network. Three critical variables are analyzed: the ratio of commodity unit revenue to the fixed cost of opening a hub, the demand scale, and the origin/destination of airplanes. First, varying the demand scale examines its influence on resource allocation and network efficiency. Second, modifying the origin and destination of airplanes explores how their placement impacts path selection and network performance. Finally, adjusting the revenue-to-cost ratio evaluates how changes in operational costs and revenue affect hub selection and profitability. These analyses provide valuable insights into how parameter changes affect network behavior, guiding better decision-making in dynamic environments. For this analysis we consider a case with 20 nodes, 20 potential hubs.

5.3.4.1 Effect of Demand Scale on Operational Strategies

We examine the influence of demand scale on resource allocation, including the selection of airplane paths and the number and location of open hubs. In this analysis, the demand is proportionally scaled based on the settings described in Section (5.3.1). Each value is adjusted upward in high-demand scenarios and downward in low-demand scenarios, with four levels: extremely high demand (200% of the standard), high demand (132.65%), standard demand (100%), and low demand (66.67%). This study examines the impact of demand scale on resource allocation and operational strategies, focusing on normalized profit, airplane average utilization, hub deployment, and the relationship between the

revenue (i.e., unit shipped) and total costs.

Figure (5.4) presents the visualization of airplane paths and hub selections for four cases. Across all scenarios, the selected locations align with target customer regions. Cases (a) and (b) choose nine nodes, while cases (c) and (d) select ten. When demand exceeds the standard level, hub selection prioritizes coverage of major demand routes, resulting in Charlotte and Jacksonville as key hubs. In contrast, under lower demand conditions, the network shifts to broaden customer reach by selecting Charleston and Jacksonville instead. Meanwhile, in case (d), the selected paths are concentrated on the eastern side of the map, while routes from the west are noticeably longer. This suggests a less efficient approach to serving customers but likely improves shipment coverage.

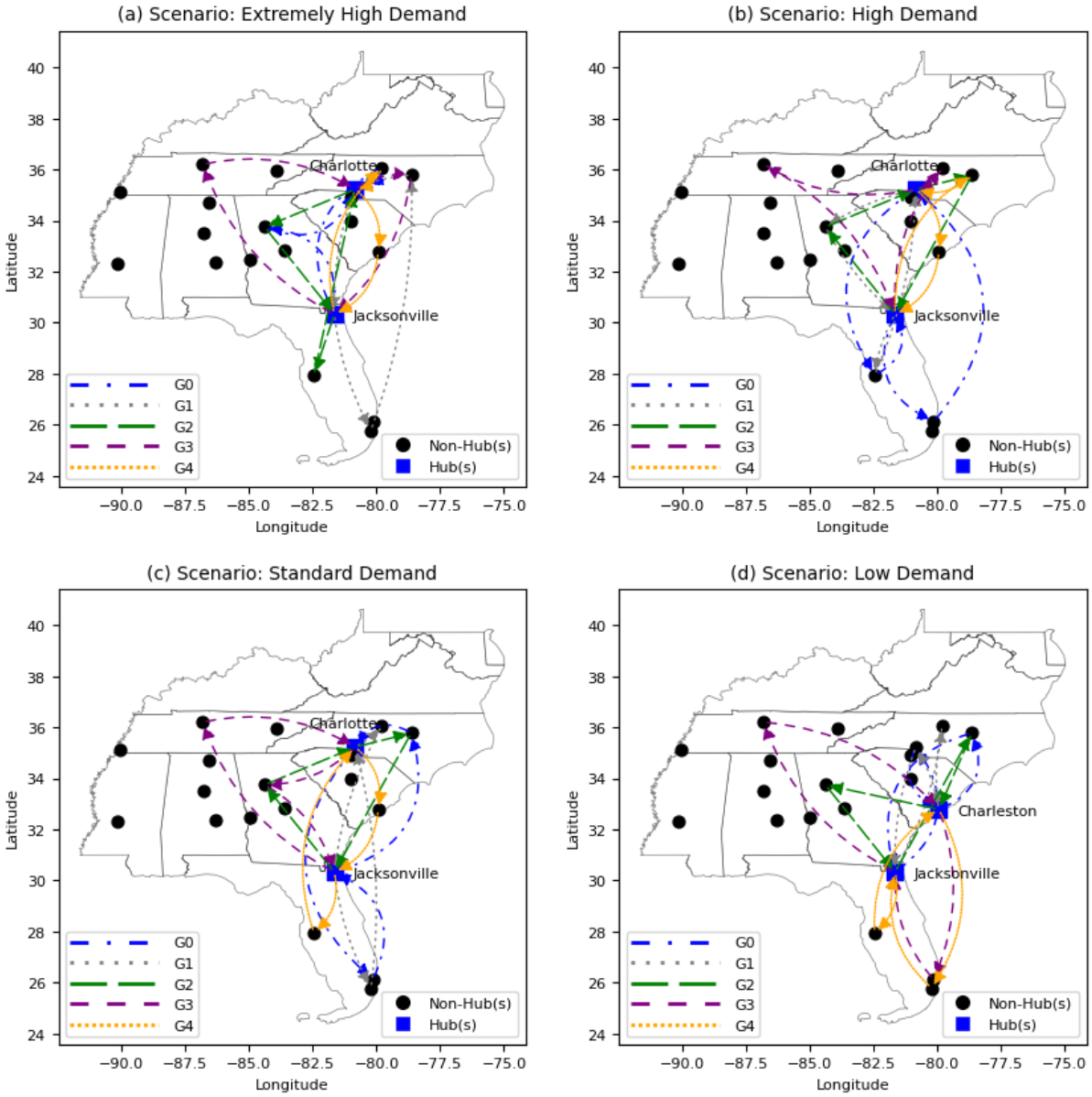

Figure 5.4: Visualization of the effect of demand scale on operational strategies.

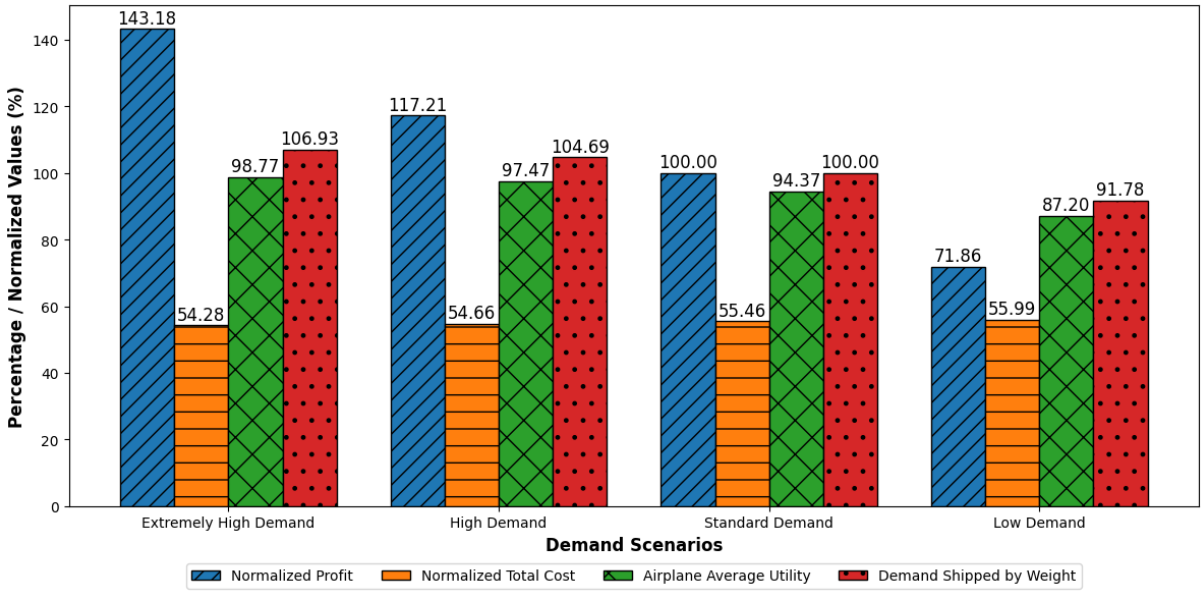

Figure 5.5: Effect of demand scale on operational strategies.

Figure (5.5) compares four scenarios by normalizing profits, with standard demand set at 100%. Under extremely high demand, profits rise to 143.18%, while high demand reaches 117.21%, and low demand drops to 71.86%. The analysis underscores how demand fluctuations influence strategic decisions. Meanwhile, total costs show a slight increase in low-demand scenarios, as the short-path approach lower the a per flight.

Under high-demand conditions, the system prioritizes routes connecting populous cities, generating a normalized profit of 117.21%. Airplane average utilization is nearly maximized at 97.47%, visiting 9 nodes, and relying on 2 hubs. This allocation strategy focuses on economies of scale, where airplanes concentrate on high-yield routes to optimize revenue while minimizing operational costs. Demand shipped increases to 104.69% by weight compared to the standard scenario, reflecting the importance of critical, high-demand paths.

These findings suggest that during periods of increased demand, businesses should emphasize the most profitable routes, strategically deploying resources to enhance profitability and operational efficiency.

In low-demand periods, the system shifts its strategy toward diversification, resulting in a normalized profit of 71.86%. Airplane utilization drops to 87.20%, while the network expands to 10 nodes with 2 hubs. Demand shipped decreases to 91.78% by weight compared to the standard scenario, reflecting lower efficiency but broader market coverage. This approach aims to sustain airplane utilization by addressing dispersed demand, even at reduced profit margins.

Notably, the consistent use of two hubs across all scenarios underscores their crucial role in maintaining operational flexibility. This stability in hub deployment, along with strategic positioning, allows for adaptive responses to fluctuations in demand. Additionally, the profit gap between high-demand (117.21%) and standard-demand (100%) cases highlights the significance of resource availability in optimizing profitability. In contrast, the reduced profit in low-demand (71.86%) scenarios emphasizes the need for strategic diversification to mitigate potential revenue losses.

By aligning resource allocation strategies with demand levels, businesses can better respond to market dynamics. Focusing resources on high-yield routes during peak demand periods maximizes profitability, while diversifying operations in low-demand periods helps maintain market visibility and ensure consistent revenue. These adaptive strategies enable businesses to optimize performance and remain agile under varying market conditions.

5.3.4.2 Influence of Airplane's Origin and Destination

The second analysis examines the influence of an airplane's origin and destination. The analysis examines four scenarios for determining airplane origins and destinations: (a) selecting the most populous city in each state, as defined in Section (5.3.1); (b) choosing the most populous cities across the entire region without state constraints; (c) prioritizing positional centrality within the map; and (d) combining positional centrality with total demand considerations. Each scenario presents distinct outcomes in profitability, total costs, airplane average utilization, and demand shipped, providing valuable insights into resource allocation and network design. The setting of four scenarios is listed below:

Table 5.5: Location setting of airplanes' origin and destination.

Scenario	Location
(a)	Charlotte, Jacksonville, Atlanta, Nashville, Charleston
(b)	Charlotte, Jacksonville, Raleigh, Miami, Fort Lauderdale
(c)	Atlanta, Macon, Columbia, Columbus, Rock Hill
(d)	Charlotte, Jacksonville, Atlanta, Birmingham, Macon

Figure (5.6) visualizes airplane paths and hub selections across four scenarios. All cases open two hubs, except for case (c), which operates with a single hub. Cases (a), (b), and (d) show similar routing patterns, though case (b) covers only nine nodes, whereas cases (a) and (d) serve ten. Notably, case (c) concentrates all flights within the central region, favoring shorter paths. This is likely due to the origin and destination of the airplanes being located in low-demand central cities, so the paths focus on reducing costs.

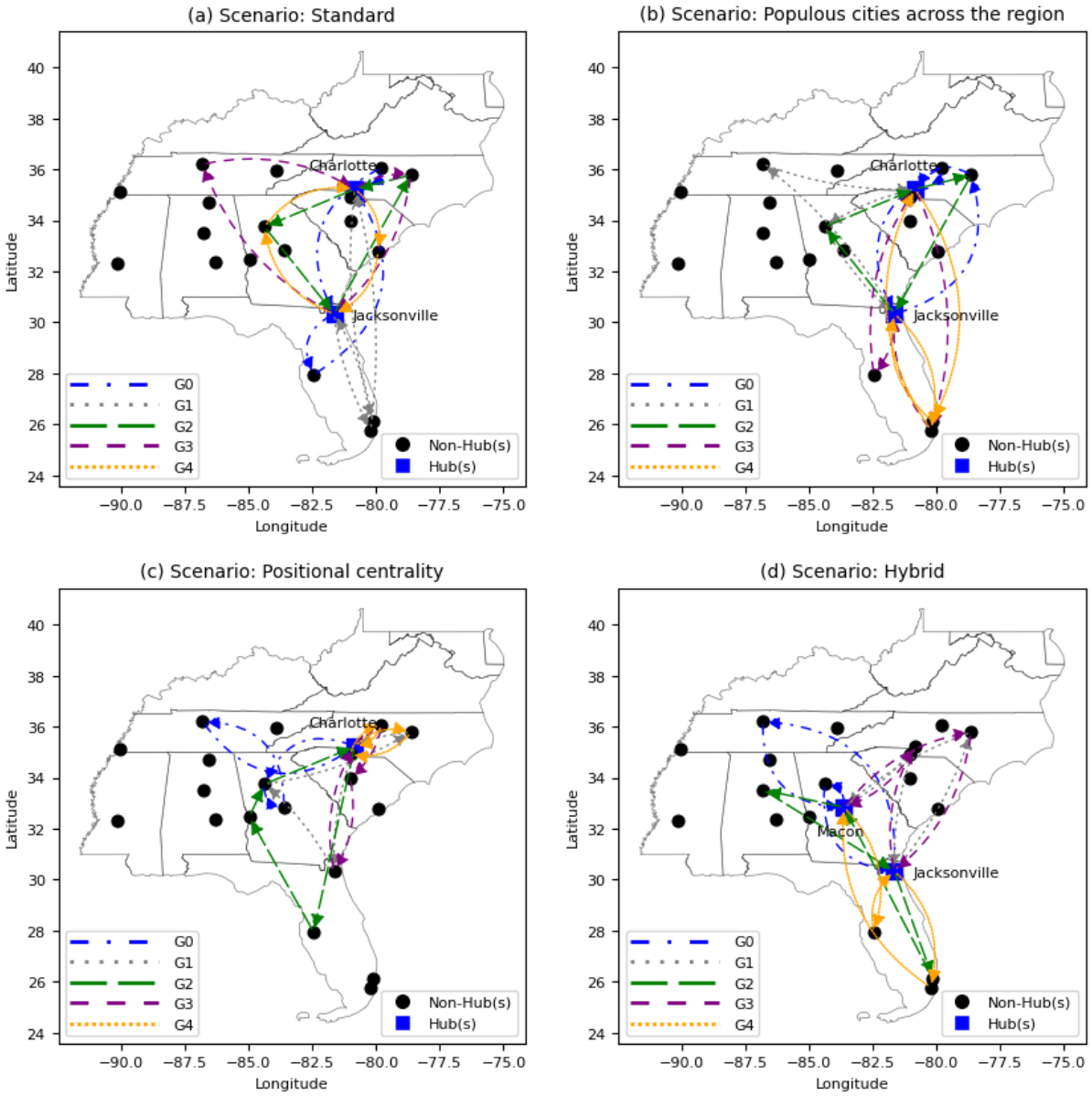

Figure 5.6: Influence of airplane origin and destinations on results.

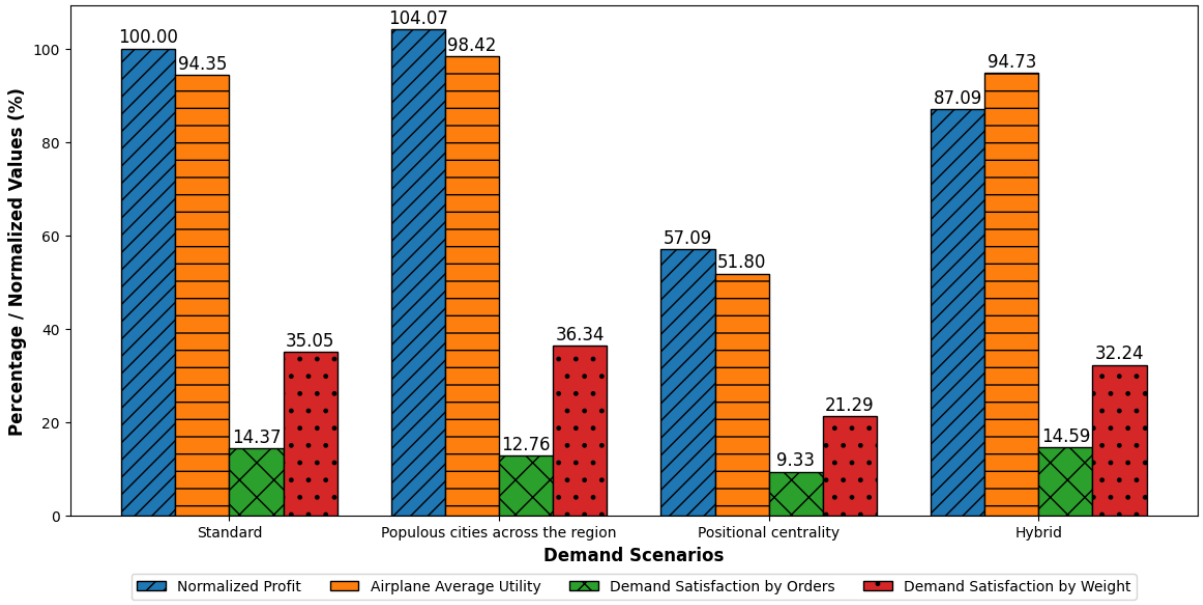

Figure 5.7: Influence of airplane's origin and destination.

Also, Figure (5.7) compares four scenarios by normalizing profits, with standard demand set at 100%. From a profitability perspective, focusing on populous cities (Case (b)) achieves the highest normalized profit (104.07%) and high airplane utilization (98.42%) by targeting high-demand areas, maximizing revenue, and leveraging economies of scale.

In contrast, positional centrality (Case (c)) reduces profitability (57.09%) and airplane utilization (51.80%) due to the nature of central locations that may not be the most profitable. The hybrid model (Case (d)), which combines centrality and demand, achieves a balanced outcome with a normalized profit of 87.09% and demand satisfaction by orders at 14.59%, ensuring both profitability and wider market coverage.

Regarding demand satisfaction, Case (c) has the lowest order fulfillment rate (9.33%) and a lower weight satisfaction (21.29%), as centrally located cities may not generate high

demand for large shipments. While central positioning may reduce travel time, the choice of airplane origins and destinations in low-demand regions limits overall efficiency.

In contrast, Case (b), focusing on populous cities, performs better in weight satisfaction (36.34%) by targeting areas with greater demand for larger shipments, though it satisfies fewer orders (12.76%). This could pose a risk if demand fluctuates or specific customers reduce their orders. Case (d) offers a balanced solution, with demand satisfaction similar to Case (a), making it an optimal choice for businesses seeking to balance profitability with broader coverage.

In summary, the populous city strategy (Case (b)) maximizes profitability and airplane utilization but offers limited coverage, depending on where the airplanes originate and where they are headed. The centrality strategy (Case (c)) provides accessibility but decreases profitability and efficiency due to its limited demand requirements. The hybrid model (Case (d)), combining centrality and demand, balances both profitability and network reach, providing a flexible approach for businesses seeking to optimize resources while expanding market coverage. Ultimately, the standard or hybrid model (Case (a), (d)) offer the best compromise between profit and service area expansion.

5.3.4.3 Impact of Revenue-to-Cost Ratio on Profitability

Finally, we analyze profitability under varying levels of unit revenue (r_k) and fixed hub opening costs (f_i). The standard scenario is defined based on the unit revenue and fixed costs presented in Table (5.1). For unit revenue, we test scenarios at 50%, 100%, 150%, and 200% of the standard value, while for fixed costs, we consider 40%, 70%, 100%, and 130%. The results are illustrated in Figure (5.8).

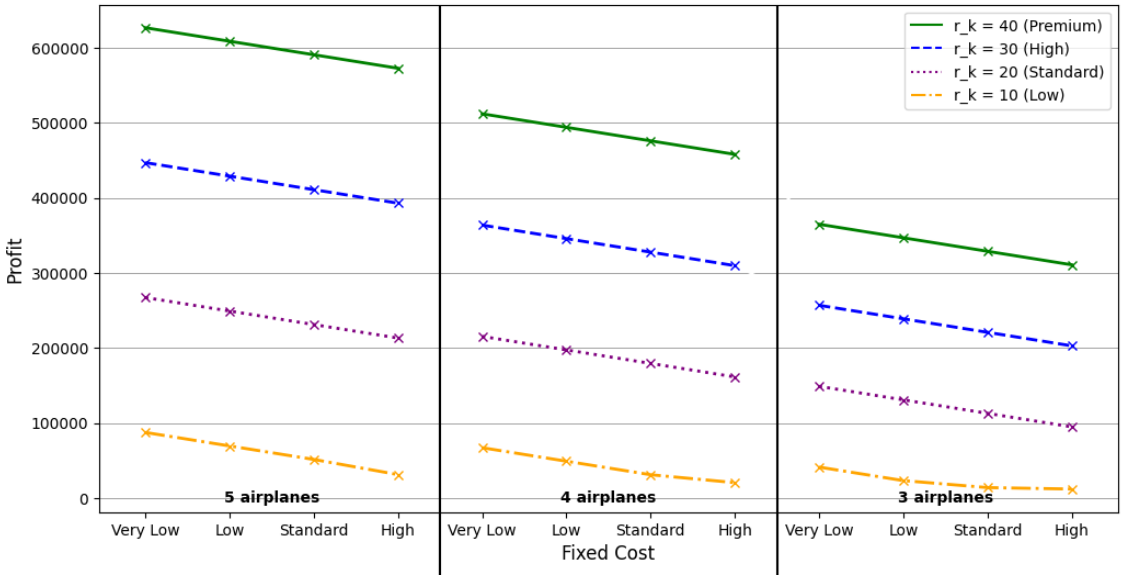

Figure 5.8: Impact of revenue-to-cost ratio on profitability.

Figure (5.8) presents the results of a sensitivity analysis examining the profit outcomes of the network design model under varying configurations of airplane numbers, unit revenue levels, and fixed costs of opening hubs. Initially, in Section (5.3.1), the unit revenue and fixed cost were set at a standard range ($r_k = 20$, $f_i = 30,000$). For the sensitivity analysis, the unit revenue and fixed cost were adjusted to low and high levels, respectively, to evaluate their impact on profitability. The figure explores these variations across fleets comprising 5, 4, and 3 airplanes, with each subplot representing a specific airplane count and distinct line styles illustrating profit trends across the revenue levels. This visualization highlights how changes in key parameters affect operational efficiency and profitability across different scenarios.

The analysis across different airplane configurations highlights that deploying 5 airplanes

offers the highest profits, particularly when revenue is high and fixed costs are low. This configuration maximizes revenue potential, but as fixed costs rise, the rate of profit decline becomes steeper, indicating that while additional airplanes increase revenue opportunities, they also make profitability more sensitive to the increased operational costs. On the other hand, 4 airplanes strike a more balanced approach, offering competitive profitability, especially at standard and high fixed cost levels. The profit curves for 4 airplanes remain close to 5 airplanes under medium revenue conditions, but start to diverge when revenue drops. With 3 airplanes, profitability is the lowest, particularly in high-cost settings, as the smaller fleet size significantly restricts revenue generation potential due to its limited operational capacity.

Furthermore, as fixed costs rise, the profit difference among different revenue scenarios becomes more evident, highlighting the importance of boosting revenue to maintain profitability. In low-revenue conditions, increasing the number of airplanes leads to diminishing returns. For instance, when fixed costs are high, the profit difference between operating 3 and 5 airplanes becomes almost negligible, indicating that using fewer airplanes may be a more effective choice when revenue is constrained. The impact of fixed costs is even more significant in low-revenue scenarios, where high operational expenses can sharply reduce profits, even with a larger number of airplanes. Based on these findings, the most effective strategy for deploying airplanes is to maximize the number in high-revenue, low-cost environments, while reducing the number of airplanes in high-cost, low-revenue conditions to optimize operational efficiency and profitability.

Note that, this analysis did not account for the purchase cost of owning airplanes, which could significantly impact the overall profitability. The costs associated with acquiring

additional planes, especially in financing and accounting, need to be considered in future evaluations. Without factoring in these expenses, the current analysis presents only the operational costs of running the planes. As the business considers expanding its aircraft capacity, these acquisition-related costs will play a critical role in determining whether the additional planes will generate sufficient returns to justify the investment. Therefore, it is essential to integrate the purchase costs into the analysis to provide a more comprehensive view of the financial effects and ensure that decisions around increasing the number of planes are based on a complete understanding of both expected revenue and operational costs.

5.4 Chapter Summary

This chapter extends the pilotless air cargo transportation network design analysis by incorporating airplane availability constraints, refining the optimization of net profit and operational efficiency. While Chapter 4 examined the impact of customer demand, unit revenue, and fixed hub opening costs on network performance, this chapter introduces an advanced formulation that explicitly considers the limited number of airplanes. To address this, we propose the HLPP-PR model, which optimizes hub locations, shipment routing, and airplane routes under capacity constraints. Additionally, we implement GA with SL and HH approach to enhance computational efficiency and improve solution quality.

The integration of the GA, SL, and HH approach improves both computational efficiency and solution quality. GA facilitates effective exploration of the solution space, ensuring adaptability to changing constraints and improving convergence toward optimal solutions. SL further refines the problem size by ranking and filtering potential solutions, reducing computational complexity. Additionally, HH strategically balances exploration and exploitation, improving search efficiency and guiding the sub-problem toward high-quality solutions. GA+SL+HH significantly reduces computational time while improving solution accuracy, making the HLPP-PR model more practical for large-scale transportation networks with airplane availability constraints.

The managerial insights in our study highlight the critical role of airplane availability in optimizing network profitability. An increase in the number of airplanes enhances net profit by improving route flexibility and demand fulfillment. However, beyond a certain

point, adding more airplanes may yield diminishing returns unless market conditions, such as demand levels and revenue structures, support further expansion.

Additionally, when the number of airplanes and hubs remains fixed, increasing the number of nodes from 10 to 30 adds complexity to the system but does not necessarily lead to higher net profit. Instead, the problem consistently prioritizes high-demand routes, reinforcing the importance of strategically selecting hubs in populous regions. Therefore, network expansion beyond an optimal point may introduce unnecessary complexity without adding meaningful opportunities, emphasizing the need for careful selection of customer locations to balance network size and performance.

The sensitivity analysis highlights how key factors—airplane count, revenue-to-cost ratio, demand scale, and airplane origin/destination—affect transportation network performance. First, the analysis shows that maximizing the number of airplanes in high-revenue, low-cost environments significantly boosts profitability. However, additional airplanes yield diminishing returns in low-revenue, high-cost scenarios, emphasizing the need for a balanced fleet strategy based on market conditions. Additionally, variations in demand scale also influence resource allocation: higher demand level prioritizes high-yield routes for optimized profit, while low-demand conditions prompt diversification to maintain airplane utilization and reach new markets. Finally, regarding airplane origin/destination, prioritizing populous cities maximizes profitability, while a hybrid model combining centrality and demand offers a balanced solution, ensuring both profitability and broader network coverage.

Chapter 6

Conclusion and Future Work

In this chapter, we first provide a brief summary and contributions of the thesis and then discuss its limitations and potential directions for future research.

Chapter (3) presents an on-demand warehousing optimization model, which accounts for price-sensitive demand fluctuations to improve resource utilization and maximize profit for both customers and warehouse operators. The integration of price-sensitive demand into the optimization model reflects real-world dynamics, where pricing strategies directly influence customer demand and profitability. To achieve high-quality solutions, a Lagrangian relaxation framework is combined with a local search heuristic to optimize dynamic warehouse allocation over multiple planning periods.

Chapter (4) introduces hub location and flight assignment optimization for pilotless air cargo transportation networks. Two formulations—path-based and arc-based—are developed to improve scalability and operational efficiency in large-scale air cargo systems. A

genetic algorithm-based decomposition approach is applied to maximize net profit while optimizing hub selection and flight assignments.

Chapter (5) extends the model in Chapter (4) by integrating airplane routing optimization into the hub location problem. The genetic algorithm approach, combined with a score-based labeling and a hybrid heuristic method, refines routing decisions to further enhance solution quality and scalability in large-scale network operations.

These applications demonstrate the need for heuristic methods in addressing large-scale optimization challenges. By bridging methodological advancements and practical implementations, this thesis contributes to optimization methodology as well as to real-world decision-making processes, particularly in logistics, warehousing, and pilotless air cargo transportation.

Despite the advantages, the proposed heuristic methods have certain limitations. First, the models rely on fixed and deterministic parameters, which restrict their ability to handle real-world uncertainties like fluctuating demand, variable costs, and regulatory constraints. Furthermore, the heuristic setting process has mainly relied on testing small examples to identify patterns of the method. This includes fine-tuning parameters such as crossover and mutation rates in GA, the base score in SL, and the learning mechanisms in HH. While this iterative approach helps improve heuristic design, it differs from traditional methods that follow a direct computational process. Although trial-and-error testing provides useful insights, it introduces a degree of subjectivity and may not always be scalable to larger or more complex problems without further adjustments.

Memory usage is another challenge associated with the heuristic method. Given the large

problem size and the need for multiple iterations with numerous sub-problems, memory consumption becomes a major concern. To address this issue, implementing multiprocessing or optimizing model logic to recycle sub-problem structures would be necessary to improve efficiency. Without such enhancements, the heuristic-based approach may result in longer processing times and higher memory demands compared to traditional models.

Future research should explore several key areas to further improve heuristic methods. Firstly, integrating machine learning techniques, such as reinforcement learning and metaheuristic tuning, could improve heuristic adaptability and reduce reliance on manual parameter adjustments. Additionally, incorporating stochastic modeling and dynamic parameter settings would enhance the ability to account for real-world uncertainties, making optimization models more resilient to market fluctuations. For on-demand warehousing, future studies should also explore the opportunity of customer commitment periods and customizable storage solutions. In air cargo operations, research should address variable costs, time-window constraints, and hub operations to create more adaptable flight assignment and airplane routing models.

References

[1] K. Unnu and J. Pazour, "Evaluating on-demand warehousing via dynamic facility location models," *IISE Transactions*, vol. 54, no. 10, pp. 988–1003, 2022.

[2] S. Ceschia, M. Gansterer, S. Mancini, and A. Meneghetti, "The on-demand warehousing problem," *International Journal of Production Research*, vol. 61, no. 10, pp. 3152–3170, 2023.

[3] A. Lahy, K. Huckle, J. Sleeman, and M. Wilson, "An Introduction to Flexible, On-Demand Warehousing: E-Space," in *Digital Supply Chain Transformation: Emerging Technologies for Sustainable Growth.* Cardiff University Press, 2022.

[4] N. Shin, "Creating shared value from collaborative logistics systems: The cases of ES3 and flexe," *Asia Pacific Journal of Information Systems*, vol. 30, no. 1, pp. 213–227, 2019.

[5] L. Parodos, O. Tsolakis, G. Tsoukos, E. Xenou, and G. Ayfantopoulou, "Business model analysis of smart city logistics solutions using the business model canvas: The case of an on-demand warehousing e-marketplace," *Future Transportation*, vol. 2, no. 2, pp. 467–481, 2022.

[6] Y. Costa and T. Melo, "Facility location modeling in supply chain network design: Current state and emerging trends," in *The Palgrave Handbook of Supply Chain Management*, J. Sarkis, Ed. Cham: Springer International Publishing, 2022, pp. 1–36.

[7] S. Kumar, B. E. Narkhede, and K. Jain, "Revisiting the warehouse research through an evolutionary lens: A review from 1990 to 2019," *International Journal of Production Research*, vol. 0, no. 0, pp. 1–23, 2021.

[8] V. Elia, M. G. Gnoni, and F. Tornese, "On-demand warehousing platforms: Evolution and trend analysis of an industrial sharing economy model," *Logistics*, vol. 8, no. 93, 2024.

[9] F. Betti Sorbelli, "UAV-based delivery systems: A systematic review, current trends, and research challenges," *ACM J. Auton. Transport. Syst.*, vol. 1, no. 3, May 2024.

[10] Y. Li, M. Liu, and D. Jiang, "Application of unmanned aerial vehicles in logistics: A literature review," *Sustainability*, vol. 14, no. 14473, 2022.

[11] M. F. Gorman, J.-P. Clarke, A. H. Gharehgozli, M. Hewitt, R. de Koster, and D. Roy, "State of the Practice: A Review of the Application of OR/MS in Freight Transportation," *Interfaces*, vol. 44, no. 6, pp. 535–554, 2014.

[12] M. SteadieSeifi, N. Dellaert, W. Nuijten, T. Van Woensel, and R. Raoufi, "Multimodal freight transportation planning: A literature review," *European Journal of Operational Research*, vol. 233, no. 1, pp. 1–15, 2014.

[13] S. A. H. Mohsan, N. Q. H. Othman, Y. Li, M. H. Alsharif, and M. A. Khan, "Unmanned aerial vehicles (UAVs): Practical aspects, applications, open challenges, secu-

rity issues, and future trends," *Intelligent Service Robotics*, vol. 16, no. 1, pp. 109–137, Mar. 2023.

[14] S. Wandelt, S. Wang, C. Zheng, and X. Sun, "AERIAL: A meta review and discussion of challenges toward unmanned aerial vehicle operations in logistics, mobility, and monitoring," *IEEE Transactions on Intelligent Transportation Systems*, vol. 25, no. 7, pp. 6276–6289, Jul. 2024.

[15] K. Unnu and J. A. Pazour, "A large-scale heuristic approach to integrate on-demand warehousing into dynamic distribution network designs," *Computers & Industrial Engineering*, vol. 186, p. 109752, 2023.

[16] S. Ceschia, M. Gansterer, S. Mancini, and A. Meneghetti, "Solving the online on-demand warehousing problem," *Computers & Operations Research*, vol. 170, p. 106760, 2024.

[17] J. Lee, C. Ko, and I. Moon, "E-commerce supply chain network design using on-demand warehousing system under uncertainty," *International Journal of Production Research*, vol. 62, no. 5, pp. 1901–1927, 2024.

[18] C. Balcazar, C. Chavez, G. Viacava, E. Ramos, and C. Raymundo, "On-demand warehousing model for open space event development services: A case study in lima, peru," in *Human Systems Engineering and Design II*, T. Ahram, W. Karwowski, S. Pickl, and R. Taiar, Eds. Cham: Springer International Publishing, 2020, pp. 953–959.

[19] E. Xenou, L. Parodos, G. Tsoukos, G. Ayfantopoulou, and Z. Maleas, "The rise of the on-demand warehousing: Is the greek market ready for this change?" in *Advances in*

Mobility-as-a-Service Systems, E. G. Nathanail, G. Adamos, and I. Karakikes, Eds. Cham: Springer International Publishing, 2021, pp. 835–844.

[20] H. Jahani, B. Abbasi, J.-B. Sheu, and W. Klibi, "Supply chain network design with financial considerations: A comprehensive review," *European Journal of Operational Research*, vol. 312, no. 3, pp. 799–839, 2024.

[21] J. P. Škrinjar, P. Škorput, and M. Furdić, "Application of unmanned aerial vehicles in logistic processes," in *New Technologies, Development and Application*, I. Karabegović, Ed. Cham: Springer International Publishing, 2019, pp. 359–366.

[22] A. Irajifar and D. van den Aker, "Roadmap to truly shared warehousing : Challenges and benefits," *Logistiek + Tijdschrift voor toegepaste logistiek*, vol. 2021, no. 11, 2021.

[23] Y. Shi, Y. Yu, and Y. Dong, "Warehousing platform's revenue management: A dynamic model of coordinating space allocation for self-use and rent," *European Journal of Operational Research*, vol. 293, no. 1, pp. 167–176, 2021.

[24] I. Correia and T. Melo, "Distribution network redesign under flexible conditions for short-term location planning," *Computers & Industrial Engineering*, vol. 174, p. 108747, 2022.

[25] J. Lee, J. Park, and I. Moon, "Inventory and commitment decisions for on-demand warehousing system," in *Advances in Production Management Systems. Artificial Intelligence for Sustainable and Resilient Production Systems*, A. Dolgui, A. Bernard, D. Lemoine, G. von Cieminski, and D. Romero, Eds. Cham: Springer International Publishing, 2021, pp. 455–463.

[26] F. Saldanha-da-Gama, "Facility location in logistics and transportation: An enduring relationship," *Transportation Research Part E: Logistics and Transportation Review*, vol. 166, p. 102903, 2022.

[27] E. Alarcon-Gerbier and U. Buscher, "Modular and mobile facility location problems: A systematic review," *Computers & Industrial Engineering*, vol. 173, p. 108734, 2022.

[28] J. Beasley, "An algorithm for solving large capacitated warehouse location problems," *European Journal of Operational Research*, vol. 33, no. 3, pp. 314–325, 1988.

[29] ——, "Lagrangean heuristics for location problems," *European Journal of Operational Research*, vol. 65, no. 3, pp. 383–399, 1993.

[30] L.-Y. Wu, X.-S. Zhang, and J.-L. Zhang, "Capacitated facility location problem with general setup cost," *Computers & Operations Research*, vol. 33, no. 5, pp. 1226–1241, 2006.

[31] A. Klose and S. Görtz, "A branch-and-price algorithm for the capacitated facility location problem," *European Journal of Operational Research*, vol. 179, no. 3, pp. 1109–1125, 2007.

[32] P. Avella, M. Boccia, A. Sforza, and I. Vasil'ev, "An effective heuristic for large-scale capacitated facility location problems," *Journal of Heuristics*, vol. 15, no. 6, pp. 597–615, Dec. 2009.

[33] G. Guastaroba and M. G. Speranza, "Kernel search for the capacitated facility location problem," *Journal of Heuristics*, vol. 18, no. 6, pp. 877–917, Dec. 2012.

[34] M. Sun, "A tabu search heuristic procedure for the capacitated facility location problem," *Journal of Heuristics*, vol. 18, no. 1, pp. 91–118, Feb. 2012.

[35] M. Fischetti, I. Ljubić, and M. Sinnl, "Benders decomposition without separability: A computational study for capacitated facility location problems," *European Journal of Operational Research*, vol. 253, no. 3, pp. 557–569, 2016.

[36] E. J. Alenezy, "Solving capacitated facility location problem using lagrangian decomposition and volume algorithm," *Advances in Operations Research*, vol. 2020, no. 1, p. 5239176, 2020.

[37] M. Caserta and S. Voß, "A general corridor method-based approach for capacitated facility location," *International Journal of Production Research*, vol. 58, no. 13, pp. 3855–3880, 2020.

[38] A. Allman and Q. Zhang, "Dynamic location of modular manufacturing facilities with relocation of individual modules," *European Journal of Operational Research*, vol. 286, no. 2, pp. 494–507, 2020.

[39] J. Ryu and S. Park, "A branch-and-price algorithm for the robust single-source capacitated facility location problem under demand uncertainty," *EURO Journal on Transportation and Logistics*, vol. 11, p. 100069, 2022.

[40] Š. Štádlerová, S. D. Jena, and P. Schütz, "Using Lagrangian relaxation to locate hydrogen production facilities under uncertain demand: A case study from Norway." *Comput Manag Sci*, vol. 20, no. 1, p. 10, 2023.

[41] K. Liu, C. Liu, X. Xiang, and Z. Tian, "Testing facility location and dynamic capacity planning for pandemics with demand uncertainty," *European Journal of Operational Research*, vol. 304, no. 1, pp. 150–168, 2023.

[42] M. Campêlo and C. T. Bornstein, "Add/drop procedures for the capacitated plant location problem," *Electronic Notes in Discrete Mathematics*, vol. 7, pp. 102–105, 2001.

[43] T. Matos, Ó. Oliveira, and D. Gamboa, "RAMP algorithms for the capacitated facility location problem," *Annals of Mathematics and Artificial Intelligence*, vol. 89, no. 8, pp. 799–813, Sep. 2021.

[44] G. Cabrera G., E. Cabrera, R. Soto, L. J. M. Rubio, B. Crawford, and F. Paredes, "A hybrid approach using an artificial bee algorithm with mixed integer programming applied to a large-scale capacitated facility location problem," *Mathematical Problems in Engineering*, vol. 2012, no. 1, p. 954249, 2012.

[45] A. Rahmani and S. MirHassani, "A hybrid Firefly-Genetic Algorithm for the capacitated facility location problem," *Information Sciences*, vol. 283, pp. 70–78, 2014.

[46] I. Harris, C. L. Mumford, and M. M. Naim, "A hybrid multi-objective approach to capacitated facility location with flexible store allocation for green logistics modeling," *Transportation Research Part E: Logistics and Transportation Review*, vol. 66, pp. 1–22, 2014.

[47] C. Lagos, G. Guerrero, E. Cabrera, S. Niklander, F. Johnson, F. Paredes, and J. Vega, "A matheuristic approach combining local search and mathematical programming," *Scientific Programming*, vol. 2016, no. 1, p. 1506084, 2016.

[48] A. Shoja, S. Molla-Alizadeh-Zavardehi, and S. Niroomand, "Adaptive meta-heuristic algorithms for flexible supply chain network design problem with different delivery modes," *Computers & Industrial Engineering*, vol. 138, p. 106107, 2019.

[49] A. Pagès-Bernaus, H. Ramalhinho, A. A. Juan, and L. Calvet, "Designing e-commerce supply chains: A stochastic facility–location approach," *International Transactions in Operational Research*, vol. 26, no. 2, pp. 507–528, 2019.

[50] C. Sauvey, T. Melo, and I. Correia, "Heuristics for a multi-period facility location problem with delayed demand satisfaction," *Computers & Industrial Engineering*, vol. 139, p. 106171, 2020.

[51] M. Rabe, J. Gonzalez-Feliu, J. Chicaiza-Vaca, and R. D. Tordecilla, "Simulation-optimization approach for multi-period facility location problems with forecasted and random demands in a last-mile logistics application," *Algorithms*, vol. 14, no. 41, 2021.

[52] A. Silva, D. Aloise, L. C. Coelho, and C. Rocha, "Heuristics for the dynamic facility location problem with modular capacities," *European Journal of Operational Research*, vol. 290, no. 2, pp. 435–452, 2021.

[53] M. R. H. Maia, M. Reula, C. Parreño-Torres, P. P. Vuppuluri, A. Plastino, U. S. Souza, S. Ceschia, M. Pavone, and A. Schaerf, "Metaheuristic techniques for the capacitated facility location problem with customer incompatibilities," *Soft Computing*, vol. 27, no. 8, pp. 4685–4698, Apr. 2023.

[54] F. B. Ozsoydan and İ. Gölcük, "A hybridisation of linear programming and genetic algorithm to solve the capacitated facility location problem," *International Journal of Production Research*, vol. 61, no. 10, pp. 3331–3349, 2023.

[55] M. E. O'Kelly, "Air freight hubs in the FedEx system: Analysis of fuel use," *Journal of Air Transport Management*, vol. 36, pp. 1–12, 2014.

[56] T. Boonekamp and G. Burghouwt, "Measuring connectivity in the air freight industry," *Journal of Air Transport Management*, vol. 61, pp. 81–94, 2017.

[57] A. Bombelli, B. F. Santos, and L. Tavasszy, "Analysis of the air cargo transport network using a complex network theory perspective," *Transportation Research Part E: Logistics and Transportation Review*, vol. 138, p. 101959, 2020.

[58] C.-C. Lin, J.-Y. Lin, and Y.-C. Chen, "The capacitated p-hub median problem with integral constraints: An application to a Chinese air cargo network," *Applied Mathematical Modelling*, vol. 36, no. 6, pp. 2777–2787, 2012.

[59] H. Oktal and A. Ozger, "Hub location in air cargo transportation: A case study," *Journal of Air Transport Management*, vol. 27, pp. 1–4, 2013.

[60] S. Yu, Z. Yang, and B. Yu, "Air express network design based on express path choices – Chinese case study," *Journal of Air Transport Management*, vol. 61, pp. 73–80, 2017.

[61] B. Yıldız and M. Savelsbergh, "Optimizing package express operations in China," *European Journal of Operational Research*, vol. 300, no. 1, pp. 320–335, 2022.

[62] B. Yıldız, M. Savelsbergh, and A. K. Dogru, "Transshipment network design for express air cargo operations in China," *EURO Journal on Transportation and Logistics*, vol. 12, p. 100120, 2023.

[63] C. Zhang, F. Xie, K. Huang, T. Wu, and Z. Liang, "MIP models and a hybrid method for the capacitated air-cargo network planning and scheduling problems," *Transportation Research Part E: Logistics and Transportation Review*, vol. 103, pp. 158–173, 2017.

[64] C. K. Lee, S. Zhang, and K. K. Ng, "Design of an integration model for air cargo transportation network design and flight route selection," *Sustainability*, vol. 11, no. 5197, 2019.

[65] F. Delgado and J. Mora, "A matheuristic approach to the air-cargo recovery problem under demand disruption," *Journal of Air Transport Management*, vol. 90, p. 101939, 2021.

[66] S. P. Gayialis, E. P. Kechagias, and G. D. Konstantakopoulos, "A city logistics system for freight transportation: Integrating information technology and operational research," *Operational Research*, vol. 22, no. 5, pp. 5953–5982, Nov. 2022.

[67] S. Alumur and B. Y. Kara, "Network hub location problems: The state of the art," *European Journal of Operational Research*, vol. 190, no. 1, pp. 1–21, 2008.

[68] J. F. Campbell and M. E. O'Kelly, "Twenty-five years of hub location research," *Transportation Science*, vol. 46, no. 2, pp. 153–169, 2012.

[69] R. Z. Farahani, M. Hekmatfar, A. B. Arabani, and E. Nikbakhsh, "Hub location problems: A review of models, classification, solution techniques, and applications," *Computers & Industrial Engineering*, vol. 64, no. 4, pp. 1096–1109, 2013.

[70] S. A. Alumur, J. F. Campbell, I. Contreras, B. Y. Kara, V. Marianov, and M. E. O'Kelly, "Perspectives on modeling hub location problems," *European Journal of Operational Research*, vol. 291, no. 1, pp. 1–17, 2021.

[71] M. J. Basallo-Triana, C. J. Vidal-Holguín, and J. J. Bravo-Bastidas, "Planning and design of intermodal hub networks: A literature review," *Computers & Operations Research*, vol. 136, p. 105469, 2021.

[72] A. Alibeyg, I. Contreras, and E. Fernández, "Hub network design problems with profits," *Transportation Research Part E: Logistics and Transportation Review*, vol. 96, pp. 40–59, 2016.

[73] G. Taherkhani and S. A. Alumur, "Profit maximizing hub location problems," *Omega*, vol. 86, pp. 1–15, 2019.

[74] G. Taherkhani, S. A. Alumur, and M. Hosseini, "Benders decomposition for the profit maximizing capacitated hub location problem with multiple demand classes," *Transportation Science*, vol. 54, no. 6, pp. 1446–1470, 2020.

[75] ——, "Robust stochastic models for profit-maximizing hub location problems," *Transportation Science*, vol. 55, no. 6, pp. 1322–1350, 2021.

[76] F. A. Oliveira, E. M. de Sá, and S. R. de Souza, "Benders decomposition applied to profit maximizing hub location problem with incomplete hub network," *Computers & Operations Research*, vol. 142, p. 105715, 2022.

[77] Y. Gao, J. Xia, and H. Ke, "A branch-and-cut algorithm for hub network design problems with profits," *Naval Research Logistics (NRL)*, vol. 69, no. 4, pp. 622–639, 2022.

[78] S. A. Alumur, S. Nickel, and F. Saldanha-da-Gama, "Hub location under uncertainty," *Transportation Research Part B*, vol. 46, no. 4, pp. 529–543, 2012.

[79] K. Govindan, M. Fattahi, and E. Keyvanshokooh, "Supply chain network design under uncertainty: A comprehensive review and future research directions," *European Journal of Operational Research*, vol. 263, no. 1, pp. 108–141, 2017.

[80] H. Topcuoglu, F. Corut, M. Ermis, and G. Yilmaz, "Solving the uncapacitated hub location problem using genetic algorithms," *Computers & Operations Research*, vol. 32, no. 4, pp. 967–984, 2005.

[81] M. Naeem and B. Ombuki-Berman, "An efficient genetic algorithm for the uncapacitated single allocation hub location problem," in *IEEE Congress on Evolutionary Computation*, 2010, pp. 1–8.

[82] Z. Stanimirović, "A genetic algorithm approach for the capacitated single allocation p-hub median problem," *Computing and Informatics*, vol. 29, pp. 117–132, Jan. 2010.

[83] H. Damgacioglu, D. Dinler, N. Evin Ozdemirel, and C. Iyigun, "A genetic algorithm for the uncapacitated single allocation planar hub location problem," *Computers & Operations Research*, vol. 62, pp. 224–236, 2015.

[84] S. Katoch, S. S. Chauhan, and V. Kumar, "A review on genetic algorithm: Past, present, and future," *Multimedia Tools and Applications*, vol. 80, no. 5, pp. 8091–8126, Feb. 2021.

[85] I. Contreras, J. A. Díaz, and E. Fernández, "Lagrangean relaxation for the capacitated hub location problem with single assignment," *OR Spectrum*, vol. 31, no. 3, pp. 483–505, Jun. 2009.

[86] Y. Wu, A. G. Qureshi, T. Yamada, and S. Yu, "Branch-and-price-and-cut algorithm for the capacitated single allocation hub location routeing problem," *Journal of the Operational Research Society*, vol. 75, no. 2, pp. 410–422, 2024.

[87] C. Zhang, X. Sun, W. Dai, and S. Wandelt, "Solving hub location problems with profits using variable neighborhood search," *Transportation Research Record*, vol. 2677, no. 1,

pp. 1675–1695, 2023.

[88] F. A. Oliveira, E. M. de Sá, S. R. de Souza, and M. J. F. Souza, "ILS-based algorithms for the profit maximizing uncapacitated hub network design problem with multiple allocation," *Computers & Operations Research*, vol. 157, p. 106252, 2023.

[89] T. Mitchell, I. Makienko, and S. Mitchell, "Making Price Elasticity A Useful Metric For Maximizing Profit," *American Journal of Business Education (AJBE)*, vol. 6, p. 565, Oct. 2013.

[90] M. Peker, B. Y. Kara, J. F. Campbell, and S. A. Alumur, "Spatial Analysis of Single Allocation Hub Location Problems," *Networks and Spatial Economics*, vol. 16, no. 4, pp. 1075–1101, Dec. 2016.